Department of Orthodontics

CASE WESTERN RESERVE UNIVERSITY

SCHOOL OF DENTAL MEDICINE

GRADUATE STUDIES

We hereby approve the thesis of

Jeffrey C. Kwong

Candidate for the degree Master of Science

in Dentistry.

Signed: _____ (Chairperson)

_____

_____

_____

_____

Date: December 20, 2006

IMAGE QUALITY PRODUCED BY DIFFERENT CBCT SETTINGS

by

JEFFREY C. KWONG

Submitted in partial fulfillment of the requirements for the degree of Master of Science in Dentistry

Thesis Advisor: J. Martin Palomo, D.D.S., M.S.D.

Department of Orthodontics

School of Dental Medicine

CASE WESTERN RESERVE UNIVERSITY

January 12, 2007

IMAGE QUALITY PRODUCED BY DIFFERENT CBCT SETTINGS

Abstract

by

JEFFREY C. KWONG

Objective: To evaluate image quality produced by different CBCT settings for three fields of view. Method: A Hitachi CB MercuRay™ was modified to allow different setting combinations. The variables consisted of 4 different mA (2, 5, 10, and 15), 2 kVp (100, and 120), presence or not of a copper filter, and 3 fields of view (6", 9", and 12"). Thirty-two scans were taken on a cadaver head and 16 scans on a skull. The groups were divided by field of view and images were ranked by at least thirty judges. Diagnostic quality was addressed in a questionnaire. Descriptive statistics and rankings were calculated using Excel 2003, and Friedman's and Wilcoxon Ranked Sign Tests using SPSS 14.0.1. Result: Changing the filter setting showed significant differences ($p < 0.006$) in two pairs of the 9". Variation in kVp showed significant differences ($p < 0.006$) in the 6" 5 mA images with filter. Altering mA

settings showed significant differences ($p < 0.008$) in the 6″ and 12″ groups. The 9″ group showed significant differences between 2 mA and 10/15 mA. Overall, the 6″, 9″ and 12″ images demonstrated diagnostic quality 56%, 99% and 99% of the time, respectively. Conclusion: Filter and kVp did not affect overall image quality. Images taken at lower mA settings showed good diagnostic quality.

DEDICATION

This thesis is dedicated to:

God, for the blessings and abilities I have been given.

My father Louis, who has given me his unconditional love and support. Thank you for your trust in me, and for the sacrifices you have made for me. You have taught me about the importance of a good education. I would not know the meaning of love or success without your guidance.

My sister Joanne, who has grown to become a strong, intelligent, beautiful young woman. Thank you for your friendship, support and love. I will always be there to protect you.

My stepmother Yvonne, who has supported me throughout my education. Thank you for the love you have given our family.

My mother Stella, for the best memories of my youth and for the example you set for me while you were with us. I would not be the person I am today without your guidance. Thank you for teaching me how to be a good person.

My grandparents, aunts, uncles, cousins, friends and loved ones who have been there in my times of greatest need. Thank you for your support and love.

ACKNOWLEDGEMENTS

Thank you Dr. Mark Hans for accepting me into your residency program and trust tree. You could not have been more right by comparing our program to a diamond in the rough. Thank you for making the program what it is. You have allowed me to fulfil my dream of becoming an orthodontist and I am truly grateful.

Thank you Dr. Martin Palomo for your friendship and mentorship throughout the residency. Your leadership throughout my project has helped me better appreciate the scientific process. Thank you for being the chair of my committee. I am grateful for the freedom you have given me, and for steering me back towards the path when I have strayed. Thank you for your deep thoughts by Martin Palomo.

Thank you Dr. Michael Landers for being a part of my thesis committee. I appreciate your guidance and help with my thesis and I am grateful for the time you have set aside to make this possible.

Thank you Dr. Manish Valiathan for your friendship and mentorship. Thank you for standing behind me when I applied to the residency, and for helping me throughout.

Thank you Sebastian for being my brother in arms in this residency. We have experienced many great trips, memories, orthodontic discussions and board exams. Thank you for your German ways.

Thank you Alika for making the residency a fun place and for being one of the guys. You are truly a great person and have always been sweet and supportive. I am thankful for your friendship.

Thank you Reid for all the laughs; you do great impressions. I am grateful for your friendship.

Thank you Boyd for being my Caucasian twin separated from birth. Lisa and I have truly enjoyed your friendship. Your stories, advice and willingness to have fun have made this residency memorable. Thank you for always being up front with me.

Thank you John for showing me how to win in Vegas. You have been a loyal friend and I am grateful for your support.

Thank you to my orthodontic little brothers, Eric and Kurt. I cannot guarantee that everything I have

taught you is right, nor can I guarantee that I have taught you anything. Thank you for your patience, and for making me a better teacher. I am grateful that you are my orthodontic little brothers.

Thanks to all my other fellow residents that have made this residency so unique: Jed, Cliff, Mike, Nadia, Gabriel, Austin, Breyn, Cynthia and Wanvadee. I have enjoyed all the fun times we experienced during this residency, and I am grateful for your friendship.

Thank you to the remarkable faculty of Case Western Reserve University Orthodontics. You have been a great inspiration. Your knowledge and generosity have created an exceptional learning environment. I appreciate all the time and effort that you have contributed towards my education. I hope that one day I might be in your position.

Thank you to Dr. Mark Schluchter, Wei Xue and Alex Figueroa for helping with my statistical design and analysis, as well as data collection. Your help has made this process a lot smoother and has been much appreciated.

Thank you to the great staff at our department: LaVerne, Shirley, Amy, Tina, Kim, and Jessica. You have

taught me a lot about myself and have made my everyday life so much easier and more pleasant.

A special thank you to Lisa. You have made these past three and a half years the best in my life. Your smile has always brightened my days. Your love, support and understanding have never wavered. Thank you for teaching me to how to be a better person and teacher. I am lucky to have you as my girlfriend.

TABLE OF CONTENTS

Page

ABSTRACT ii

DEDICATION iv

ACKNOWLEDGEMENTS v

TABLE OF CONTENTS ix

LIST OF FIGURES xi

LIST OF TABLES xvii

LIST OF TABLES xvii

LITERATURE REVIEW 1

STATEMENT OF HYPOTHESIS 33

MANUSCRIPT 34

1. IRB Approval 69

2. Instructions and Questionnaires 71

3. Six Inch Bitewing Images 81

4. Nine Inch Panoramic Images 98

5. Twelve Inch Lateral Cephalogram Images 115

6. Raw Data: Six Inch 132

7. Raw Data: Nine Inch 137

8. Raw Data: Twelve Inch 142

Page

9. Friedman and Wilcoxon Signed Ranks Tests for 6″ Images 147

10. Friedman and Wilcoxon Signed Ranks Tests for 9″ Images 155

11. Friedman and Wilcoxon Signed Ranks Tests for 12″ Images 161

12. Intraexaminer and Interexaminer Reliability 170

REFERENCES 182

LIST OF FIGURES

Figure Page

1. Radiographic image obtained at settings of 6" field of view, 2 mA and 100 kVp without filter. 82

2. Radiographic image obtained at settings of 6" field of view, 2 mA and 100 kVp with filter.. 83

3. Radiographic image obtained at settings of 6" field of view, 2 mA and 120 kVp without filter.. 84

4. Radiographic image obtained at settings of 6" field of view, 2 mA and 120 kVp with filter.. 85

5. Radiographic image obtained at settings of 6" field of view, 5 mA and 100 kVp without filter.. 86

6. Radiographic image obtained at settings of 6" field of view, 5 mA and 100 kVp with filter.. 87

7. Radiographic image obtained at settings of 6" field of view, 5 mA and 120 kVp without filter.. 88

8. Radiographic image obtained at settings of 6" field of view, 5 mA and 120 kVp with filter.. 89

9. Radiographic image obtained at settings of 6" field of view, 10 mA and 100 kVp without filter.. 90

Figure Page

10. Radiographic image obtained at settings of 6" field of view, 10 mA and 100 kVp with filter.. 91

11. Radiographic image obtained at settings of 6" field of view, 10 mA and 120 kVp without filter.. 92

12. Radiographic image obtained at settings of 6" field of view, 10 mA and 120 kVp with filter.. 93

13. Radiographic image obtained at settings of 6" field of view, 15 mA and 100 kVp without filter.. 94

14. Radiographic image obtained at settings of 6" field of view, 15 mA and 100 kVp with filter.. 95

15. Radiographic image obtained at settings of 6" field of view, 15 mA and 120 kVp without filter.. 96

16. Radiographic image obtained at settings of 6" field of view, 15 mA and 120 kVp with filter. 97

17. Radiographic image obtained at settings of 9" field of view, 2 mA and 100 kVp without filter.. 99

18. Radiographic image obtained at settings of 9" field of view, 2 mA and 100 kVp with filter.. 100

19. Radiographic image obtained at settings of 9" field of view, 2 mA and 120 kVp without filter.. 101

Figure Page

20. Radiographic image obtained at settings of 9" field of view, 2 mA and 120 kVp with filter.. 102

21. Radiographic image obtained at settings of 9" field of view, 5 mA and 100 kVp without filter.. 103

22. Radiographic image obtained at settings of 9" field of view, 5 mA and 100 kVp with filter.. 104

23. Radiographic image obtained at settings of 9" field of view, 5 mA and 120 kVp without filter.. 105

24. Radiographic image obtained at settings of 9" field of view, 5 mA and 120 kVp with filter.. 106

25. Radiographic image obtained at settings of 9" field of view, 10 mA and 100 kVp without filter.. 107

26. Radiographic image obtained at settings of 9" field of view, 10 mA and 100 kVp with filter.. 108

27. Radiographic image obtained at settings of 9" field of view, 10 mA and 120 kVp without filter.. 109

28. Radiographic image obtained at settings of 9" field of view, 10 mA and 120 kVp with filter.. 110

29. Radiographic image obtained at settings of 9" field of view, 15 mA and 100 kVp without filter.. 111

Figure Page

30. Radiographic image obtained at settings of 9" field of view, 15 mA and 100 kVp with filter.. 112

31. Radiographic image obtained at settings of 9" field of view, 15 mA and 120 kVp without filter.. 113

32. Radiographic image obtained at settings of 9" field of view, 15 mA and 120 kVp with filter. 114

33. Radiographic image obtained at settings of 12" field of view, 2 mA and 100 kVp without filter.. 116

34. Radiographic image obtained at settings of 12" field of view, 2 mA and 100 kVp with filter. 117

35. Radiographic image obtained at settings of 12" field of view, 2 mA and 120 kVp without filter.. 118

36. Radiographic image obtained at settings of 12" field of view, 2 mA and 120 kVp with filter.. 119

37. Radiographic image obtained at settings of 12" field of view, 5 mA and 100 kVp without filter.. 120

38. Radiographic image obtained at settings of 12" field of view, 5 mA and 100 kVp with filter.. 121

39. Radiographic image obtained at settings of 12" field of view, 5 mA and 120 kVp without filter.. 122

Figure Page

40. Radiographic image obtained at settings of 12" field of view, 5 mA and 120 kVp with filter.. 123

41. Radiographic image obtained at settings of 12" field of view, 10 mA and 100 kVp without filter.. 124

42. Radiographic image obtained at settings of 12" field of view, 10 mA and 100 kVp with filter.. 125

43. Radiographic image obtained at settings of 12" field of view, 10 mA and 120 kVp without filter.. 126

44. Radiographic image obtained at settings of 12" field of view, 10 mA and 120 kVp with filter.. 127

45. Radiographic image obtained at settings of 12" field of view, 15 mA and 100 kVp without filter.. 128

46. Radiographic image obtained at settings of 12" field of view, 15 mA and 100 kVp with filter.. 129

47. Radiographic image obtained at settings of 12" field of view, 15 mA and 120 kVp without filter.. 130

48. Radiographic image obtained at settings of 12" field of view, 15 mA and 120 kVp with filter.. 131

49. The Kendall's tau-b of 6" ranking by each operator at time 1 and time 2 and the pooled tau-b of all operators. 173

Figure Page

50. The Kendall's tau-b of 9" ranking by each operator at time 1 and time 2 and the pooled tau-b of all operators. 175

51. The Kendall's tau-b of 12" ranking by each operator at time 1 and time 2 and the pooled tau-b of all operators. 180

LIST OF TABLES

Table		Page
1.	Scanning Parameters for Conventional CT	24
2.	Scanning Parameters for Helical CT	24
3.	Six Inch Ranking Raw Data and Descriptive Statistics	133
4.	Six Inch Diagnosis* Raw Data and Descriptive Statistics	134
5.	Six Inch Ranking Reliability Raw Data	135
6.	Six Inch Diagnosis* Reliability Raw Data	136
7.	Nine Inch Ranking Raw Data and Descriptive Statistics	138
8.	Nine Inch Diagnosis* Raw Data and Descriptive Statistics	139
9.	Nine Inch Ranking Reliability Raw Data	140
10.	Nine Inch Diagnosis* Reliability Raw Data	141
11.	Twelve Inch Ranking Raw Data and Descriptive Statistics	143
12.	Twelve Inch Diagnosis* Raw Data and Descriptive Statistics	144
13.	Twelve Inch Ranking Reliability Raw Data	145
14.	Twelve Inch Diagnosis* Reliability Raw Data	146
15.	Ranks for 6" Image Pairs Comparing Filter	148

Table Page

16. Wilcoxon Signed Rank Test Comparing Effect of Filter on 6" Images 149

17. Ranks for 6" Image Pairs Comparing kVp 149

18. Wilcoxon Signed Rank Test Comparing kVp on 6" Images 150

19. Friedman Test for 6" 100 kVp Without Filter Images 150

20. Ranks for 6" 100 kVp Without Filter Images 150

21. Wilcoxon Signed Rank Test Comparing mA on 6" 100 kVp Without Filter 151

22. Friedman Test for 6" 100 kVp With Filter Images 151

23. Ranks for 6" 100 kVp With Filter Images 151

24. Wilcoxon Signed Rank Test Comparing mA on 6" 100 kVp With Filter 152

25. Friedman Test for 6" 120 kVp Without Filter Images 152

26. Ranks for 6" 120 kVp Without Filter Images 152

27. Wilcoxon Signed Rank Test Comparing mA on 6" 120 kVp Without Filter 153

28. Friedman Test for 6" 120 kVp With Filter Images 153

29. Ranks for 6" 120 kVp With Filter Images 153

30. Wilcoxon Signed Rank Test Comparing mA on 6" 120 kVp With Filter 154

31. Ranks for 9" Image Pairs Comparing Filter 156

Table Page

32. Wilcoxon Signed Rank Test Comparing Effect of Filter on 9" Images 157

33. Ranks for 9" Image Pairs Comparing kVp 157

34. Wilcoxon Signed Rank Test Comparing Effect of kVp on 9" Images[c]..... 158

35. Friedman Test for 9" 100 kVp Without Filter Images 158

36. Ranks for 9" 100 kVp Without Filter Images 158

37. Wilcoxon Signed Rank Test Comparing mA on 9" 100 kVp Without Filter 159

38. Friedman Test for 9" 100 kVp With Filter Images[a]..... 159

39. Friedman Test for 9" 120 kVp Without Filter Images[a]..... 159

40. Friedman Test for 9" 120 kVp With Filter Images 159

41. Ranks for 9" 120 kVp With Filter Images 160

42. Wilcoxon Signed Rank Test Comparing mA on 9" 120 kVp With Filter[c]..... 160

43. Ranks for 12" Image Pair Comparing Filter 162

44. Ranks for 12" Image Pairs Comparing Filter[c]..... 163

45. Ranks for 12" Image Pairs Comparing kVp 163

46. Wilcoxon Signed Rank Test Comparing Effect of kVp on 12" Images[c]..... 164

47. Friedman Test for 12" 100 kVp Without Filter Images[a]..... 164

48. Ranks for 12" 100 kVp Without Filter Images 165

Table Page

49. Wilcoxon Signed Rank Test Comparing mA on 12" 100 kVp Without Filter 165

50. Friedman Test for 12" 100 kVp With Filter Images 165

51. Ranks for 12" 100 kVp With Filter Images 166

52. Wilcoxon Signed Rank Test Comparing mA on 12" 100 kVp With Filter 167

53. Friedman Test for 12" 120 kVp Without Filter Images 167

54. Ranks for 12" 120 kVp Without Filter Images 167

55. Wilcoxon Signed Rank Test Comparing mA on 12" 120 kVp Without Filter[c]..... 168

56. Friedman Test for 12" 120 kVp With Filter Images[a]..... 168

57. Ranks for 12" 120 kVp With Filter Images 168

58. Wilcoxon Signed Rank Test Comparing mA on 12" 120 kVp With Filter 169

59. Kendall's tau-b of 6" Ranking by Each Operator at Time 1 and Time 2 with Pooled Coefficient. 172

60. Kendall's tau-b of 9" Ranking by Each Operator at Time 1 and Time 2 with Pooled Coefficient. 174

61. Kendall's Coefficient of Concordance of 6" Ranking by Each Individual at Two Time Points with P-values. 176

62. Kendall's Coefficient of Concordance of 9" Ranking by Each Individual at Two Time Points with P-values. 177

Table Page

63. Kendall's tau-b of 12" Ranking by Each Operator and Pooled Coefficient with 95% CI 179

64. Kendall's Coefficient of Concordance for Each Individual at Two Time Points with P-values. 181

LITERATURE REVIEW

Recently, cone beam computed tomography (CBCT) has been utilized for its capability of providing reliable information compared to conventional methods (Bodner et al. 2001). CBCT provides excellent tissue contrast, eliminating blurring and overlapping of adjacent teeth and offers orthogonal views eliminating projection effects (Elefteriadis et al. 1996). In addition to the advantages of CBCT, this technology offers reduced cost relative to medical CT and significantly reduced radiation exposure.

With CBCT technology, all possible craniofacial radiographs can be taken in under a minute. Dental clinicians now have in a single image, the possibility of producing periapicals, panoramic, cephalograms, occlusal radiographs, and TMJ views, along with views that cannot be produced by regular radiographic machines such as axial and cross-sectional views. A number of clinical applications have already been reported in the literature (Danforth et al. 2003; Mah et al. 2003; Aboudara et al. 2003; Hatcher et al. 2003; Hamada et al. 2005).

The two principal differences that distinguish cone beam computed tomography from traditional CT are the type of imaging source-detector complex and the method of data acquisition. The X-ray source for CT is a high-output rotating anode generator while that for CBCT can be a low-energy fixed anode tube similar to that used in dental panoramic machines. Computed tomography employs a fan-shaped X-ray beam and records the data on solid state image detectors arranged in a 360-degree array around the patient. Cone beam computed tomography uses a cone shaped X-ray beam with a special image intensifier and a solid-state sensor or an amorphous silicon plate for capturing the image. Conventional medical CT devices image patients in a series of axial plane slices that are captured either as individual stacked slices or from a continuous spiral motion over the axial plane. Cone beam CT on the other hand uses one rotational sweep of the patient (Danforth et al. 2003).

Unlike two dimensional digital images that are composed of distinct picture elements or 'pixels', three dimensional volumes are formed by volume elements or 'voxels' (Farman 2003). The gray level in each pixel is related to X-ray attenuation from both the radiodensity

and thickness of the tissue penetrated in addition to the selected exposure factors. Similarly, each voxel is also assigned an attenuation value (density) that corresponds to a shade of grey. Small voxel sizes of approximately 0.3mm would allow feature detection size and dimensional accuracy in the range of 0.5 mm (Hatcher et al. 2003). Currently, regional CBCT devices such as those developed for the evaluation of implant sites, have better resolution. However, it has been noted that image resolution in CBCT is much less than plain film radiography (Danforth et al. 2003).

Although cone beam technology is able to provide volumetric images with up to four times less radiation than a conventional CT, the resulting effective radiation is dependent on the settings used, namely kilovoltage peak (kVp) and milliamperage (mA) (Shulze et al. 2004a, Shulze et al. 2004b). Capturing images using a lower mA setting with or without collimation are ways to reduce the dose of radiation. Patient effective exposure dose from a CBCT machine has been reported to be as low as 45 microsieverts (μSv) to as high as 650 μSv. Exposure for an analog full mouth series has been reported as 150 μSv, for an analog panoramic radiograph as 54 μSv, while a

roundtrip from Paris to Tokyo adds 139 μSv of effective dose per passenger (Fredriksen 1995; Kiefer et al. 2004a; Kiefer et al. 2004b; Bottollier-Depois et al. 2003; Bottollier-Depois et al. 2004). However, lowering the mA setting may produce a lower image quality.

The ADA Council on Scientific Affairs recommends the use of techniques that would reduce the amount of radiation received during dental radiography. Known as the "As Low As Reasonably Achievable" or ALARA principle, this includes taking radiographs based on the patient's needs (as determined by an examination), using the fastest film compatible with the diagnostic task, collimating the beam to a size as close to that of the film as feasible and using lead aprons and thyroid shields. An accepted ratio between exposure and image quality needs to be reached in order to use this principle.

The ideal imaging modality should produce the desired diagnostic information while minimizing the cost and risk to the patient (Hatcher et al. 2003). However, better quality images can be produced by use of techniques which give higher radiation doses to patients (Martin et al. 1999). Thus in choosing the level of

image quality required, the potential risk from loss of diagnostic information from application of a lower dose technique must be weighed against the increased risk that would result from use of a higher radiation exposure (Martin et al. 1999). There is a trade-off between dose and resolution that should be viewed as task dependent.

Before a reasonable assessment of image quality can be made, proper requirements for image quality need to be defined. The ideal set of parameters describing image quality should give a measure of the effectiveness with which an image can be used for its intended purpose, namely answering the clinical questions posed. The parameters should relate to the ability of the image to reveal disease and to demarcate anatomical structures which are relevant to detection, differential diagnosis and localization. Image quality requirements will vary for different types of examination or even different tasks within single examinations (Martin et al. 1999).

Image quality is essentially a descriptor of the subjective interpretation of visual data and as such cannot have a simple analytical definition. It can only be fully understood in relation to a specific medical task and images should convey sufficient information to

the clinician to allow a medical decision to be made with an acceptable degree of certainty.

Image Quality in Traditional Film-Screen Radiography

In traditional film radiography, the quality of the radiographic image can be defined as the ability of the film to record each point in the object as a point on the film (Curry et al. 1990). In radiology, point-for-point reproduction is never perfect due to the diffusion of photons by intensifying screens. There is no general agreement as to what should be included when considering image quality, but it is influenced by radiographic mottle, sharpness and resolution (Curry et al. 1990).

Radiographic Mottle

If a film is exposed to a homogeneous x-ray beam the resultant film will not exhibit uniform density but will have an irregular mottled appearance. This uneven appearance is caused by small differences in density and is termed "radiographic mottle." Radiographic mottle has two components: film graininess and screen mottle. Film graininess refers to the nonhomogeneous composition of silver crystals in a gelatinous film and contributes minimally to radiographic mottle. Film graininess can only be observed at magnifications of five to ten times.

Screen mottle has two components: structure mottle and quantum mottle. Structure mottle is caused by defects in the intensifying screen, such as an irregular thickness or physical defects in the phosphor layer. However, the quality control in the production of films is good, and thus it is rare to have structure mottle. Quantum mottle is the only important cause of radiographic mottle. Quantum mottle is seen when intensifying screens are used. It is caused by the statistical fluctuation in the number of quanta (discrete energy units, i.e., x-ray photons) per unit area absorbed by the intensifying screen. The actual number of x-ray photons per mm^2 obeys the law of probability because the emission of x-rays by the x-ray tube is a random event. Hence, an x-ray film is exposed to a nonuniform pattern of light on the surface of the intensifying screen. The fewer quanta used, the greater the statistical fluctuation and hence, the greater the quantum mottle (Curry et al. 1990).

Sharpness

Sharpness is the ability of the x-ray film to define an edge. Sharpness and contrast are closely related in the sense that an unsharp edge can be easily seen if contrast is high, but a sharp edge may be poorly visible

if contrast is low. The sharpness of a film is affected by geometric unsharpness, motion unsharpness, absorption unsharpness, screen unsharpness, and parallax unsharpness (Curry et al. 1990).

Geometric unsharpness or penumbra occurs because the focal spot acts as if it were composed of multiple point sources of x-rays, with each point source forming its own image of an object. Penumbra is the region of partial illumination that surrounds the umbra (or complete image). Penumbra can be minimized by using a small focal spot and keeping magnification as small as possible. Motion unsharpness is affected mainly by movement of the object and can be minimized by using a short exposure time. Absorption unsharpness results when imaging an object that does not have nice sharp edges, and is greatest for round or ovoid objects. Screen unsharpness is caused by light diffusion through the screen phosphor layer and can be minimized with good screen-film contact. Parallax unsharpness is caused by viewing an object at an angle and is seen only with double emulsion films. It is a result of images on two emulsions separated by the width of the film base (Curry et al. 1990).

Resolution

Resolution refers to the ability to record separate images of small objects that are placed very close together. The resolution of a film-screen system is evaluated by how many line pairs per millimeter can be clearly seen in the developed radiograph. However, the resolving power measures a limit. That is, given the resolution of a system, an image cannot be produced with a greater number of line pairs per millimeter. Additionally, the resolution (in line pairs per mm) of a system does not provide any information about image quality at a lesser resolution (fewer line pairs) (Curry et al. 1990).

Image Quality in Digital Radiography

The quality of a digital image is affected by the spatial resolution, the association of the gray level values of the pixels to the optical density of the radiograph, and the image display. The number of gray levels and pixels that are necessary to produce an image of suitable quality will vary depending on the image itself. Highly detailed images depend more on the number of pixels rather than the number levels of gray.

Spatial Resolution

Spatial resolution is the ability to record separate images of small objects that are placed in close proximity. As in film-screen radiography, spatial resolution is measured in line pairs per mm (lp/mm). As pixel size decreases, the image becomes more detailed and hence the resolution increases. Since the smallest detail detectable by the human eye is 0.1 by 0.1 mm, pixels no larger than 0.1 mm are required to produce digital radiographs with at least as much information as is available in the original conventional radiograph (Gray 1984). Loss of some diagnostic accuracy can result from the use of pixel sizes substantially larger than 0.1 mm. The optimal pixel size for a given application will be the one just small enough to allow an acceptable level of diagnostic accuracy while reducing data storage requirements to a minimum. Usually, musculoskeletal radiology requires a spatial resolution of 8 lp/mm. The spatial resolution of most film/screen combinations used for musculoskeletal radiography is equivalent to 10-12 lp/mm. In general, increasing resolution generally results in a poorer ability to identify structures

amongst background noise unless dose is increased proportionately (Farman 2003).

Optical Density

Film darkness is measured by optical density. The quality of digital images is related to the number of gray levels. Specifically, the quality is related to the relationship between the range of gray level values and the optical density of the region of interest on the conventional radiograph. However, image enhancement techniques, such as histogram equalization, can be used to ensure maximum use is being made of the gray scale available and may improve the diagnostic quality of the image. Wenzel, in assessing the requirements of 3 x 4 cm intraoral periapical radiographs, found that diagnostic accuracy was maintained when the gray levels were reduced to six bits (Wenzel 1987). A six bit image allows sixty-four possible values for each pixel, ranging from 0, which represents a black area on the image, to 63, which represents a white area (Forsyth et al. 1996a).

Image Quality in Computed Tomography

Image quality in computed tomography is not well defined, but it can be thought of as the visibility of diagnostically important structures in the CT image. The

factors affecting image quality are interrelated and can be described using similar terms described for film-screen radiographs: quantum mottle (noise), resolution and patient exposure (Curry et al. 1990).

Quantum Mottle

Precision in computed tomography is a measure of background (matrix) consistency. When homogenous objects are examined using a CT scanner, all voxels in the matrix should have exactly the same CT number. Deviations from uniformity represent statistical fluctuations called quantum mottle or noise. The quantum mottle is due to the statistical emission of photons from the x-ray tube. The statistical fluctuation is a function of the number of photons emitted. Noise can be measured as a standard deviation of the number of photons (i.e., $\sigma = (\sqrt{N})/N$). Hence, decreasing mottle is seen with increasing photon count rates (Curry et al. 1990).

The x-ray beam is generated in the x-ray tube, carried through the patient, and recorded by the detectors. Noise is the variation in the number of x-ray photons absorbed by the detector. Hence, it can only be seen when photons are absorbed by the detector. The only way to decrease noise is to increase the number of

photons absorbed by the detector by increasing x-ray dose to the patient (Curry et al. 1990).

Photon counting statistics are intimately related to voxel size. Assuming that other factors remain constant, reducing voxel size decreases the number of counts per each element. If counting statistics (precision) are kept constant, the enhanced resolution of the smallest sized voxel can only be realized with an increase in patient exposure. Noise tends to increase at higher resolution (smaller voxel sizes) if exposure remains the same.

Matrix size, field size and pixel/voxel size are interrelated. The matrix size is defined as the number of points in a volume matrix, and is dependent on voxel size. Field size refers to the outside dimensions of the CT slice and dictates the maximum size of anatomic part that can be examined. If the matrix or field size is increased, so does the number of voxels. Hence, enlarging the matrix or field size requires an increase in patient dose if the same precision (counting statistics) is required (Curry et al. 1990).

Resolution

Resolution has two components, spatial resolution and contrast resolution. Spatial resolution of a CT unit is its ability to display, as separate images, two objects that are very close to each other. In computed tomography, spatial resolution is expressed in line pairs per centimeter. Contrast resolution is the ability to display areas with small differences in density as distinct images. Contrast and spatial resolution are closely related to each other and to the radiation dose absorbed by the detector (i.e., quantum mottle). Efforts to improve spatial resolution may cause increased noise levels that decrease contrast resolution. Attempts to improve contrast resolution by increasing scan times (i.e. a larger dose) may decrease spatial resolution by increasing the possibility of motion artifacts (Curry et al. 1990).

Spatial resolution measurements are determined by using test objects of high contrast, which differ significantly in density. High contrast test objects and make it possible to ignore the effect of quantum mottle on spatial resolution measurements. High contrast

spatial resolution is determined by the scanner design, computer reconstruction and the display.

The scanner design includes x-ray tube focal spot size, detector size and magnification. CT scanners have small focal spots that range from just under 1mm to slightly over 1 mm. Detector size places a limit on the maximum spatial resolution of a CT scanner. To increase resolution, it is necessary to use aperture in front of the detector (to effectively reduce detector size). Also, minimizing magnification by increasing the object to source distance is difficult. The minimum detector size can be calculated by multiplying the magnification by the object size.

Although computer reconstruction is a determining factor of resolution it does not play a large role. The resolution capability is actually determined by the scanner design. The reconstruction matrix needs to be large enough to distinguish the high contrast resolution. In order to calculate the size of a reconstruction matrix, it is necessary to assume that a minimum of one pixel for one an opaque line and one pixel for the adjacent space. For example, if a 10 lp/cm resolution is required for a CT field size of 40 cm, then 20 pixels are

required per cm. A 40 cm field would require an 800 X 800 pixel matrix, or 640,000 matrix points. The reconstruction matrix must be large enough to reconstruct the available data, otherwise information will be lost.

The display is the unit that presents the captured CT scan. For an image to be viewed effectively, the display should have a resolution that is equal to or greater than that of the reconstruction matrix. However, if the resolution of the reconstruction matrix is larger than that of the display, the quality of the image cannot be appreciated. This problem can be overcome by viewing only parts of matrix that are smaller than the full field (Curry et al. 1990).

Contrast resolution is the ability of an imaging system to display an image of an object (2-3 mm) that is only slightly different in density from its surroundings. For the object to be visible, it must produce enough change in the number of transmitted photons to overcome the statistical fluctuations in transmitted photons caused by noise. Hence, low contrast visibility is limited by the amount of noise in surrounding the object (Seibert 1991). A homogenous background allows better visibility of low contrast images. Better counting

statistics produce a more homogeneous background. Counting statistics improve with larger pixel/voxel size by minimizing statistical fluctuations. Hence, the only way to improve low contrast resolution is to improve counting statistics. Contemporary CT scanners can display objects of 3 mm in diameter with density differences of 0.5% or less. Film-screen radiography on the other hand requires a density difference of approximately 10% for contrast resolution. Hence, computer tomography technology has an improved capability of detecting density differences over film-screen radiography (Curry et al. 1990).

Patient Exposure

Theoretically, exposure of tissues only occurs during the time that the slice containing the tissue is being scanned. At other times the tissue is exposed only to scatter radiation, which is minimized by a narrow beam width. A conventional dose for a medical grade CT scan ranges from 2 cGy (rads) to 4 cGy (Curry et al. 1990).

Dose is closely related to contrast resolution and spatial resolution. Again, contrast resolution improves with improved counting statistics, and the only way to improve counting statistics is with more x-ray photons.

Improved spatial resolution requires smaller pixel/voxel size. If the size of the voxel is decreased and the dose (photon count) is kept constant, the dose per volume element will decrease (i.e., fewer photons per voxel). Hence, improved spatial resolution will be at the expense of increased noise unless dose is increased. Improvement of both contrast resolution and spatial resolution always requires increased patient dose (Curry et al. 1990).

Artifacts in Computed Tomography Images

An artifact can be defined as a structure or feature not normally present but visible as a result of an external agent or action. Artifacts in computed tomography occur when there is a discrepancy between the reconstructed CT numbers and true attenuation coefficients, as a result of errors in the x-ray transmission measurements (Seibert 1991). Common artifacts include motion artifacts, streak artifacts beam-hardening artifacts, and ring artifacts.

Motion artifacts have an overwhelming effect on image quality. Since motion is random and unpredictable, the reconstruction program does not have the ability to make the necessary corrections. Motion artifacts are displayed as a streak in the direction of motion. The

intensity of the streak artifact will depend on the density of the object in motion. The density of the pixels in the area of the streak artifacts will be averaged. Objects with greater differences in density than the surrounding area will produce more intense motion artifacts.

Scatter radiation causes streaks by matching or exceeding the true signal level of the area surrounding a dense object (Seibert 1991). Scatter is most deleterious behind dense objects and is difficult to correct because the amount of scatter radiation varies from patient to patient. Streak artifacts can also occur when transmission of photons is reduced by a high density material. If the detector records no transmission, this violates a basic assumption and the reconstruction program cannot account for the violation. As a result, streak artifacts will occur (Gould 1991).

The x-ray beam used to produce a CT image is a heterogenous x-ray beam that contains photons with different energies. The energy in the x-ray beam is reported as an averaged kVp. Low energy photons are readily absorbed by the patient. Hence, the x-ray beam leaving the patient contains a lower percentage of energy

photons than the entering beam. This effect is called beam hardening (Gould 1991). In beam hardening artifacts, lower CT numbers are obtained in the middle of the object than at the edge (Seibert, 1991). That is, the reconstructed image will be less dark in the center than at the periphery (Gould 1991).

Ring artifacts occur as a result of miscalibration or failure of one or more detectors. A miscalibrated detector will record incorrect data in every position and is constructed as a ring in the image. Ring artifacts are associated with older scanner geometries and have almost disappeared from contemporary CT units (Gould, 1990).

The Effect of Dose Variation on Image Quality

CBCT is a fairly new modality and there has been little research done in the area of dose reduction and cone beam CT image quality. The effect of dose variation and image quality has been studied using medical and dental grade CT scanners. The current trend in dental and medical diagnostic imaging is to minimize the radiation dose to the patient. The use of a higher radiation dose does not guarantee a better image quality and surveys of a number of medical radiographic

examinations have shown no correlation between image quality and patient entrance surface dose (Warren-Forward and Millar 1996; European Commission 1996a,b; Badr et al. 1997). It has also been shown by Ortiz et al., in 1995, that the reduction of radiation dose has had minimal effect on the diagnostic capabilities of medical clinical images. The aim in balancing radiation dose and image quality is to provide an image which is adequate for the clinical task with the minimum radiation dose to the patient (Martin et al. 1999).

Haaga et al. (1981) studied the effects of mA variation upon computed tomography image quality of both *in vivo* images of patients, and in-vitro images of a performance phantom. The images were captured at 120 kVp with one millimeter of aluminum filtration at 6, 20, 40 and 100 mAs. The scans were two seconds in duration and all were obtained in the same anatomical area, the abdomen. After 152 scans were collected, two radiologists were asked to subjectively evaluate the images based on diagnostic quality (grainy texture, spatial and contrast resolution). The results indicated that very few patients were successfully scanned at a dose of 6 mA due to increasing noise. The *in vitro* study

revealed that decreasing the dose from 100 mA to 6 mA resulted in a twofold increase in the amount of quantum mottle. However, the resolution did not change significantly, and varied only between the different structures within the performance phantom.

In order to determine the minimal tube current (mAs) required for consistently good image quality, Mayo et al. (1995) evaluated chest CT for thirty consecutive patients. Patients had a conventional chest CT taken on a single CT scanner using the standard technique (120 kVp, 400 mAs) followed by four additional sections imaged using reduced tube currents (200, 140, 80 and 20 mAs) at two anatomical levels. The images were evaluated in a random order by two independent observers using a five point scale (non-diagnostic to excellent). The observers also evaluated for the presence of parenchymal or mediastinal abnormalities using the standard settings as the control. Images were reconstructed using two different algorithms and the window settings were adjusted to appropriately view the lungs and mediastinum. Data analysis revealed a significant linear relationship between the subjective image quality scores and the square root of the tube current. In general, higher

image quality scores were consistently obtained with higher tube current. As well, no significant differences were detected in image quality between the images taken at the standard current (400 mAs) and the 200 mAs or 140 mAs. However, significant differences in image quality were detected between the standard current and the 80 mAs and 20 mAs levels. No significant differences were observed in detecting parenchymal or mediastinal abnormalities with decreasing milliamperage settings. A dose reduction of nearly threefold is seen when milliamperage is changed from 400 mAs to 140 mAs. Mayo et al. concluded that a tube current of 140 mA was necessary to obtain consistently good quality chest CT images.

Cohnen et al. (2000) researched the relationship between the image quality of intracranial scans and dose reduction by use of reduced current and kilovoltage. Scanning parameters for two medical grade CT scanners (Toshiba Xpress SX, Siemens Somatom AR.SP) were systematically changed and analyzed using a formalin fixed cadaver head as the phantom. The scans were acquired in both conventional and helical modes, and the adjustable parameters included mA and kVp. Scanning

parameters were reduced stepwise in the fashion shown in Table 1 and 2 below:

TABLE 1.--Scanning Parameters for Conventional CT

Toshiba Conventional Scan		Siemens Conventional Scan	
kVp	mA	kVp	mA
120	100	110	63
135	200	130	83
	270		105

TABLE 2.--Scanning Parameters for Helical CT

Toshiba Helical Scan		Siemens Helical Scan	
kVp	mA	kVp	mA
80	50	110	63
100	100	130	83
120	150		105
	185		

Radiation dose was measured using lithium-fluoride-thermoluminescent dosimeters. To create a standard reference rank order, the images were ranked and numbered according to descending surface dose. This assumed that image quality degradation varied inversely with a reduced surface dose. Subsequently the films were randomly assigned and presented in a blinded fashion. Five examiners were asked to subjectively rank the films according to image quality. Image quality differences between modes obtained from the same scanner were

assessed semiquantitatively using a Likert scale. The authors found that the subjective rating according to image quality was incongruent to the ranking according to descending radiation dose. Generally, films scanned with 100% to 60% of the initial dose could not be reliably identified by subjective assessment of image quality, that is, there was very little difference in image quality. As well, images acquired from both scanners with less than 30 mGy skin entrance doses were judged as non-diagnostic. It was also found that there was a nearly linear inverse relation between surface dose and image noise. The author's also confirmed that variation of kVp and mA reduced radiation exposure. The data shows that a maximal dose reduction up to 70% in conventional scanning and 65% in helical CT may be achievable without a significant change in image quality.

Sohaib et al. (2001) evaluated the effect of reducing mAs on the diagnostic quality of images and the radiation dose to the orbits in patients undergoing sinus CT. Forty consecutive patients were scanned in four groups at 200, 150, 100 and 50 mAs respectively. Image quality was assessed by two blinded independent observers using a semi-quantitative scale that evaluated six

different anatomic structures. The results indicated that there was no significant difference in image quality between the four groups. However, this may attributed to the grading system that was based on visibility or lack thereof of anatomical structures. Although the structures were visible, the images provided in their paper showed a clear difference in amount of noise present. Another limitation in the study is the use of forty different patients which exhibited different sinus anatomy. Overall, the mean radiation dose to the orbit was reduced by 77% from 13.5 mGy at 200 mAs to 3.1 mGy at 50 mAs.

Loubele et al. (2005) examined the tradeoff between radiation dose and image quality for low dose CT protocols of the head as related to maxillofacial surgery and oral implant planning. The low dose protocol was derived by lowering mAs and kVp, and increasing the pitch (i.e., the slice thickness) using a multi-slice CT scanner. Dose was measured using thermoluminescence dosimeters, while image quality was assessed using a spine phantom and skull phantom of known geometry. Image quality differences were quantified by linear measurements (distances) between segmentations obtained

with the low-dose imaging protocol and a reference clinical protocol. The low dose protocol allowed a reduction of radiation dose to 12.7% of the effective dose of the standard clinical protocol. The image quality results showed that the measurements and corresponding standard deviations obtained using the low dose protocol were at least twofold greater than those measured using the clinical protocol. Loubele et al. noted that the:

> "dose reduction with acceptable image quality was possible because only the bone surface is of interest for indications of maxillofacial surgery and oral implant planning, and not the contrast of the different soft tissues."

The authors concluded that although the measurements were larger using the low dose protocol, they were still acceptable for the purpose of maxillofacial surgery planning and image-based oral implant planning.

Gündogdu et al.(2005) looked at the relationship between tube current, image quality and adult head size in cranial CT. The experimental group consisted of sixty adult patients who underwent a non-contrast cranial CT examination. The sixty patients were divided into three groups based on the region of interest in the scan. Each patient received four scans using dose reduction scanning

protocols. The mA was varied between dose reduction protocols (140 mA and two seconds, 140 mA and one second, 120 mA, and 90 mA) while kVp was maintained at 140. Two radiologists were blinded for scanning parameters and were asked to qualitatively assess randomized image sets. The radiologists were given a short seven question assessment with questions concerning image quality and image noise and were asked to rate the images on a five point scale. The image quality scores and noise measurements were correlated with the dimensions of the patient's head. The radiologists were found to have a moderate to good level of interobserver agreement (r: 0.59-0.72) in the image quality and subjective noise scores. A significant difference in image quality and objective noise was found between the four protocols. In general, as the dose decreased so did the image quality and subjective noise scores. The average scores were still considered between good and acceptable. At 50% decreased dose protocol, there was no poor quality score at any level. Nonetheless, at a dose reduction of approximately 70%, protocol four was graded in the poor category 23% of the time by the two radiologists. Significant differences were found when image noise was

correlated to head size, however, no correlation was found between image quality and head size. Gündogdu et al. concluded that at a 50% dose reduction, image quality was not affected for CT scans of intracranial structures.

In order to evaluate the possibility of minimizing radiation dose during dental CT, Rustemeyer et al.(2004) compared two dose protocols using the Siemens Somatom Plus 4 scanner. A corpse was used to collect scans of the mandible. The first (standard) protocol had a tube current of 165 mA, a rotation time of 1s and a 1mm pitch. The second protocol, developed in a previous study by Rustemeyer et al., in 1999, had a tube current of 50 mA, rotation time of 0.7 s, and a 2 mm pitch. Radiation dose was detected by use of the Alderson-Rando Phantom with lithium fluoride thermoluminescent dosimeters rods. Eight radiologists were blinded and asked to evaluate the images independently by use of a six point rank scale. They were asked to judge differentiation of the lower jaw cortical bone, general picture quality, and visibility of bone and soft tissue structures. As well, measurements of the height and width of the lower jaw were made in eight definite positions for both dosing protocols. These measurements were compared with measurements taken

directly from the cadaver. The comparison of protocols between judges showed no difference in contrast and visibility of the cortical boundary, bony structures, differentiation of soft tissue or image quality, and no significant difference in measurements were found in the diameter alveolar canal or heights and widths of the ridges. Quantum mottle was more visible in the images acquired using the low dose protocol, but did not make a significant difference in image quality. The dose in the standard protocol was nine times greater than that in the low dose protocol. Hence the authors were able to conclude that the low dose protocol allowed a reduction of dose by a factor of nine without loss of picture quality.

Bianchi et al. (2005) subjectively evaluated and quantitatively measured image quality of low dose dental CT to investigate changes in image quality in relation to scan parameters that affect dose. In dental CT the structures of interest are high contrast objects, namely teeth and bone. Generally, high contrast structures are more easily visualized in CT radiography and require a lower dose to be visualized. The CT scans were performed using a multislice CT (General Electric Lightspeed 16Pro)

and images of two phantoms were captured. A geometric phantom (Catphan 500) and an anatomical phantom (mandibular tract inserted in a geometrical water phantom) were used to test image quality. Many acquisition protocols were tested by changing different parameters; tube currents ranged from 10 to 160 mA, pitch factors ranged from 0.562 to 1.75, and a tube potential of 120 kVp was kept constant. Subjective image quality was evaluated by six judges, a radiologist and residents in radiology and in maxillofacial surgery. The judges were asked to rank the images using a five point Likert scale ranging from insufficient to good. Image quality was evaluated based on three anatomical structures, the spongy bone, the mandibular canal and the alveolar crest edge. The judges showed a high level of interobserver reliability (kappa = 0.82). Quantitative evaluation of image quality was measured using spatial resolution, noise and contrast to noise ratio (CNR). The results of the study showed that the relationship between dose and noise followed an antilogarithmic pattern. In general, low mA images had considerable image noise compared to high mA images. As well, holding mA constant, high pitch values gave images with more noise than low pitch values.

The relationship of contrast to noise ratio to dose showed a logarithmic pattern with CNR rising with increased tube current. With tube current held constant, images with greater pitch (i.e., noise) showed a lower CNR value. The quantitative measures were only reported and not tested statistically. There was no statistical difference between image quality scores for images captured at 40 mA or higher for the three anatomical areas chosen and for all pitch levels. Tube current was held constant at 40 mA to evaluate the effect of pitch level on image quality score. Significant differences detected were when a pitch of 0.562 (lowest pitch value) was compared to pitches higher than 0.938 only when evaluating the image quality score of spongy bone. There were no significant differences between image quality scores with varying pitches for the other two anatomical areas. The authors concluded that the changing from the standard CT protocol (120 mA, pitch 0.5) to a low dose protocol (40 mA, pitch 1.75) could allow a possible dose reduction of 90% before a difference in image quality could be detected.

STATEMENT OF HYPOTHESIS

The purpose of this study is to describe differences in image quality for cone beam computed tomographic images acquired using the Hitachi CB MercuRay™. It is hypothesized that there is no difference in image quality between cone beam computed tomographic images captured using different settings, including milliamperage (mA), kilovolt peak (kVp), and presence or absence of a copper filter. If rejected, there would be a difference in the image quality of images captured at different operator settings. It is also hypothesized that images captured at lower settings will not be diagnostic. If rejected, the images captured at lower settings will be considered diagnostic.

IMAGE QUALITY PRODUCED BY DIFFERENT CBCT SETTINGS

Authors: Jeffrey Kwong D.D.S.[1]

J. Martin Palomo D.D.S., M.S.D.[2]

Michael A. Landers D.D.S, M.A.[3]

Alex Figueroa[4]

Mark G. Hans D.D.S. M.S.D.[5]

1. Resident, Department of Orthodontics at Case School of Dental Medicine in Cleveland, OH
2. Associate Professor, Department of Orthodontics at Case School of Dental Medicine in Cleveland, OH
3. Associate Professor, Department of Oral Diagnosis and Radiology at Case School of Dental Medicine in Cleveland, OH
4. Dental Student, Case School of Dental Medicine in Cleveland, OH
5. Professor and Chairman, Department of Orthodontics at Case School of Dental Medicine in Cleveland, OH

Corresponding Author:

J. Martin Palomo, D.D.S., M.S.D.
Case Western Reserve University
School of Dental Medicine
Department of Orthodontics
10900 Euclid Ave.
Cleveland, OH 44106

American Journal of Orthodontics & Dentofacial Orthopedics
Manuscript Draft

Title: Image quality produced by different CBCT settings

Article Type: Original article

Keywords: Cone beam computed tomography, image quality, diagnostic quality, mA, kVp, copper filter, Hitachi CB MercuRay™

Objectives: To evaluate image quality produced by different CBCT settings for three fields of view. **Methods:** A Hitachi CB MercuRay™ was modified to allow different setting combinations. The variables consisted of 4 different mA (2, 5, 10, and 15), 2 kVp (100, and 120), presence or not of a copper filter, and 3 fields of view (6", 9", and 12"). Thirty-two scans were taken on a cadaver head and 16 scans on a skull. The groups were divided by field of view and images were ranked by at least 30 judges. Diagnostic quality was addressed in a questionnaire. Descriptive statistics and rankings were calculated using Excel 2003, and Friedman's and Wilcoxon Ranked Sign Tests using SPSS 14.0.1. **Results:** Changing the filter setting showed significant differences ($p < 0.006$) in two pairs of the 9". Variation in kVp showed significant differences ($p < 0.006$) in the 6" 5 mA images with filter. Altering mA settings showed significant differences ($p < 0.008$) in the 6" and 12" groups. The 9" group showed significant differences between 2 mA and 10/15 mA. Overall, the 6", 9" and 12" images demonstrated diagnostic quality 56%, 99% and 99% of the time, respectively. **Conclusions:** Filter and kVp did not affect overall image quality. Images taken at lower mA settings showed good diagnostic quality.

INTRODUCTION

Cone beam computed tomography (CBCT) has been utilized for its capability of providing reliable information compared to conventional methods[1]. CBCT provides excellent tissue contrast, eliminates blurring and overlapping of adjacent teeth and offers orthogonal views eliminating projection effects[2]. Additional advantages of CBCT include reduced cost and significantly reduced radiation exposure relative to medical CT.

Although cone beam technology can produce volumetric images with up to four times less radiation than a conventional CT, the resulting effective radiation is dependent on the settings used; namely kilovoltage peak (kVp) and milliamperage (mA)[3,4]. The ADA Council on Scientific Affairs recommends the use of techniques that would reduce the amount of radiation received during dental radiography. Known as the "As Low As Reasonably Achievable" or ALARA, principle, this includes taking radiographs based on the patient's needs (as determined by an examination), using the fastest film compatible with the diagnostic task, collimating the beam to a size as close to that of the film as feasible and using lead aprons and thyroid shields. An accepted ratio between exposure and image quality needs to be reached in order to use this principle.

Image quality in traditional radiography has been defined by Curry as "the ability to record each point in the object as a point on the film"[5]. The definition of image quality for CT images is not as accurately defined but has been described as the visibility of diagnostically important structures in the CT image. The quality of CBCT images has yet to be evaluated, however, the quality of CT images has been evaluated. Previous studies have shown that lower settings in medical-grade CT units can achieve image

quality comparable to higher settings [6,7,8,9,10]. Sohaib et al. evaluated the quality of maxillary sinus CT images in forty patients holding kVp constant and varying mA. Although judges noticed an increase in graininess, they found no significant differences in image quality between high and low settings groups[6]. Two studies have evaluated the image quality of intracranial scans. Cohnen et al. evaluated image quality with many combinations of mA and kVp settings, and Gündogdu et al. evaluated the quality of 240 images holding kVp constant and varying mA[7,8]. Both studies showed that scans taken at higher settings showed similar image quality, while scans at lower settings showed unacceptable image quality. Two studies using dental CT have evaluated image quality in CT scans of the mandible. Rustemeyer et al. evaluated the quality of 16 images holding kVp constant while varying mA and found no significant differences in the visibility of mandibular structures[9]. Bianchi et al. evaluated 28 images holding kVp constant while changing mA and found that images captured at low settings were significantly different than those captured at mid to high settings[10]. The literature revealed the following: there is no single way to analyze image quality, more than one setting was rarely isolated to study the effects of different, and rarely was a reliability analysis included.

This descriptive study seeks to compare the quality of images captured using the CB MercuRay CBCT (Hitachi Medical Systems – Tokyo, Japan) unit. For the purpose of this study, we have defined image quality as the ability of the image to answer our diagnostic questions. Multiple CBCT images of a cadaver head and skull were captured at different operator settings. The images were divided into three groups based on the

field of view (FOV, 6", 9" and 12") and used in a subjective test of image quality. The object of this study is to evaluate image quality for different CBCT settings for three fields of view. The null hypothesis is that no difference in image quality exists within each field of view, and should a difference exist, it would make no difference on the diagnostic ability of the images.

MATERIALS AND METHODS

The Case Western Reserve University Institutional Review Board (IRB) approved the experimental protocol. The CB MercuRay CBCT has user controlled variables that may affect image quality. These settings include mA, kVp, field of view, hardware filter, and reconstruction algorithm (see Table 1). By varying the mA, kVp, presence or absence of a filter and FOV, a total of 48 images were captured. Thirty two images of a fresh human cadaver head and 16 images of a dry skull were captured. A fresh cadaver head was chosen since it is the closest possible subject to a live human and to exhibit image quality for a subject with dental work. Images of the cadaver head were captured in the 6" and 12" FOV. The skull was chosen to demonstrate what images might look like in an ideal situation. Images of the skull were captured in the 9" FOV. The cadaver head was not used for the 9" FOV because the condyles and dentition could not be imaged simultaneously.

The selection criteria for the cadaver head were as follows: 1) no chemical preservation to maintain the integrity of the soft tissue, 2) majority of natural teeth present and 3) minimal number of full coverage restorations. The skull was selected



from the Hamann-Todd collection based on 1) having majority of the dentition present, 2) no restorations, and 3) the presence of undamaged condyles.

Cadavers were screened by the co-investigator (JK) and a minimal oral exam was completed. When the inclusion criteria were satisfied, the head was acquired with the goal of reproducing a natural head position. A scout image was taken to validate the findings of the oral examination. The cadaver head was stored in a cold room at a temperature of approximately 32°F between periods of image acquisition. The positions of the cadaver head and skull were standardized using cross-hair projections from the CB MercuRay^{TM} in the frontal and lateral positions. All images were captured within a 1 week period to prevent any cadaver deterioration.

The CB Works 2.0 software (Cybermed Inc - Seoul, Korea) was used in conjunction with the CB MercuRay^{TM} to reconstruct and segment the volumes. The images were segmented by the co-investigator after standardizing the window levels and widths. Three groups of sixteen images were made based on the FOV. Specific images were made to represent each FOV based on the manufacturer recommended settings. The 6" FOV was designed to capture only the dentition and the images taken in this FOV were made to resemble a bitewing radiograph. The 9" FOV was designed to capture the dentition and condyles and were made to resemble a panoramic radiograph. The 12" FOV was designed to capture the entire face and images taken and were made to resemble lateral cephalograms. Each image was identified by a serial number that consisted of mA, kVp, FOV and filter settings respectively.

All images were printed on glossy photo paper for ease of simultaneous viewing. The 12" images were printed directly from CB Works using a Codonics Horizon printer (Codonics inc - Middleburg Heights, OH). The 6 and 9" images were exported from CB Works, converted to 16-bit grayscale .tiff images using Adobe Photoshop CS2 (Adobe Systems inc – San Jose, CA) and printed using an Epson Stylus Photo R300 printer (Epson America Inc – Long Beach, CA), with Epson premium glossy photo paper and ink.. Serial numbers were coded and labeled on the backs of the images so that judges were unaware of the settings used to acquire the images.

The judges were chosen from faculty and residents at Case Western Reserve School of Dental Medicine and were selected based on the following criteria: 1) experience viewing the images and 2) absence of visual impairment. The judges were asked only to examine images they use on a daily basis. The lateral cephalograms were viewed only by orthodontists and oral surgeons, the panoramic views were viewed by orthodontists, oral surgeons and general clinicians, and the bite wings were only viewed by general clinicians. An experienced oral maxillofacial radiologist judged all three groups of images. Each of the three groups of images was evaluated by at least 30 judges. The evaluators were asked to rank the images from best to worst overall image quality using a technique called 'Q-sorting'[11]. Each image in the set was assigned a rank from 1 through 16, where 1 represented the image of best quality and 16 the image of poorest quality. The ranks were recorded by the co-investigator and a research assistant while the clinician filled out a short survey.

The survey addressed the inclusion criteria, as well as the diagnostic quality of each image. Specifically, the clinician was asked whether each image (in the order it was ranked) was of diagnostic quality. For the bitewing images, the clinicians were asked if the images were of diagnostic quality to be used an adjunct to make a periodontal diagnosis (i.e. were the bone levels and structures of the periodontium adequately visible). For the panoramic images, the clinicians were asked if the images were of diagnostic quality for a general screening (i.e. was the image of diagnostic quality to view bone levels, frank caries, condyles, sinuses, trabeculation and pathology). For the lateral cephalogram images, the clinicians were asked if the images were of diagnostic quality to make an orthodontic diagnosis (i.e. was the image of diagnostic quality to view the relative positions of the jaws to the cranial base, and teeth in relation to their respective jaws).

The rank and diagnosis data were transferred by the co-investigator (JK) to a Microsoft Excel 2003 (Microsoft Co. – Redmond, WA) spreadsheet. To minimize skewing, the ranks were recoded from 1 through 16, to a scale from +8 through -8 (excluding zero), respectively.

DATA ANALYSIS AND STATISTICAL METHODS

Descriptive statistics were used to depict the clinicians' image preferences and calculated (see tables 2, 3, and 4). The data was transferred into SPSS 14.0 (: SPSS Inc - Chicago, IL) for further analysis to compare the effect of the filter, kVp, and mA settings. To test for the effect of a specific setting, other settings were held constant and the mean ranks of images were compared. The Friedman test was used to test image quality

differences in groups of images larger than two, while the Wilcoxon Signed Ranks tests were used for pair wise comparisons. The alpha value was set at 0.05 and Bonferroni correction was applied for multiple comparisons. The data for diagnostic quality was recorded as the percentage of clinicians who felt the image was of diagnostic quality.

RELIABILITY

A reliability study was conducted one month after the first sitting, and ten clinicians per group were randomly chosen to repeat the Q-sort and diagnosis survey. The intra-rater reliability was tested using Kendall's value of concordance (W) which is applicable to rank ordinal data. Kendall's coefficient of concordance ranges from 0 (no concordance) to 1 and can be converted to a spearman correlation.

RESULTS

Six inch Images

The 6" bitewing images were rated by 37 judges; three of which were excluded for visual acuity problems. The 15 mA images were ranked the highest followed by the 10 mA, 5 mA, and 2 mA images. The image of best quality had a mean score of 4.12 with a standard deviation of 3.08 (see figure 1), and the image of poorest quality had a mean score -5.97 with a standard deviation of 2.71 (see figure 2). The maximum and minimum ranks for each image showed a variation in ranking between judges, and the largest variation showed a range of +8 to -8. The lowest diagnostic quality image (2 mA, 120 kVp with the filter) was considered diagnostic 32% of the time. The most diagnostic quality image (15 mA, 100 kVp without a filter) was considered diagnostic 88% of the time.

Nine inch Images

The 9" panoramic images were judged by 34 clinicians; three of which were excluded for visual acuity problems, and one for the inability to detect a difference between the images. The image captured at 5 mA, 120 kVp with a filter was rated as the best image. However, 15 mA were generally most preferred, while the 2 mA films were least favored. The image of best quality had a mean score of 2.77 with a standard deviation of 4.95 (see figure 3), while the image of poorest quality had a mean score -3.87 with a standard deviation of 4.61 (see figure 4). The maximum and minimum ranks for each image showed a variation in ranking and ten images showed a range of +8 to -8. The two images rated least diagnostic were deemed diagnostic 87% of the time. The most diagnostic image (15 mA, 120 kVp with the filter) was considered diagnostic 100% of the time.

Twelve inch Images

The 12" images were examined by 30 clinicians. The 10 mA images were most preferred followed by the 15 mA, 5 mA, and 2 mA images. The image of best quality had a mean rank of 2.63 and standard deviation of 5.20 (see figure 5), while the image of poorest quality had a mean rank of -3.53 and standard deviation of 3.46 (see figure 6). The standard deviations were fairly high and consistent between the 16 images; while the mean image quality scores were low. There was a sizeable amount of variation in ranking between judges, and the largest variation showed a range of +8 to -8. The least diagnostic image (15 mA, 120 kVp without filter) was considered diagnostic 93% of the

time. Twelve images were rated as the most diagnostic and were rated as diagnostic 100% of the time.

The Effect of the Filter

When isolating the presence and absence of a filter, significant differences were found ($p < 0.006$) only in the 9" FOV (see table 5). When significant differences were detected, images captured with the presence of the filter were preferred. Overall, the presence of the copper filter did not affect the quality of CBCT images.

The Effect of kVp

When kVp was varied, a single significant difference ($p < 0.006$) was found in the 6" FOV (see table 6). In general, the quality of images captured at 100 kVp was no different than images captured at 120 kVp.

The Effect of mA

For the 6" images, the effect of varying mA showed significant differences ($p < 0.05$) in the following subgroups of images: 100 kVp without filter, 100 kVp with filter, 120 kVp with filter and 120 kVp without filter. Further tests within each group showed significant differences ($p < 0.008$) in each subgroup (see table 7). For the 9" images, the variation of mA showed significant differences in image quality ($p < 0.05$) in the following groups of images: 100 kVp without filter and 120 kVp with filter. Further tests showed significant differences ($p < 0.008$) in the 100 kVp without filter group (see table 8). For the 12" images, the change in mA settings showed significant differences ($p < 0.05$) in the following subgroups of images: 100 kVp without filter, 100 kVp with filter, 120 kVp with filter and 120 kVp without filter. Further tests showed significant

differences ($p < 0.008$) in each of the subgroups (see table 9). When a significant difference was detected, the image captured at the higher mA setting was always preferred.

Reliability

Kendall's coefficient of concordance (W) was calculated and averaged across the ten judges. The average W value was 0.888, 0.567 and 0.653 for the 6", 9", and 12" rankings, respectively. The coefficients of concordance were converted to spearman correlations of 0.78, 0.13 and 0.31 respectively for the 6", 9" and 12" groups. The judges showed a high level of agreement between the two time points when ranking the 6" images. On the other hand, the judges showed a low level of agreement between the two time points when ranking the 9" and 12" images.

DISCUSSION

Image quality is essentially a descriptor of the subjective interpretation of visual data and hence cannot have a simple analytical definition. The quality of an image can only be related to a specific medical task and the image should convey enough information to allow a medical decision to be made with an acceptable degree of certainty.

Previous studies have shown that low settings used in medical CT machines can achieve comparable image quality in medical head and neck imaging to higher settings[6,7,8]. Other studies comparing dental CT images also showed that low settings can produce images without loss of quality[9,10]. Our study suggests that depending on the

FOV, CBCT images captured at lower settings are comparable to those captured at higher settings while maintaining adequate diagnostic image quality.

Differences in image quality were detected in the 6" group when the mA setting was varied. The 6" FOV has the smallest voxel size and the highest resolution. However, high resolution does not necessarily imply high image quality. Voxel size, mA and image quality are intimately related. The mA setting controls the number of photons released by the x-ray tube, and subsequently the number of photons that reach the detector voxels. If the number of photons released is held constant (by holding the mA setting and capture time constant), and the size of the voxel on the detector is changed, the number of photons that strike each voxel will change (see figure 7). In this case, smaller voxels are struck by fewer photons, while larger voxels are struck by more photons. When more photons strike each voxel, more information is generated for each voxel, thus contributing to a difference in image quality[5]. This difference in image quality may lead to a blurry or grainy image. When voxel size is decreased more photons are required increase the photon per voxel count if the image quality is to remain the same. For the purposes of our study, images within each FOV were compared. The comparison of image quality between FOVs was not a focus of our study.

Within the 9" group, variation of mA did not have a great effect on image quality. Few significant differences were detected, and the standard deviations and range in the maximum and minimum rankings suggest that the differences are not clinically significant. The 6" images were constructed in a similar manner yet showed considerable differences, suggesting that the presence of soft tissue may play a role in the image

quality. Theoretically, the skull is more likely to produce a consistent image because only high density structures are present. The lack of soft tissue leads to less attenuation of the x-ray photons by objects such as the soft tissue. CBCT produces higher amounts of scattered radiation, thus negatively affecting image quality[12]. Scattered radiation affects structures of low density; and hence was not a factor in the case of the skull.

The 12" group showed significant image quality differences when the mA was varied. The overall ranks showed that all 10 mA images were ranked greater than the 15 mA images. After reviewing matched 10 and 15 mA images, their histograms revealed a minor shift towards the right from 10 mA to 15 mA. This suggests not only that the judges preferred images of less darkness, but that a small change in density was visually detectable. Although there was considerable variation in the ranking as shown by the maximum and minimum rankings, the judges considered the diagnostic quality of all images very high; implying that a clinically significant difference between the images may not exist.

Few significant differences were found as a result of varying kVp. In all radiographic imaging, increasing the kVp increases the average photon energy and decreases the grayscale resolution. Siegel et al. found that in pediatric CT imaging, a decrease in tube voltage from 140 to 80 kVp resulted in a decrease in image quality[13]. A direct comparison to our study cannot be drawn for a few reasons: 1) Siegel et al. measured image quality based on the evaluation of grayscale resolution and 2) a reduction in tube current of 60 kVp is not equivalent to a reduction of 20 kVp. CBCT

image quality with the Hitachi CB MercuRay can be maintained when tube current is reduced from 120 to 100 kVp.

The copper filter only affected image quality in the 6" images. The copper filter altered the beam quality by removing low energy photons from the x-ray beam[14]. Low energy photons do not penetrate the subject and tend to be absorbed by the patient/subject. Gonçalves et al. studied the effect of copper aluminum alloy and aluminum filters and found no difference in plain film image quality[15]. Although our study cannot be directly compared to Gonçalves et al., our results agree that the addition of a copper filter did not affect the overall image quality of the Hitachi CB MercuRay.

Although the examiners were not calibrated there was a good level of agreement between two time points when evaluating the 6" images. This suggests that the examiners agreed where image quality differed. The 9 and 12" images showed a low level of agreement. Although differences in image quality existed, it was difficult for clinicians to agree where the where differences existed.

For the diagnosis data, at the first time point 56%, 99% and 99% of the judges felt that the 6", 9" and 12" images were diagnostic, respectively. At the second time point, 86%, 96% and 100% of the clinicians graded the 6", 9" and 12" images as diagnostic time, respectively. The variation between the two time points for the 6" images suggests that the judges may have become more comfortable with the images, or that they were more lenient with their grading. The variation in diagnostic quality also suggests that that image quality could be improved for the 6" images.

Our study highlighted the difficulties in defining and quantifying clinical image quality. The judges commented that image scoring was difficult in the 9 and 12" groups, despite efforts to be as consistent as possible. A limitation in our study was that the ranking system did not allow two images to be ranked the same. It is possible that image quality differences did not exist between images. Another limitation is that our study evaluates only two dimensional images reconstructed from a 3D volume. We chose to use the 2D images as a tool for image quality evaluation because clinicians are familiar with 2D images. It is the opinion of the authors that the use of this new technology to produce familiar images may limit the usefulness of the 3D data for diagnosis. The key issue in terms of image quality is whether an image enables an appropriate diagnosis to be made. To answer diagnostic questions appropriately, the proper images need to be segmented.

CONCLUSION

Our results indicate that it is possible to lower the CBCT settings in the CB MercuRay and maintain diagnostic quality. To minimize the dose to the patient, images should be captured using 100 kVp, and in the presence of a copper filter. The choice for mA setting depends on the field of view chosen. Many significant differences were detected for the 6" FOV. Overall, the 5 mA and 10 mA views were considered diagnostic for periodontal structures, 68% and 78% of the time, respectively. Before choosing between the 5 mA and 10 mA views, the clinician should consider that images acquired with lower mA settings were generally less preferred. Our study suggests that although statistically significant differences in image quality were detected in the 9" and

12" images, clinically significant differences do not exist in the diagnostic quality. To minimize radiation dose to the patient, the 2 mA images should be sufficient for the 9" and 12" images. For a good balance between the ALARA principle and the image quality needed, it seems that the ability to select different mA settings could be helpful. As a final thought, the clinician should consider that "image quality requirements vary for different types of examination or even different tasks within single examinations"[16].

Table 1.—Hitachi CB MercuRay™ Operator Settings

Field of View	**6”**		**9”**	**12”**
Milliamperage	**2 mA**	**5 mA**	**10 mA**	**15 mA**
Kilovolt peak	**100 kVp**		**120 kVp**	
Hardware filter – copper filter	**Filter present**		**Filter absent**	
Reconstruction algorithm	**Soft***		**Hard**	

*Held constant for all images captured

Table 2.—Ranks for Six inch Images (Bitewing)

6 inch Image Settings	15 [a] 100 [b] 06Y [c]	15 120 06Y	15 100 06N	10 100 06Y	10 120 06Y	05 120 06Y	05 120 06N	10 120 06N	15 120 06N	10 100 06N	05 100 06N	05 100 06Y	02 120 06N	02 100 06N	02 120 06Y	02 100 06Y
Overall Rank	1	2	3	4	5	6	7	8	9	10	11	12	13	14	15	16
Mean Rank	4.12	3.74	3.50	3.38	2.53	2.21	2.00	1.56	1.24	0.41	-1.09	-1.59	-4.62	-5.62	-5.79	-5.97
SD	3.08	3.59	4.73	3.47	3.65	4.18	3.98	4.20	4.09	4.62	3.43	3.20	2.81	3.35	2.61	2.71
Median	5	4.5	5	3	3	2.5	3	2	2	1	-2	-3	-5	-7	-6	-7
Max	8	8	8	8	8	8	8	8	8	8	8	6	2	6	6	3
Min	-4	-4	-8	-2	-6	-5	-5	-7	-8	-8	-8	-7	-8	-8	-8	-8
% Diagnostic	82	76	88	82	71	74	76	79	85	79	62	59	41	38	32	38

[a] mA value (02, 05, 10 or 15 mA)

[b] kVp value (100 or 120 kVp)

[c] presence or absence of copper filter (N or Y)

Table 3.—Ranks for Nine inch Images (Panoramic)

9 inch Image Settings	05 [a] 120 [b] 09Y [c]	15 120 09Y	15 100 09N	15 120 09N	15 100 09Y	10 120 09N	05 100 09Y	02 100 09Y	10 100 09N	10 120 09Y	02 120 09Y	05 100 09N	10 100 09Y	05 120 09N	02 120 09N	02 100 09N
Overall Rank	1	2	3	4	5	6	7	8	9	10	11	12	13	14	15	16
Mean Rank	2.77	2.20	0.90	0.80	0.77	0.73	0.67	0.53	0.50	0.43	-0.63	-1.20	-1.33	-1.50	-1.77	-3.87
SD	4.95	4.53	5.66	4.95	4.82	4.53	4.72	4.45	5.59	4.21	5.31	5.55	5.08	4.87	3.78	4.61
Median	4.5	3	1.5	2	1	1.5	0.5	1	0.5	1.5	-2.5	-3	-1.5	-2.5	-1.5	-6
Max	8	8	8	8	8	7	8	8	8	6	8	8	7	8	4	8
Min	-7	-8	-8	-8	-7	-7	-8	-8	-8	-7	-8	-8	-8	-8	-7	-8
% Diagnostic	93	93	97	100	87	93	93	93	90	97	93	87	90	93	93	90

[a] mA value (02, 05, 10 or 15 mA)

[b] kVp value (100 or 120 kVp)

[c] presence or absence of copper filter (N or Y)

Table 4.—Ranks for Twelve inch Images (Lateral Cephalograms)

12 inch Image Settings	10 [a] 100 [b] 12N [c]	10 100 12Y	10 120 12Y	10 120 12N	15 100 12N	15 120 12N	15 100 12Y	05 100 12N	15 120 12Y	05 120 12N	05 100 12Y	02 120 12N	05 120 12Y	02 100 12N	02 120 12Y	02 100 12Y
Overall Rank	1	2	3	4	5	6	7	8	9	10	11	12	13	14	15	16
Mean Rank	2.63	2.47	2.00	1.97	1.83	1.80	1.63	0.87	0.10	-0.47	-0.83	-1.57	-2.77	-3.00	-3.13	-3.53
SD	5.20	4.01	3.60	4.92	5.87	5.55	4.13	3.76	4.84	4.23	4.95	4.76	4.04	5.38	4.87	3.46
Median	3.5	3	2	3	4	3	2	1	0	-1	-2	-3	-4	-5	-5	-4.5
Max	8	8	8	8	8	8	7	8	8	7	7	6	7	6	8	5
Min	-8	-7	-6	-7	-8	-8	-5	-6	-8	-7	-8	-8	-8	-8	-8	-8
% Diagnostic	100	100	100	100	100	93	100	100	100	100	100	100	97	100	97	97

[a] mA value (02, 05, 10 or 15 mA)

[b] kVp value (100 or 120 kVp)

[c] presence or absence of copper filter (N or Y)

Table 5.--The Effect of Filter vs. No Filter on Image Quality. The mean rank (μ) and standard deviations were compared for images taken with a filter and without a filter.

			Filter No	Filter Yes	
FOV	mA	kVp	μ ± S.D.	μ ± S.D.	P-value[a]
6	2	100	-5.62 ± 3.35	-5.97 ± 2.71	0.523
		120	-4.62 ± 2.81	-5.79 ± 2.61	0.034
	5	100	-1.09 ± 3.43	-1.59 ± 3.20	0.655
		120	2.00 ± 3.98	2.21 ± 4.18	0.797
	10	100	0.41 ± 4.62	3.38 ± 3.47	0.012
		120	1.56 ± 4.20	2.53 ± 3.65	0.333
	15	100	3.50 ± 4.73	4.12 ± 3.08	0.637
		120	1.24 ± 4.09	3.74 ± 3.59	0.015
9	2	100	-3.87 ± 4.61	0.53 ± 4.45	0.006 †
		120	-1.77 ± 3.78	-0.63 ± 5.31	0.393
	5	100	-1.20 ± 5.55	0.67 ± 4.72	0.240
		120	-1.50 ± 4.87	2.77 ± 4.95	0.004 †
	10	100	0.50 ± 5.59	-1.33 ± 5.08	0.187
		120	0.73 ± 4.53	0.43 ± 4.21	0.918
	15	100	0.90 ± 5.66	0.77 ± 4.82	0.861
		120	0.80 ± 4.95	2.20 ± 4.53	0.257
12	2	100	-3.00 ± 5.38	-3.53 ± 3.46	0.861
		120	-1.57 ± 4.76	-3.13 ± 4.87	0.216
	5	100	0.87 ± 3.76	-0.83 ± 4.95	0.103
		120	-0.47 ± 4.23	-2.77 ± 4.04	0.071
	10	100	2.63 ± 5.20	2.47 ± 4.01	0.749
		120	1.97 ± 4.92	2.00 ± 3.60	0.984
	15	100	1.83 ± 5.87	1.63 ± 4.13	0.734
		120	1.80 ± 5.55	0.10 ± 4.84	0.110

[a] Based on Wilcoxon Ranked Sign Test, † $p < 0.006$ after Bonferroni correction

Table 6.--The Effect of 100 vs. 120 kVp on Image Quality. The mean rank (μ) and standard deviations were compared for images taken with at 100 kVp and 120 kVp.

			100 kVp	120 kVp	
FOV	mA	Filter	μ ± S.D.	μ ± S.D.	P-value[a]
6	2	N	-5.62 ± 3.35	-4.62 ± 2.81	0.126
		Y	-5.97 ± 2.71	-5.79 ± 2.61	0.556
	5	N	-1.09 ± 3.43	2.00 ± 3.98	0.007
		Y	-1.59 ± 3.20	2.21 ± 4.18	0.001 †
	10	N	0.41 ± 4.62	1.56 ± 4.20	0.461
		Y	3.38 ± 3.47	2.53 ± 3.65	0.337
	15	N	3.50 ± 4.73	1.24 ± 4.09	0.012
		Y	4.12 ± 3.08	3.74 ± 3.59	0.292
9	2	N	-3.87 ± 4.61	-1.77 ± 3.78	0.059
		Y	0.53 ± 4.45	-0.63 ± 5.31	0.398
	5	N	-1.20 ± 5.55	-1.50 ± 4.87	0.967
		Y	0.67 ± 4.72	2.77 ± 4.95	0.147
	10	N	0.50 ± 5.59	0.73 ± 4.53	0.805
		Y	-1.33 ± 5.08	0.43 ± 4.21	0.101
	15	N	0.90 ± 5.66	0.80 ± 4.95	0.967
		Y	0.77 ± 4.82	2.20 ± 4.53	0.180
12	2	N	-3.00 ± 5.38	-1.57 ± 4.76	0.177
		Y	-3.53 ± 3.46	-3.13 ± 4.87	0.893
	5	N	0.87 ± 3.76	-0.47 ± 4.23	0.317
		Y	-0.83 ± 4.95	-2.77 ± 4.04	0.181
	10	N	2.63 ± 5.20	1.97 ± 4.92	0.523
		Y	2.47 ± 4.01	2.00 ± 3.60	0.509
	15	N	1.83 ± 5.87	1.80 ± 5.55	0.789
		Y	1.63 ± 4.13	0.10 ± 4.84	0.232

[a] Based on Wilcoxon Ranked Sign Test, † $p < 0.006$ after Bonferroni correction

Table 7.--The Effect of Varying mA on Image Quality for 6" FOV. The mean rank (μ) and standard deviations were compared for images taken at different mA values.

kVp	Filter	mA_1	$\mu_1 \pm$ S.D.	mA_2	$\mu_2 \pm$ S.D.	p-Value[a]
100	No	2	-5.62 ± 3.35	5	-1.09 ± 3.43	0.000 †
			-5.62 ± 3.35	10	0.41 ± 4.62	0.000 †
			-5.62 ± 3.35	15	3.50 ± 4.73	0.000 †
		5	-1.09 ± 3.43	10	0.41 ± 4.62	0.187
			-1.09 ± 3.43	15	3.50 ± 4.73	0.000 †
		10	0.41 ± 4.62	15	3.50 ± 4.73	0.002 †
	Yes	2	-5.97 ± 2.71	5	-1.59 ± 3.20	0.000 †
			-5.97 ± 2.71	10	3.38 ± 3.47	0.000 †
			-5.97 ± 2.71	15	4.12 ± 3.08	0.000 †
		5	-1.59 ± 3.20	10	3.38 ± 3.47	0.000 †
			-1.59 ± 3.20	15	4.12 ± 3.08	0.000 †
		10	3.38 ± 3.47	15	4.12 ± 3.08	0.296
120	No	2	-4.62 ± 2.81	5	2.00 ± 3.98	0.000 †
			-4.62 ± 2.81	10	1.56 ± 4.20	0.000 †
			-4.62 ± 2.81	15	1.24 ± 4.09	0.000 †
		5	2.00 ± 3.98	10	1.56 ± 4.20	0.625
			2.00 ± 3.98	15	1.24 ± 4.09	0.532
		10	1.56 ± 4.20	15	1.24 ± 4.09	0.790
	Yes	2	-5.79 ± 2.61	5	2.21 ± 4.18	0.000 †
			-5.79 ± 2.61	10	2.53 ± 3.65	0.000 †
			-5.79 ± 2.61	15	3.74 ± 3.59	0.000 †
		5	2.21 ± 4.18	10	2.53 ± 3.65	0.560
			2.21 ± 4.18	15	3.74 ± 3.59	0.155
		10	2.53 ± 3.65	15	3.74 ± 3.59	0.050

[a] Based on Wilcoxon Ranked Sign Test, † $p < 0.008$ after Bonferroni correction

Table 8.--The Effect of Varying mA on Image Quality for 9" FOV. The mean rank (μ) and standard deviations were compared for images taken at different mA values.

kVp	Filter	mA_1	$\mu_1 \pm$ S.D.	mA_2	$\mu_2 \pm$ S.D.	p-Value[a]
100	No	2	-3.87 ± 4.61	5	-1.20 ± 5.55	0.082
			-3.87 ± 4.61	10	0.50 ± 5.59	0.005 †
			-3.87 ± 4.61	15	0.90 ± 5.66	0.005 †
		5	-1.20 ± 5.55	10	0.50 ± 5.59	0.376
			-1.20 ± 5.55	15	0.90 ± 5.66	0.144
		10	0.50 ± 5.59	15	0.90 ± 5.66	0.781
	Yes	2	0.53 ± 4.45	5	0.67 ± 4.72	n/a
			0.53 ± 4.45	10	-1.33 ± 5.08	n/a
			0.53 ± 4.45	15	0.77 ± 4.82	n/a
		5	0.67 ± 4.72	10	-1.33 ± 5.08	n/a
			0.67 ± 4.72	15	0.77 ± 4.82	n/a
		10	-1.33 ± 5.08	15	0.77 ± 4.82	n/a
120	No	2	-1.77 ± 3.78	5	-1.50 ± 4.87	n/a
			-1.77 ± 3.78	10	0.73 ± 4.53	n/a
			-1.77 ± 3.78	15	0.80 ± 4.95	n/a
		5	-1.50 ± 4.87	10	0.73 ± 4.53	n/a
			-1.50 ± 4.87	15	0.80 ± 4.95	n/a
		10	0.73 ± 4.53	15	0.80 ± 4.95	n/a
	Yes	2	-0.63 ± 5.31	5	2.77 ± 4.95	0.016
			-0.63 ± 5.31	10	0.43 ± 4.21	0.422
			-0.63 ± 5.31	15	2.20 ± 4.53	0.032
		5	2.77 ± 4.95	10	0.43 ± 4.21	0.059
			2.77 ± 4.95	15	2.20 ± 4.53	0.483
		10	0.43 ± 4.21	15	2.20 ± 4.53	0.095

[a] Based on Wilcoxon Ranked Sign Test, † $p < 0.008$ after Bonferroni correction

Table 9.--The Effect of Varying mA on Image Quality for 12" FOV. The mean rank (μ) and standard deviations were compared for images taken at different mA values.

kVp	Filter	mA_1	$\mu_1 \pm$ S.D.	mA_2	$\mu_2 \pm$ S.D.	p-Value[a]
100	No	2	-3.00 ± 5.38	5	0.87 ± 3.76	0.007†
			-3.00 ± 5.38	10	2.63 ± 5.20	0.002†
			-3.00 ± 5.38	15	1.83 ± 5.87	0.003†
		5	0.87 ± 3.76	10	2.63 ± 5.20	0.073
			0.87 ± 3.76	15	1.83 ± 5.87	0.257
		10	2.63 ± 5.20	15	1.83 ± 5.87	0.277
	Yes	2	-3.53 ± 3.46	5	-0.83 ± 4.95	0.049
			-3.53 ± 3.46	10	2.47 ± 4.01	0.000†
			-3.53 ± 3.46	15	1.63 ± 4.13	0.000†
		5	-0.83 ± 4.95	10	2.47 ± 4.01	0.004†
			-0.83 ± 4.95	15	1.63 ± 4.13	0.074
		10	2.47 ± 4.01	15	1.63 ± 4.13	0.347
120	No	2	-1.57 ± 4.76	5	-0.47 ± 4.23	0.288
			-1.57 ± 4.76	10	1.97 ± 4.92	0.009
			-1.57 ± 4.76	15	1.80 ± 5.55	0.035
		5	-0.47 ± 4.23	10	1.97 ± 4.92	0.038
			-0.47 ± 4.23	15	1.80 ± 5.55	0.084
		10	1.97 ± 4.92	15	1.80 ± 5.55	0.829
	Yes	2	-3.13 ± 4.87	5	-2.77 ± 4.04	0.598
			-3.13 ± 4.87	10	2.00 ± 3.60	0.000†
			-3.13 ± 4.87	15	0.10 ± 4.84	0.011
		5	-2.77 ± 4.04	10	2.00 ± 3.60	0.000†
			-2.77 ± 4.04	15	0.10 ± 4.84	0.017
		10	2.00 ± 3.60	15	0.10 ± 4.84	0.085

[a] Based on Wilcoxon Ranked Sign Test, † $p < 0.008$ after Bonferroni correction

Figure 1. 6" image of highest quality (15 mA, 100 kVp with copper filter).

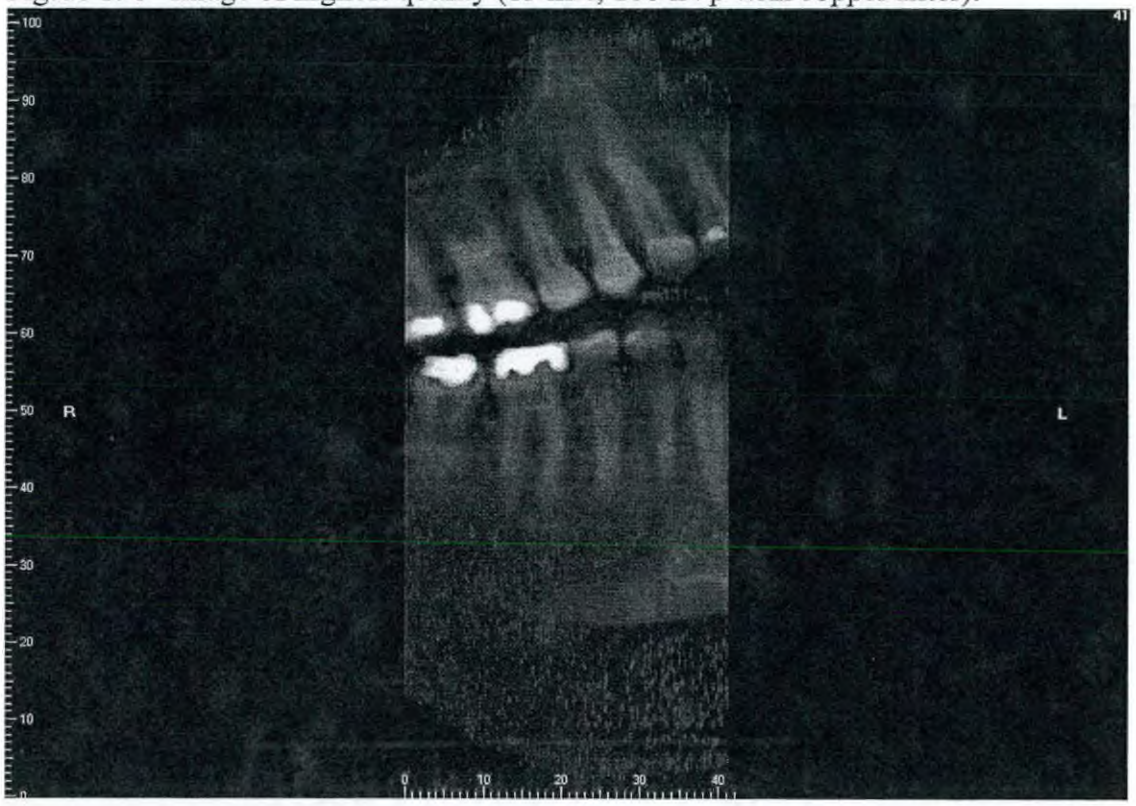
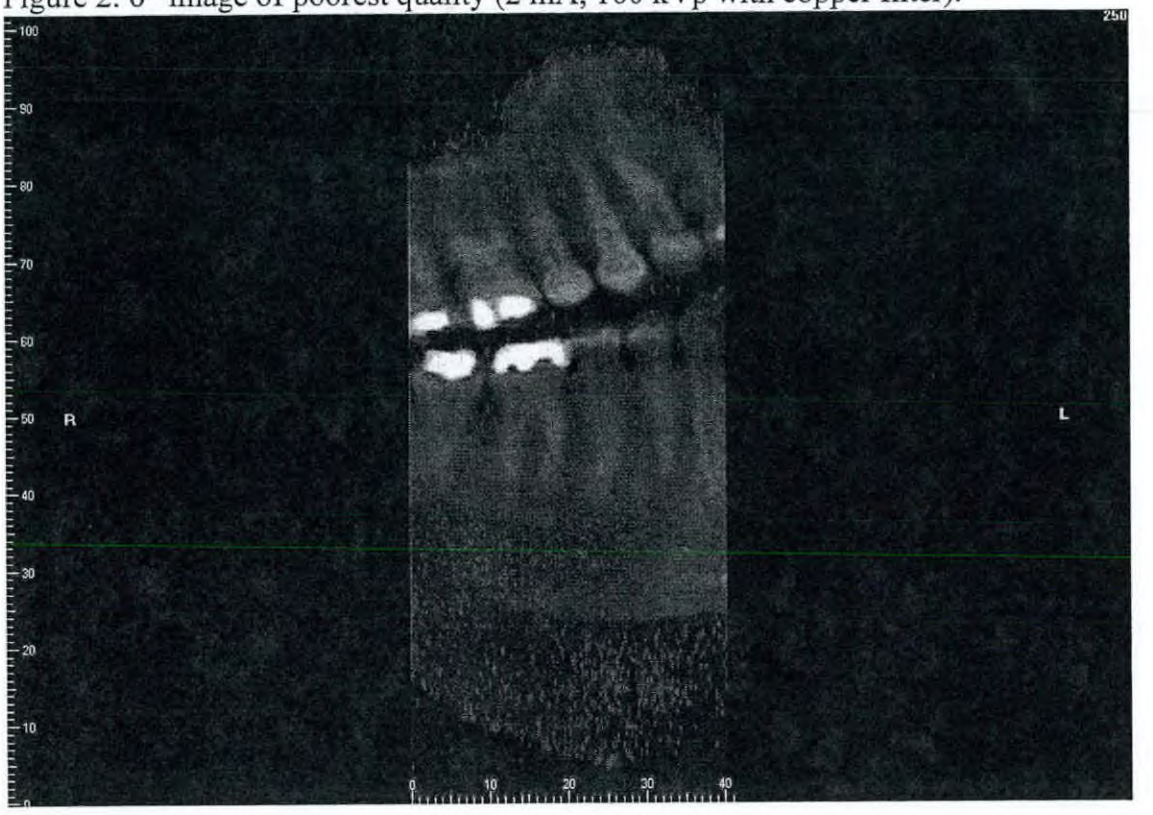


Figure 2. 6" image of poorest quality (2 mA, 100 kVp with copper filter).



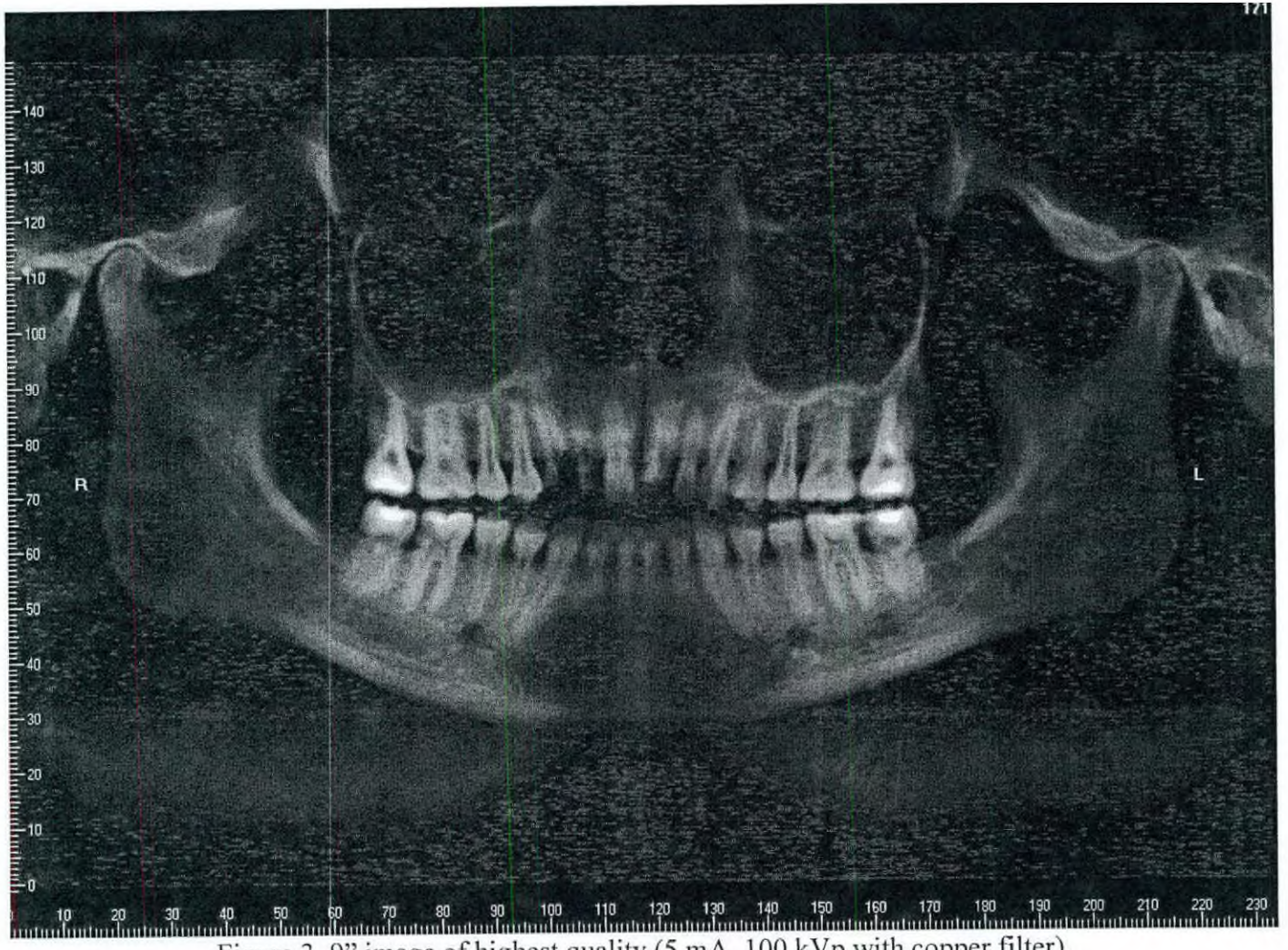


Figure 3. 9" image of highest quality (5 mA, 100 kVp with copper filter).

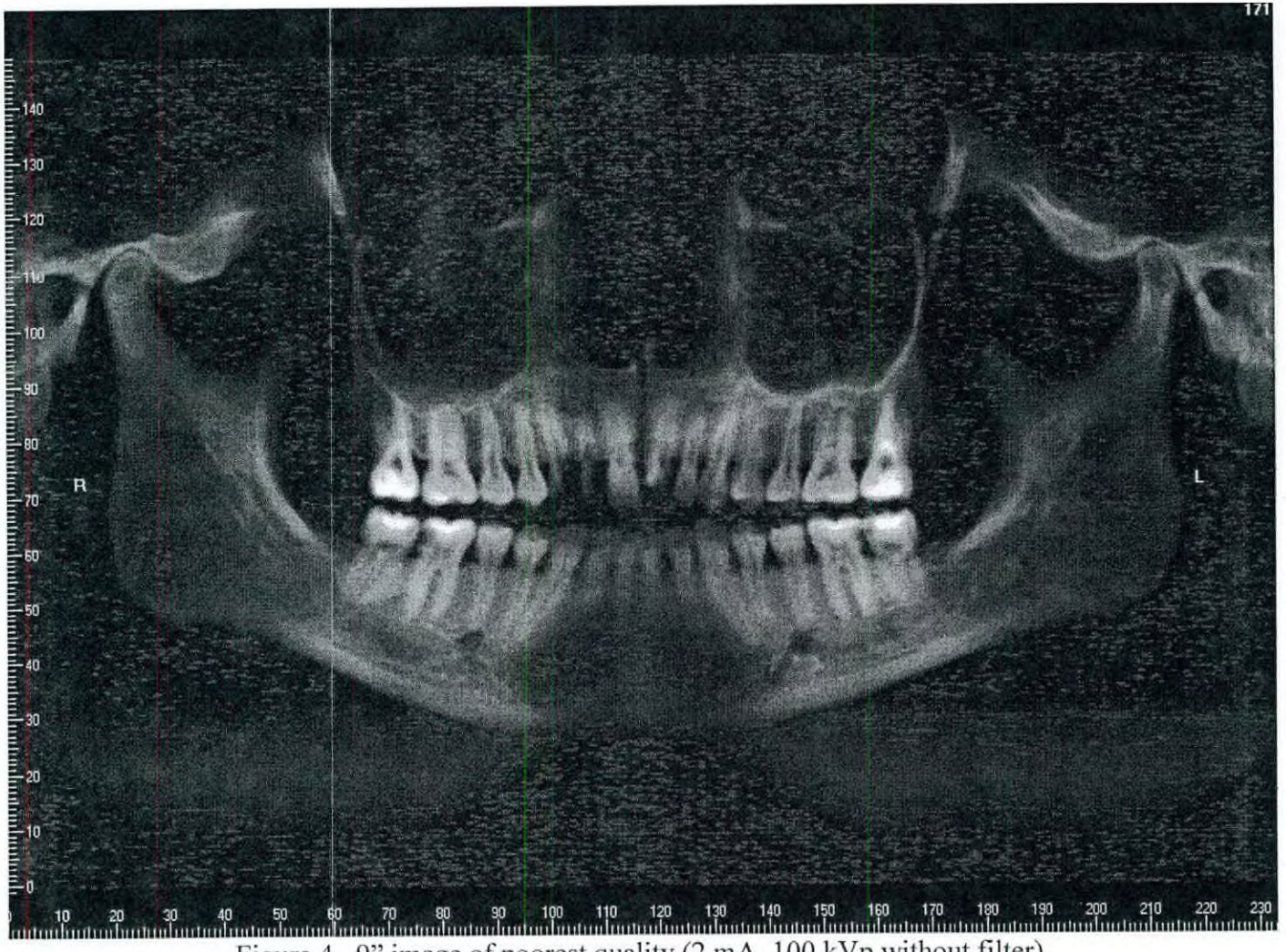


Figure 4. 9" image of poorest quality (2 mA, 100 kVp without filter).

Figure 5. 12" image of highest quality (10 mA, 100 kVp without copper filter).

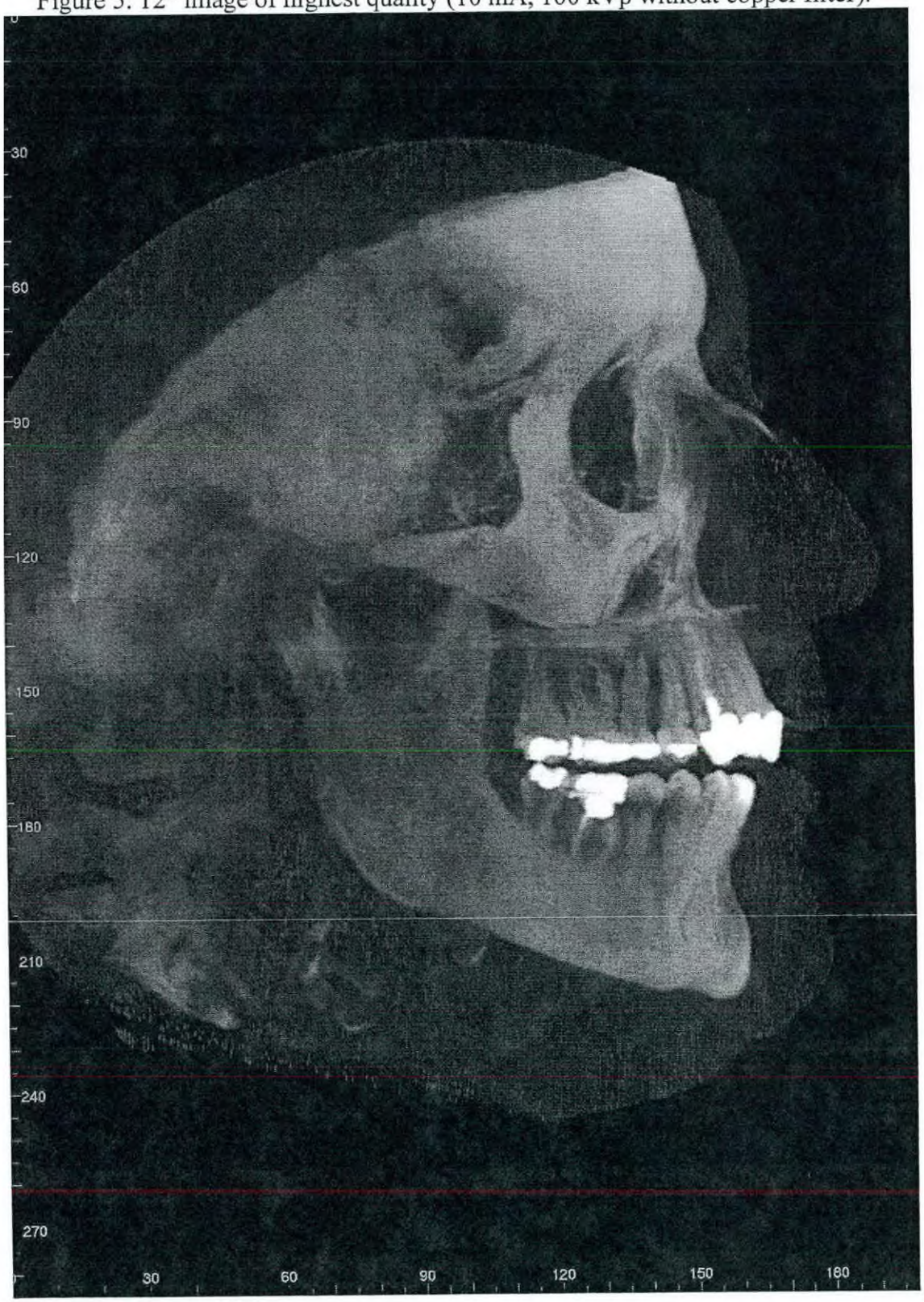


Figure 6. 12" image of poorest quality (2 mA, 100 kVp with copper filter).

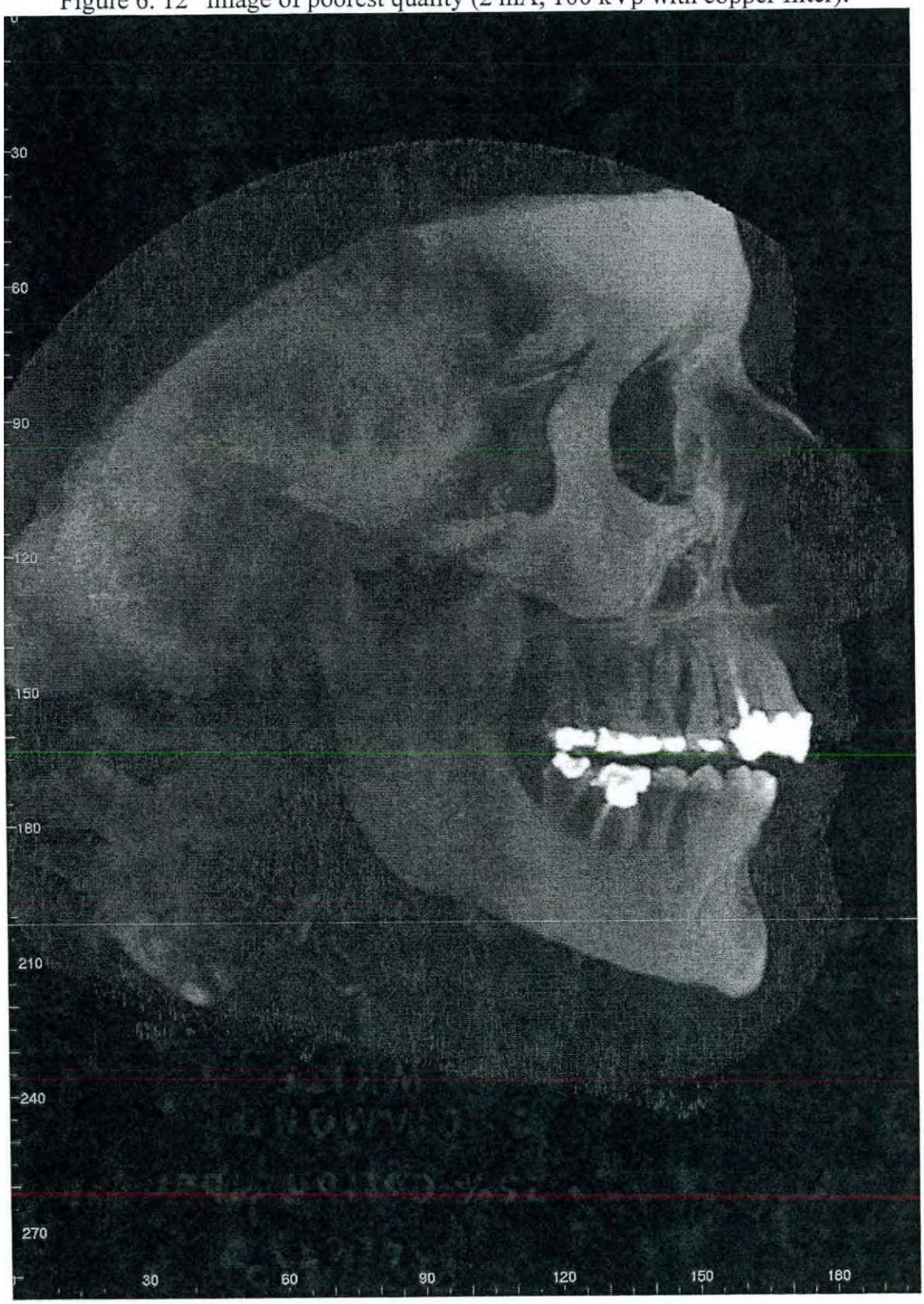
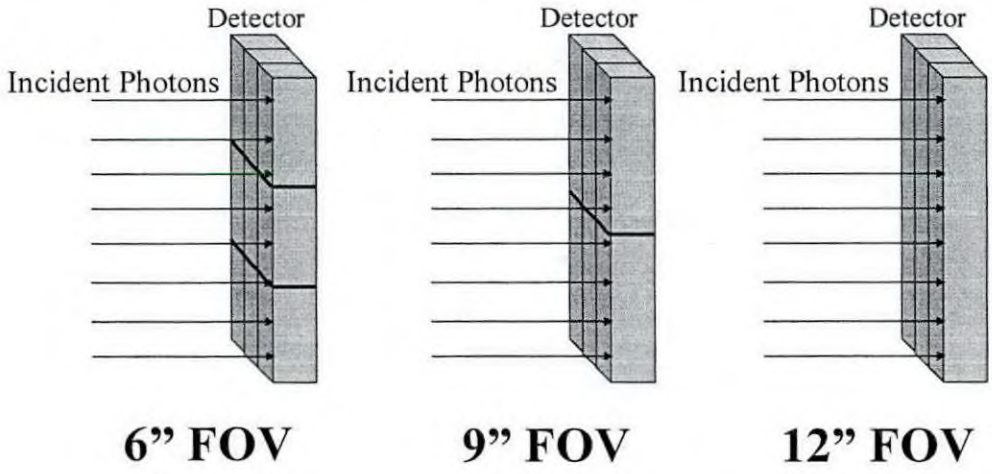


Figure 7. The relationship between voxel size, mA and image quality. Depending on the FOV, the size of the element at the level of the detector will vary. Small fields of view correspond with small detector elements (voxels). If the number of photons is held constant, the voxel size limits the number of incident photons that can strike each voxel. For example, it is shown above that the 6", 9" and 12" FOV are struck by 3, 4 and 8 incident photons per voxel, respectively. The number of photons that strike each voxel affects the quality of a digital image. The photon count is controlled by the mA setting and capture time (which remains constant in the Hitachi CB MercuRay). Better image quality is associated with a larger number of photons/voxel.



REFERENCES

1. Bodner L, Bar-Ziv J, Becker A. Image accuracy of plain film radiography and computerized tomography in assessing morphological abnormality of impacted teeth. Am J Orthod Dentofacial Orthop 2001;120:623-8.

2. Elefteriadis JN, Athanasiou AE. Evaluation of impacted canines by means of computerized tomography. Int J Adult Ortho Orthognath Surg 1996;11:257-64.

3. Schulze D, Heiland M, Thurmann H, Adam G. Radiation exposure during midfacial imaging using 4 and 16 slice computed tomography, cone beam computed tomography systems and conventional radiography. Dentomaxillofac Radiol 2004;33(2):83-6.

4. Schulze D, Heiland M, Schmelzle, R, Rother, UJ. Diagnostic possibilities of cone-beam computed tomography in the facial skeleton. In *Proceedings of the 18th International Congress and Exhibition, Chicago, USA, June 23 26, 2004*, by International Congress Series 1268, 1179-1183.

5. Curry TS, Dowdey JE, and Murry RC. 1990. *Christensen's Physics of Diagnostic Radiology.* 4th ed. Philedelphia: Lippincott, Williams and Wilkins

6. Sohaib SA, Peppercorn PD, Horrocks JA, Keene MH, Kenyon GS, Reznek RH. The effect of decreasing mAs on image quality and patient dose in sinus CT. Br J Radiol 2001;74:157-161.

7. Cohnen M, Fischer H, Hamacher J et al. CT of the head by use of reduced current and kilovoltage: relationship between image quality and dose reduction. Am J Neuroradiol 2000;21:1654–1660.

8. Gündogdu S, Mahmutyazicioglu K, Ozdemir H, Savranlar A, Asil K. Assessment of image quality of a standard and three dose-reducing protocols in adult cranial CT. Eur Radiol 2005;15(9):1959-1968.

9. Rustemeyer P, Streubühr U, Suttmoeller J. Low-dose dental computed tomography: significant dose reduction without loss of image quality. Acta Radiol 2004;45:847–853.

10. Bianchi SD, Rampado O, Luberto L, Genovesio AF, Bianchi CC, Ropolo R. Image quality analysis and low dose dental CT. In. *Proceedings of the 19th International Congress and Exhibition in Berlin, Germany, June 22 - 25, 2005,* by International Congress Series 1281, 1177–1181.

11. Mrtek RG, Tafesse E, Wigger UI. Q-Methodology and Subjective Research. J Soc Adm Pharm 1996;13(2)54-64.

12. Endo M, Tsunoo T, Nakamori N, Yoshida T. Effect of scattered radiation on image noise in cone beam CT. Med Phys 2001;28(4):469-474.

13. Siegel MJ, Schmidt B, Brdaley D, Suess C, Hildebolt C. Radiation dose and image quality in pediatric CT: effect of technical factors and phantom size and shape. Radiology 2004;233(2):515-522.

14. Franklin, JB. The Effect of Aluminum Filter Disks In Roentgenographic Cephalometry. Angle Orthod 1962;32(4):252–269.

15. Gonçalves A, Rollo JMD, Gonçalves M, Haiter Neto F, Bóscolo FN. Effects of Aluminum-Copper Alloy Filtration on Photon Spectra, Air Kerma Rate and Image Contrast. Braz Dent J 2004;15(3):214-219.

16. Martin CJ, Sutton DG, Sharp PF. Measurement of image quality in diagnostic radiography. Appl Radiat Isot 1999;50:21-38.

APPENDIX 1

IRB Approval

Case Western Reserve University
Institutional Review Board
NOTICE OF APPROVAL

Responsible Investigator: **J. Martin Palomo**
Department:
IRB Protocol #: **20060425**
Title: ***Determination of the Lowest mA and kVp Setting for a Diagnostic Cone Beam Computed Tomographic Image***
Co-Investigator: **Jeffrey Kwong**

Approval Date: **June 16, 2006**
Continuing Review Deadline: **June 1, 2007**
Expiration Date: **June 15, 2007**

The Institutional Review Board (IRB) has APPROVED the above new protocol through the expedited review process. It has been determined that this study involves minimal risk, and that no vulnerable populations will be involved. As an investigator of human subjects, your responsibilities include the following (see full description of responsibilities at our website):

1. Report all adverse events and unanticipated problems involving human subjects to the IRB Office, located in the Office of Research Compliance (ORC), within three (3) business days of your knowledge of the occurrence.
2. Provide the IRB with a complete Continuing Review form (available at the CWRU IRB Web Pages, or from the ORC) by the continuing review deadline noted above, and when the study is terminated.
3. Discontinue all work pertaining to this protocol if a continuing review approval is not finalized by the expiration date noted above.
4. Submit all proposed changes to the protocol to the IRB, and receive approval from the IRB, before implementation of the change.
5. Keep all research data and original consent documents in your possession for at least three (3) years after the study is terminated.

Questions? Please visit our website: http://ora.ra.cwru.edu/orc_humansubjects_CWRU_IRB.asp
OR
contact our administrative office...

Isabel Sanchez, IRB Administrator
216.368.6993
Maureen Dore-Arshenovitz, IRB Assistant
216.368.6925
Fax: 216.368.3737

CASE Institutional Review Board
Office of Research Compliance
Sears Building 657
Cleveland, OH 44106-7230

APPENDIX 2

Instructions and Questionnaires

CASE
SCHOOL OF DENTAL MEDICINE

Department of Orthodontics

Determination of the lowest mA and kVp setting for a diagnostic quality CBCT image

You are being asked to participate in a research study about the determination of the lowest mA and kVp setting for a diagnostic quality CBCT image. You were selected as a possible participant because of your knowledge of radiographs and clinical experience. Please read this form and ask any questions that you may have before agreeing to be in the research.

Researchers at Case Western Reserve University are conducting this study.

Background Information

There has been an escalating interest in three-dimensional imaging devices over the last decade. Medical and dental clinicians are beginning to appreciate the advantages that the third dimension gives to clinical diagnosis, treatment planning and patient education. CBCT technology provides only a fraction of radiation exposure when compared to axial CT (CAT scan) machine. The radiation exposure is primarily linked to the mA and kVp settings used to take the image. The higher these settings are, the more radiation exposure the patient receives, but there is also an image quality increase with the increase of these values.

Objective

The purpose of this study is to find out if images taken with lower mA and kVp settings could be differentiated from the images with higher settings, and if they would still be considered of diagnostic quality. A diagnostic quality image would be an image which would be able to answer the questions the clinician or researcher would look for and expect to see in that particular radiographic view.

Confidentiality

The records of this research will be kept private. In any sort of report we might publish, we will not include any information that will make it possible to identify a participant. Research records will be kept in a locked file, and access will be limited to the researchers, the University review board responsible for protecting human participants, and regulatory agencies.

Voluntary Nature of the Study

Your participation is voluntary. If you choose not to participate, it will not affect your current or future relations with the University. There is no penalty or loss of benefits for not participating or for discontinuing your participation.

Findings from this study will be available to you upon request.

Your response to the survey will assume that you consent to participate in this study.

EXPIRES
MAY 07 2007
CWRU IRB

Procedures

If you agree to be a participant in this research, we would ask you to Q-sort 16 images and answer a short questionnaire. Q-sorting works by taking a set of data (a Q-set), and arranging it based on given statements. In this situation the Q-set will consist of 16 images.

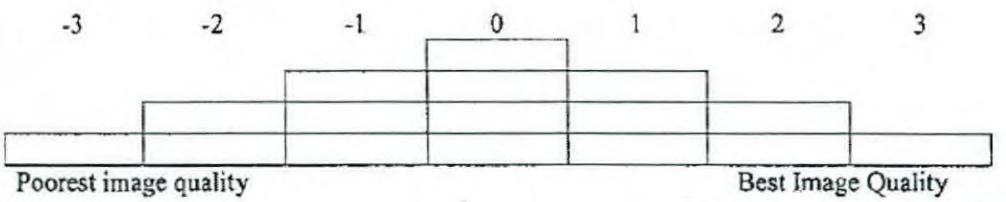
The object of the Q-sort is for the clinician to sort the images based on image quality (poorest image quality to best image quality). The 16 images will be laid out on a table such that they can all be viewed simultaneously.

It is the responsibility of the clinician to then sort through the images, and choose the image of best quality image and the image of poorest quality.

Each image will be placed aside, the best quality image to the clinician's right, and the poorest quality image to the clinician's left. From the remaining 14 images, the clinician will then choose the two best quality images and two poorest quality images and place them aside as previously described. From the remaining 10 images, the clinician will then choose the three best quality images and three poorest quality images and place them aside. When the sort is complete there will be four images remaining. At this point, please confirm that you are comfortable with your choice of sorting. Beginning with the column on the right, please arrange the images in each column in descending order based on image quality, i.e. the best image at the top, the poorest image at the bottom.

Step by Step Instructions for Q-Sorting

1. Count and confirm that there are 16 images
2. Begin by evaluating and looking through all 16 images
3. YOU MAY CHOOSE TO EITHER REMOVE THE IMAGES FROM THE PROTECTIVE SLEEVES *OR* LEAVE THE IMAGES IN THE PROTECTIVE SLEEVES. **HOWEVER, YOU MUST VIEW EACH IMAGE THE SAME WAY, i.e.** ***ALL IMAGES OUT OF THE PROTECTIVE SLEEVES OR ALL IMAGES IN THE PROTECTIVE SLEEVES.***
4. Choose the image of best quality and place it aside on the right
5. Choose the image of poorest quality and place it aside on the left
6. From the remaining images, choose two images of best quality and place them beside the image of best quality
7. From the remaining images, choose two images of poorest quality and place them beside the image of poorest quality
8. From the remaining images, choose three images of best quality and place them beside the image of best quality
9. From the remaining images, choose three images of poorest quality and place them beside the image of poorest quality
10. When the sort is complete, four images should remain and the images should be arranged in piles that resemble the following diagram:



EXPIRES
MAY 07 2007
CWRU IRB

11. Please confirm that you are comfortable with your choice of sorting.
12. Starting with the column on the right, please arrange the images in each column in descending order based on image quality, i.e. the best image at the top, the poorest image at the bottom.
13. Please fill out the questionnaire

Contacts and Questions

The researchers conducting this study are Dr. J. Martin Palomo or Jeffrey Kwong. You may ask any questions you have now. If you have any questions later, you may contact them at (216) 368-2449.

If the researchers cannot be reached, or if you would like to talk to someone other than the researcher(s) about; (1) concerns regarding this study, (2) research participant rights, (3) research-related injuries, or (4) other human subjects issues, please contact Case Western Reserve University's Institutional Review Board at (216) 368-6925 or write: Case Western Reserve University; Institutional Review Board; 10900 Euclid Ave.; Cleveland, OH 44106-7230.

Thank you in advance for your cooperation.

EXPIRES
MAY 07 2007
CWRU IRB

Questionnaire for 6" images

Please take the time to fill out the following Questionnaire

Do you wear glasses of any sort or have any visual acuity problems?
a) Glasses
b) Contact lenses
c) Bifocals
d) Visual acuity problem, please clarify: _____
e) Other, please clarify: _____

What year did you (will you) graduate from your most recent training?:
_____

Do you have experience viewing bitewing radiographs? Yes / No

Please check off the amount of time used to view this set of images:
a) less than 15 minutes
b) between 15-20 minutes
c) greater than 20 minutes

What considerations did you take into account when classifying an image as having better image quality?

What considerations did you take into account when classifying an image as having poorer image quality?

Considering each individual image, arranged in the position that you have sorted them, please answer the following question: Is the image of sufficient diagnostic quality for making a **periodontal** diagnosis?

-3	-2	-1	0	1	2	3
			Yes/No			
		Yes/No	Yes/No	Yes/No		
	Yes/No	Yes/No	Yes/No	Yes/No	Yes/No	
Yes/No	Yes/No	Yes/No	Yes/No	Yes/No	Yes/No	Yes/No
Poorest image quality					Best Image	
Quality						

If you have chosen "No" for any image please explain why you feel the image is not of diagnostic quality. If you have any comments, you may also use the space provided below:

Questionnaire for 9" images

Please take the time to fill out the following Questionnaire

Do you wear glasses of any sort or have any visual acuity problems?
a) Glasses
b) Contact lenses
c) Bifocals
d) Visual acuity problem, please clarify: _____
e) Other, please clarify: _____

What year did you (will you) graduate from your most recent training?:
_____

Do you have experience viewing panoramic radiographs? Yes / No

Please check off the amount of time used to view this set of images:
a) less than 15 minutes
b) between 15-20 minutes
c) greater than 20 minutes

What considerations did you take into account when classifying an image as having better image quality?

What considerations did you take into account when classifying an image as having poorer image quality?

Considering each individual image, arranged in the position that you have sorted them, please answer the following question: Is the image of sufficient diagnostic quality for making a **general** diagnosis?

-3	-2	-1	0	1	2	3
			Yes/No			
		Yes/No	Yes/No	Yes/No		
	Yes/No	Yes/No	Yes/No	Yes/No	Yes/No	
Yes/No	Yes/No	Yes/No	Yes/No	Yes/No	Yes/No	Yes/No

Poorest image quality Best Image
Quality

If you have chosen "No" for any image please explain why you feel the image is not of diagnostic quality. If you have any comments, you may also use the space provided below:

Questionnaire for 12" images

Please take the time to fill out the following Questionnaire

Do you wear glasses of any sort or have any visual acuity problems?
a) Glasses
b) Contact lenses
c) Bifocals
d) Visual acuity problem, please clarify: _____
e) Other, please clarify: _____

What year did you (will you) graduate from your most recent training?:
_____

Do you have experience viewing lateral cephalograms? Yes / No

Please check off the amount of time used to view this set of images:
a) less than 15 minutes
b) between 15-20 minutes
c) greater than 20 minutes

What considerations did you take into account when classifying an image as having better image quality?

What considerations did you take into account when classifying an image as having poorer image quality?

Considering each individual image, arranged in the position that you have sorted them, please answer the following question: Is the image of sufficient diagnostic quality for making an **orthodontic** diagnosis?

-3	-2	-1	0	1	2	3
			Yes/No			
		Yes/No	Yes/No	Yes/No		
	Yes/No	Yes/No	Yes/No	Yes/No	Yes/No	
Yes/No	Yes/No	Yes/No	Yes/No	Yes/No	Yes/No	Yes/No

Poorest image quality Best Image
Quality

If you have chosen "No" for any image please explain why you feel the image is not of diagnostic quality. If you have any comments, you may also use the space provided below:

APPENDIX 3

Six Inch Bitewing Images



Figure 1. Radiographic image obtained at settings of 6" field of view, 2 mA and 100 kVp without filter.

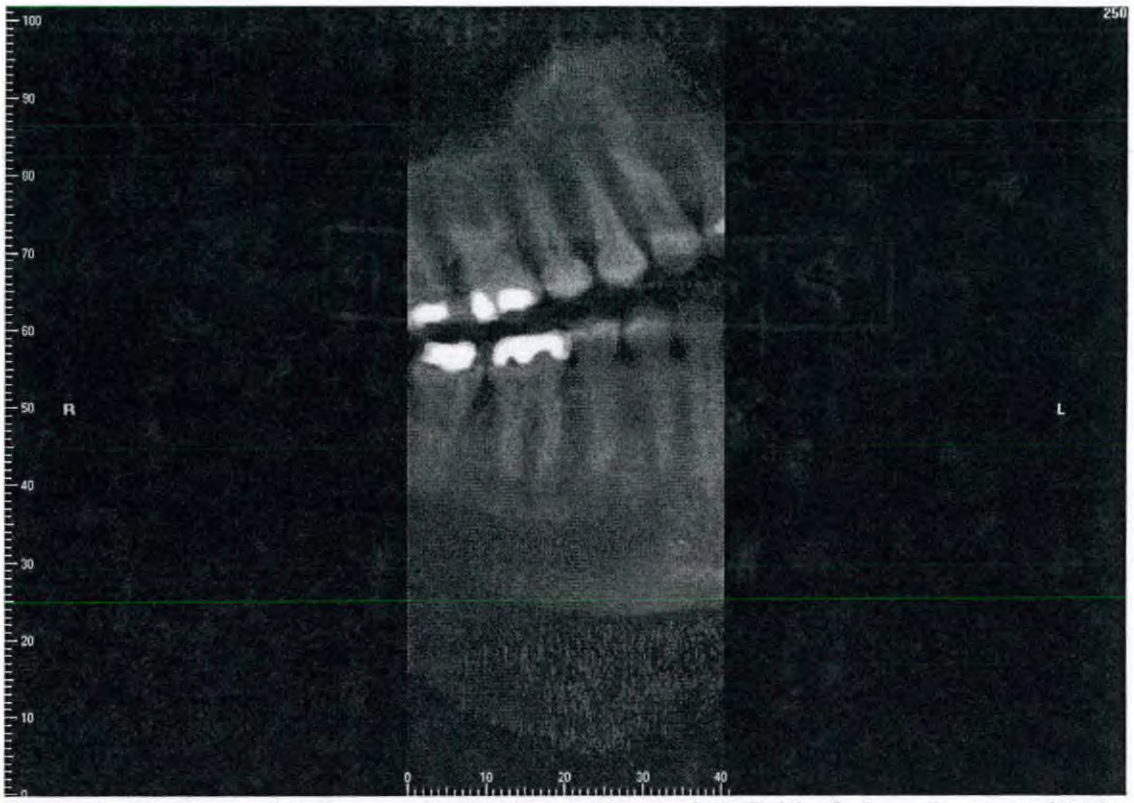


Figure 2. Radiographic image obtained at settings of 6" field of view, 2 mA and 100 kVp with filter.

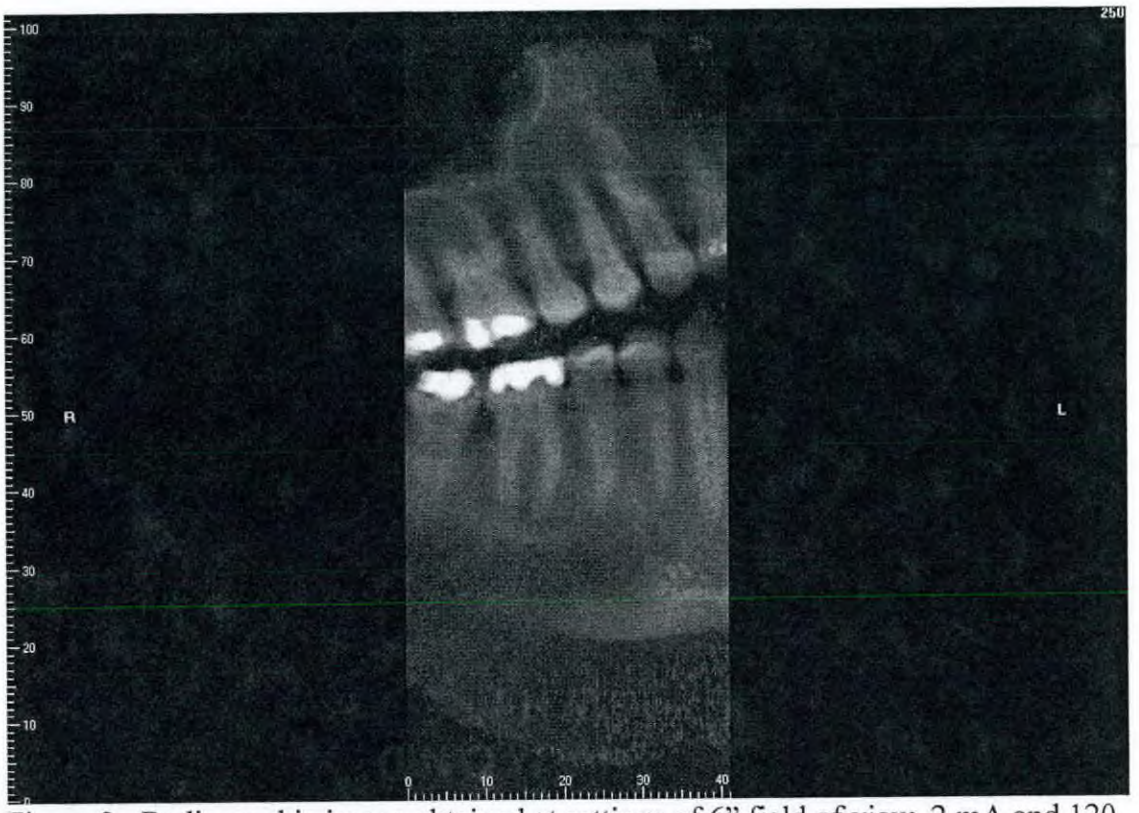


Figure 3. Radiographic image obtained at settings of 6" field of view, 2 mA and 120 kVp without filter.

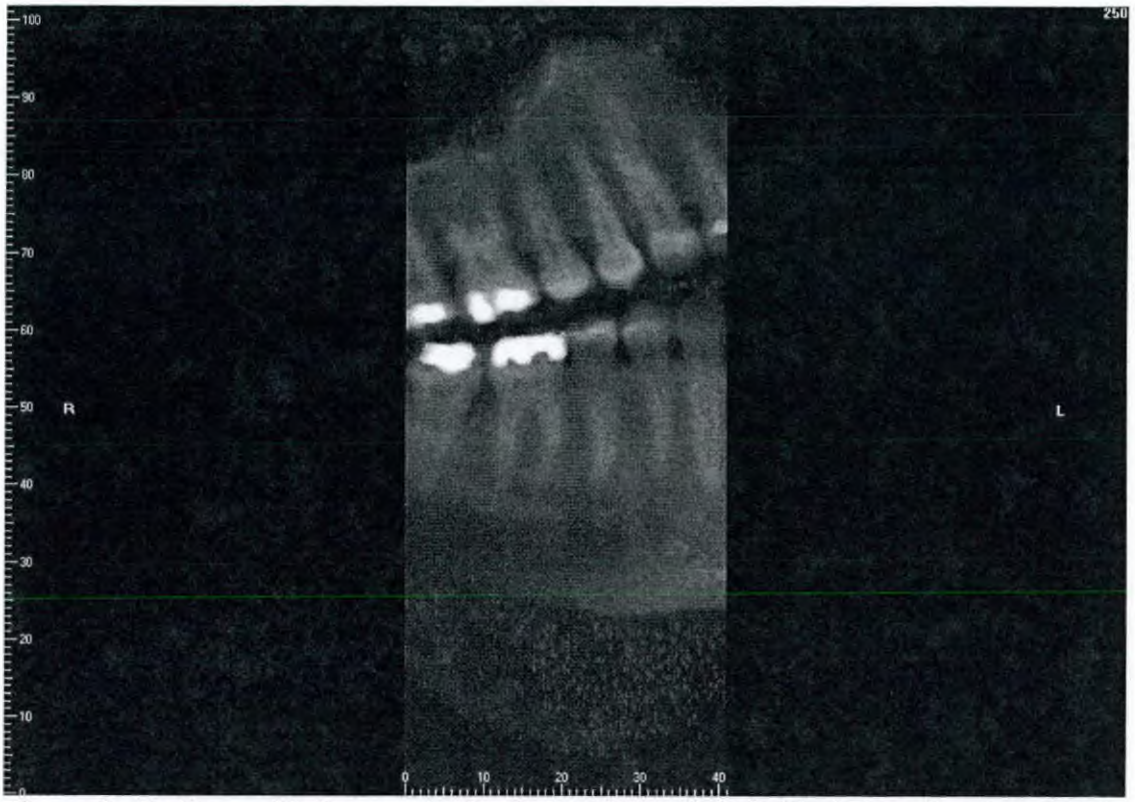


Figure 4. Radiographic image obtained at settings of 6" field of view, 2 mA and 120 kVp with filter.

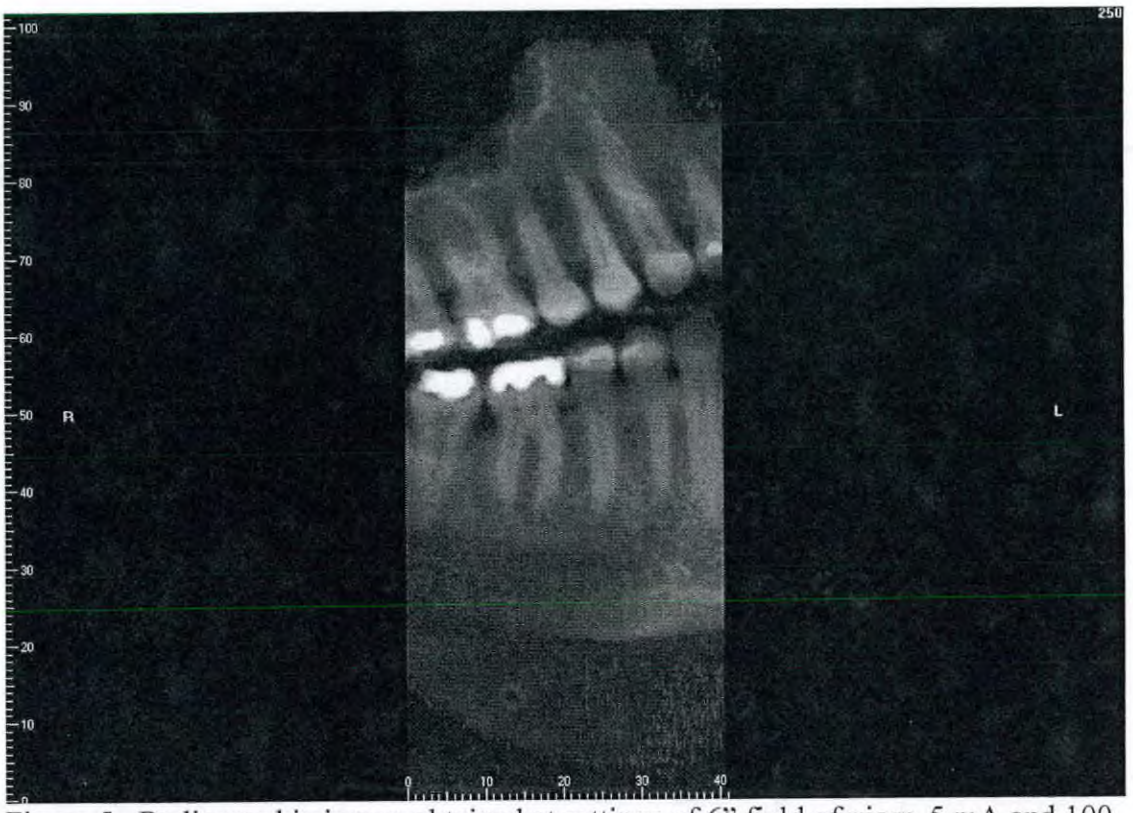


Figure 5. Radiographic image obtained at settings of 6" field of view, 5 mA and 100 kVp without filter.

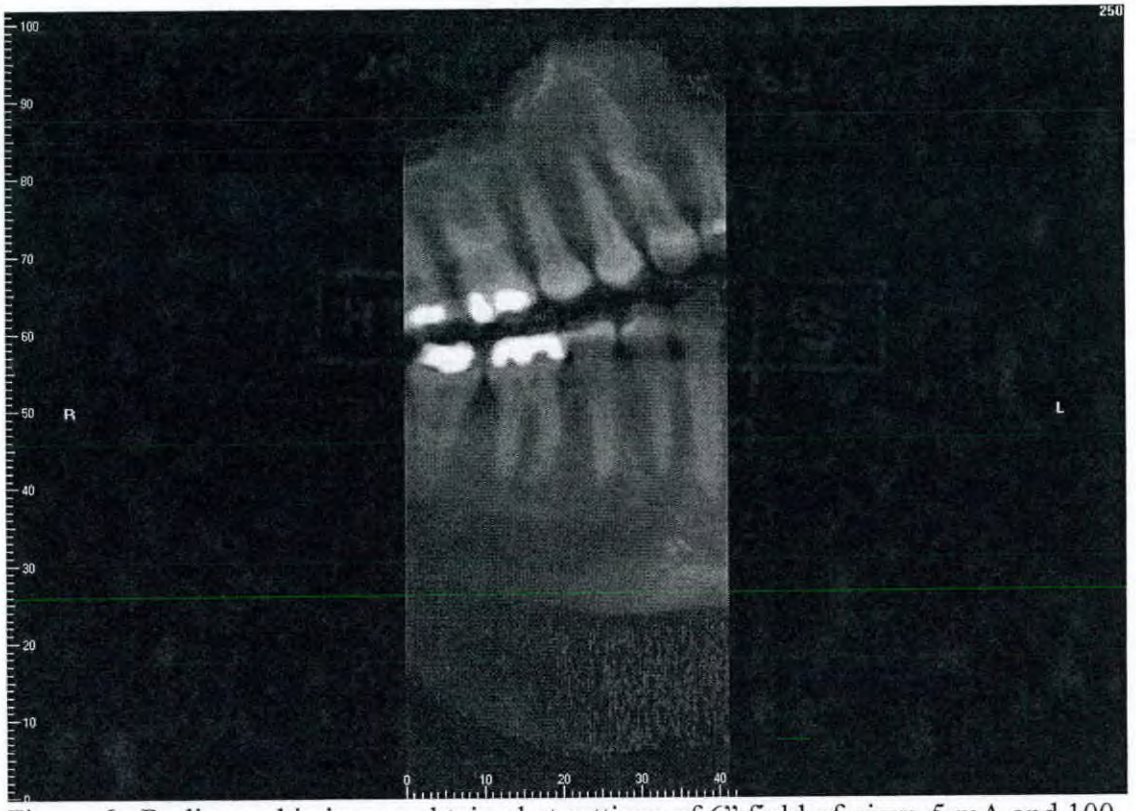


Figure 6. Radiographic image obtained at settings of 6" field of view, 5 mA and 100 kVp with filter.

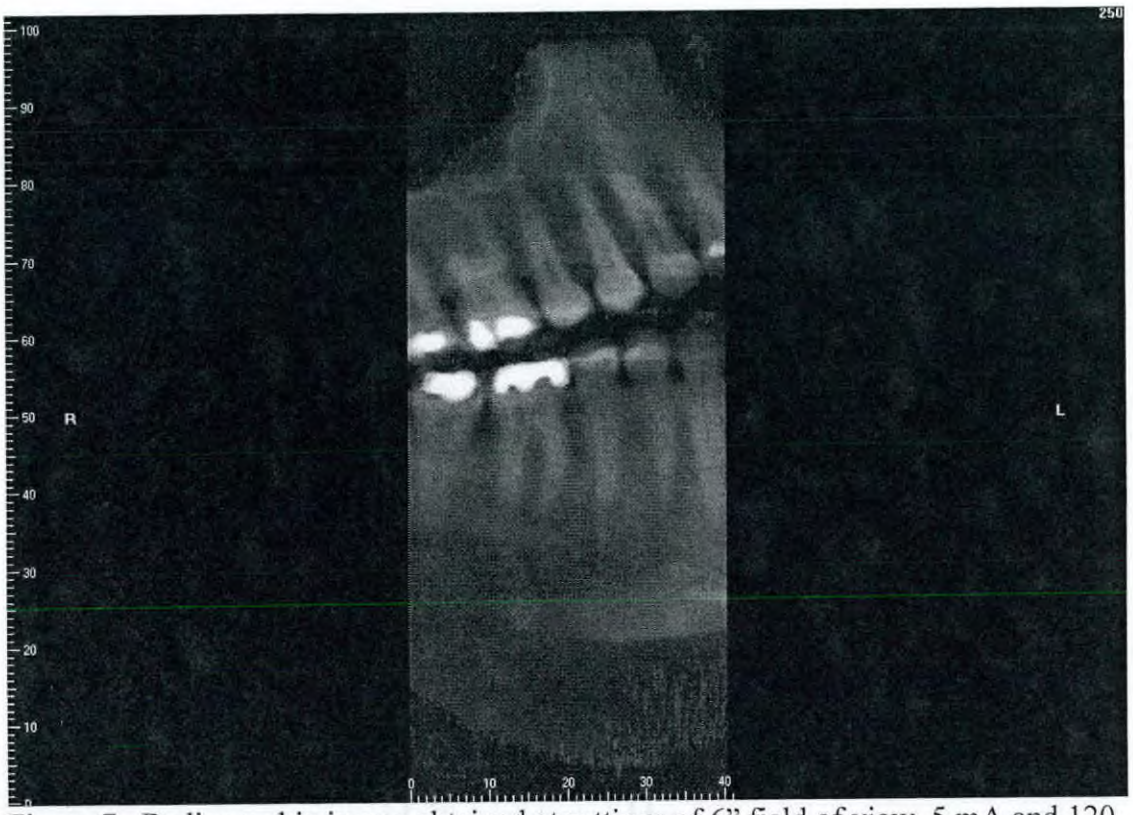


Figure 7. Radiographic image obtained at settings of 6" field of view, 5 mA and 120 kVp without filter.

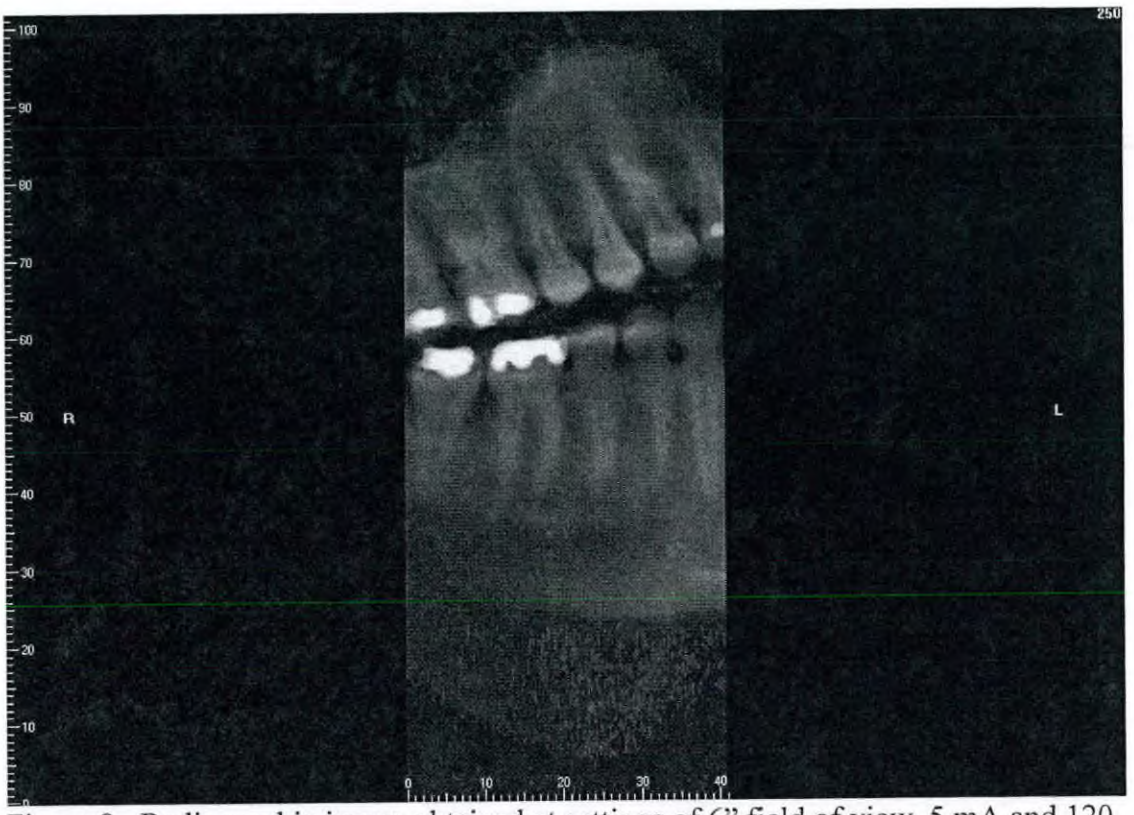


Figure 8. Radiographic image obtained at settings of 6" field of view, 5 mA and 120 kVp with filter.

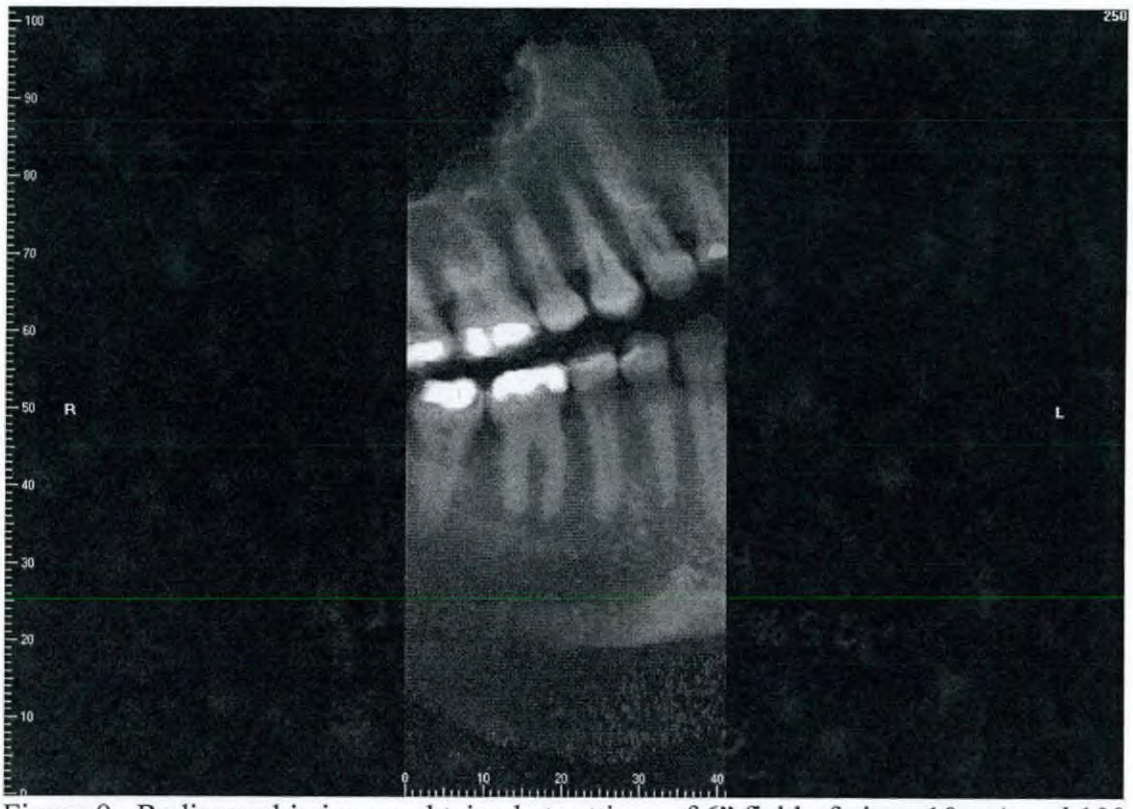


Figure 9. Radiographic image obtained at settings of 6" field of view, 10 mA and 100 kVp without filter.



Figure 10. Radiographic image obtained at settings of 6" field of view, 10 mA and 100 kVp with filter.

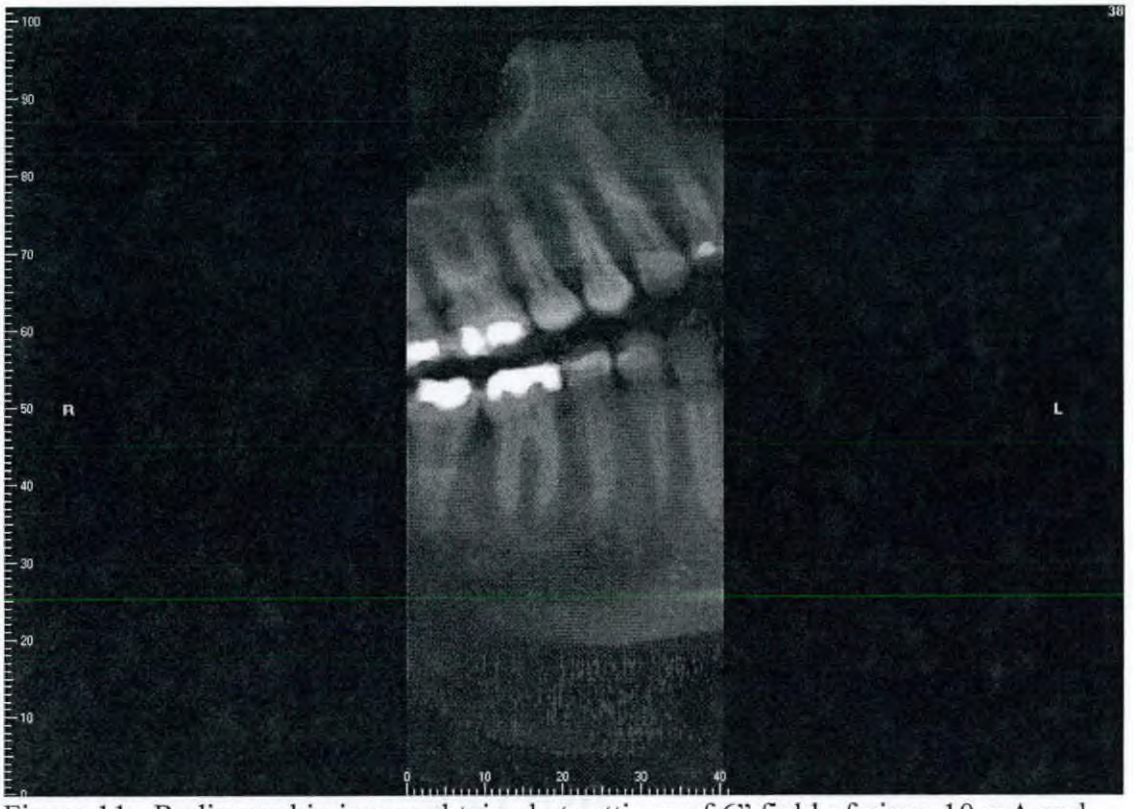


Figure 11. Radiographic image obtained at settings of 6" field of view, 10 mA and 120 kVp without filter.

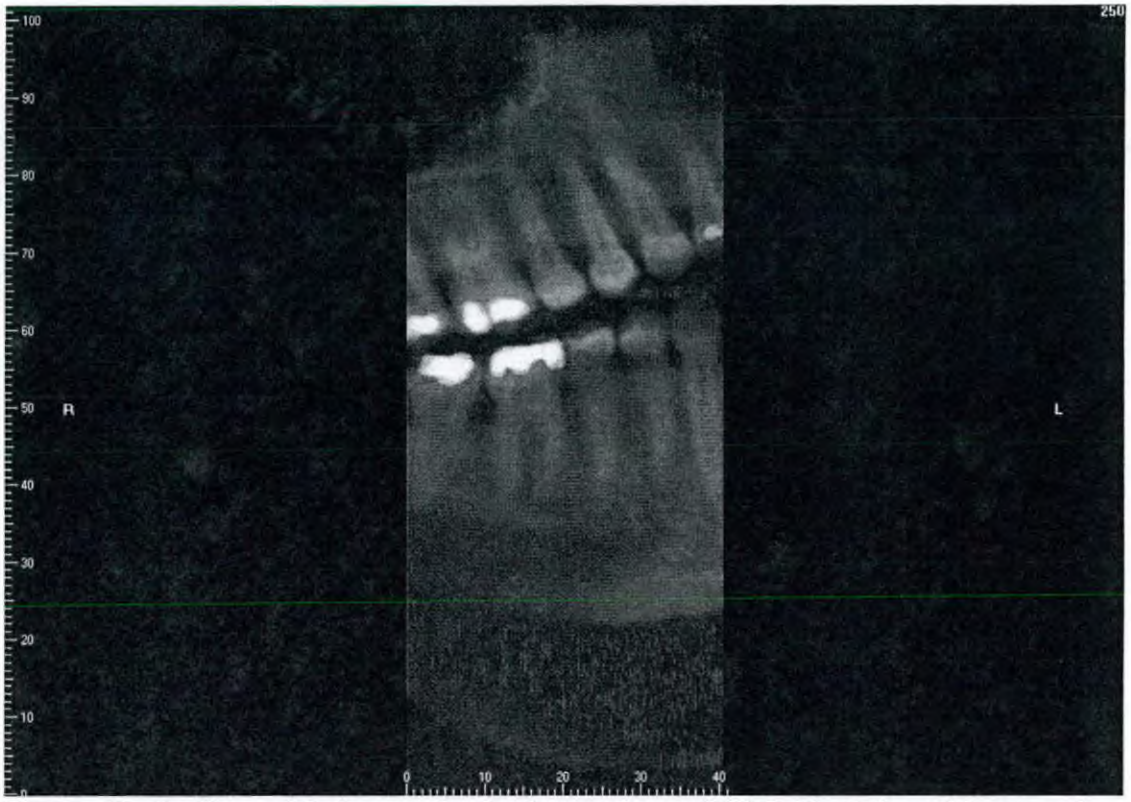


Figure 12. Radiographic image obtained at settings of 6" field of view, 10 mA and 120 kVp with filter.

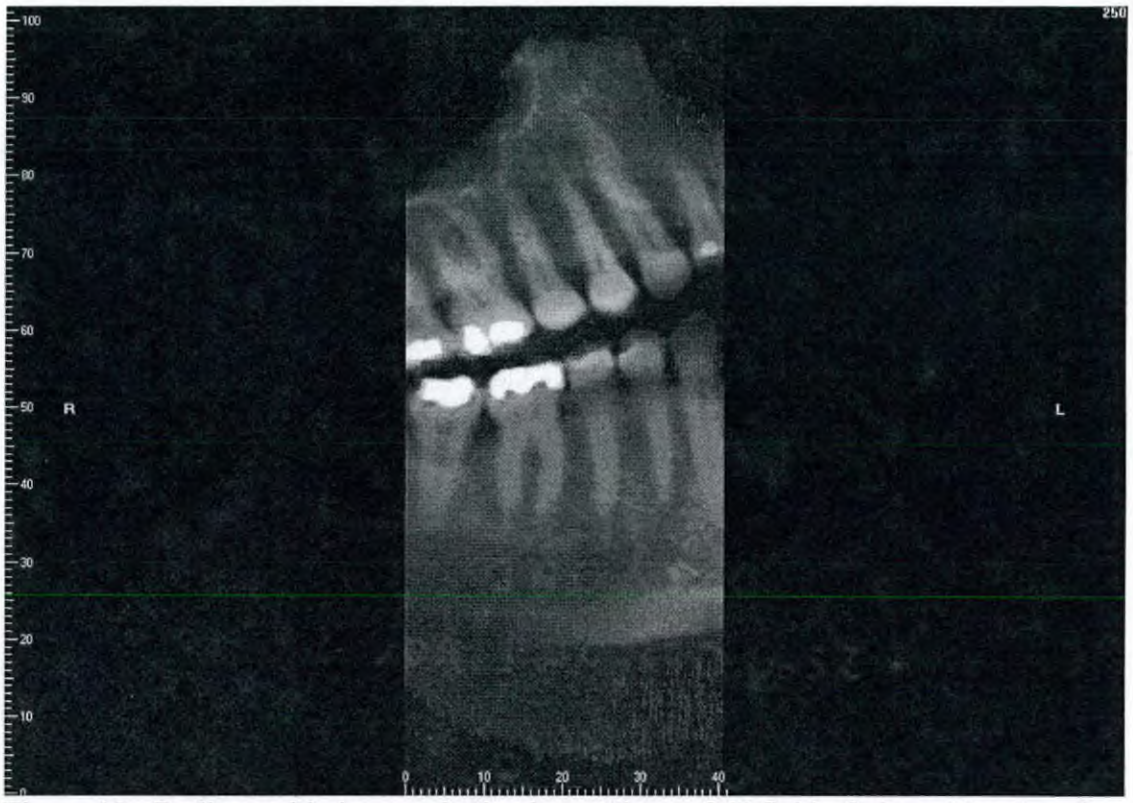


Figure 13. Radiographic image obtained at settings of 6" field of view, 15 mA and 100 kVp without filter.



Figure 14. Radiographic image obtained at settings of 6" field of view, 15 mA and 100 kVp with filter.

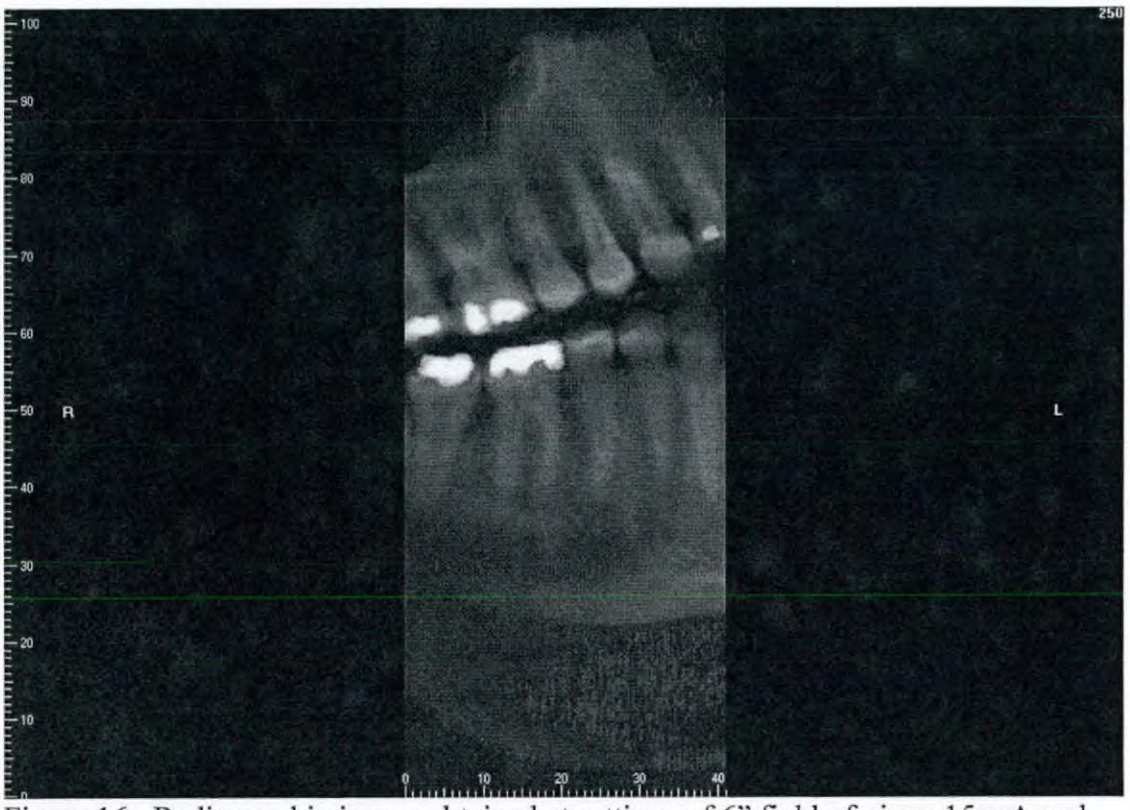


Figure 16. Radiographic image obtained at settings of 6" field of view, 15 mA and 120 kVp with filter.

APPENDIX 4

Nine Inch Panoramic Images

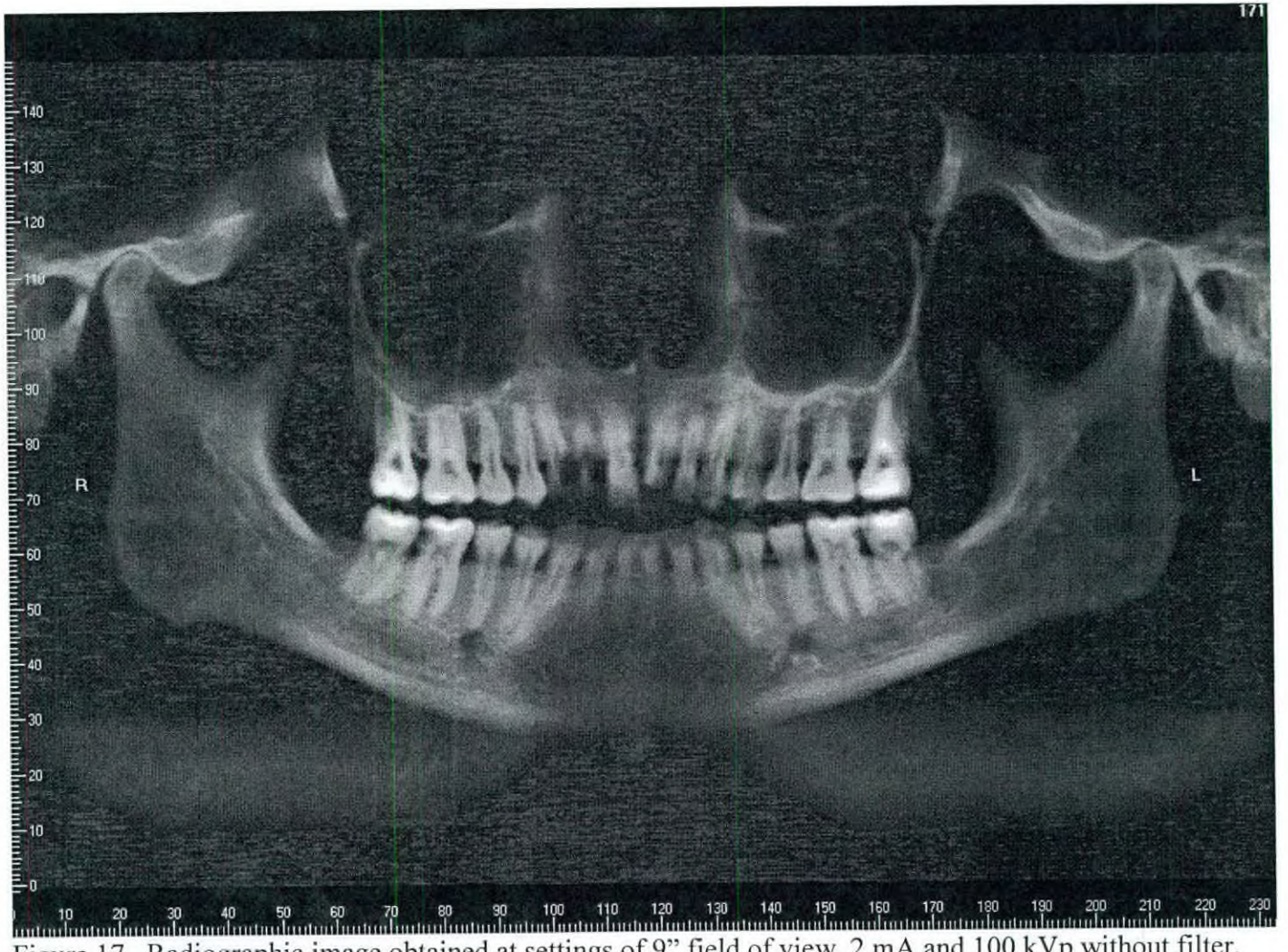


Figure 17. Radiographic image obtained at settings of 9" field of view, 2 mA and 100 kVp without filter.

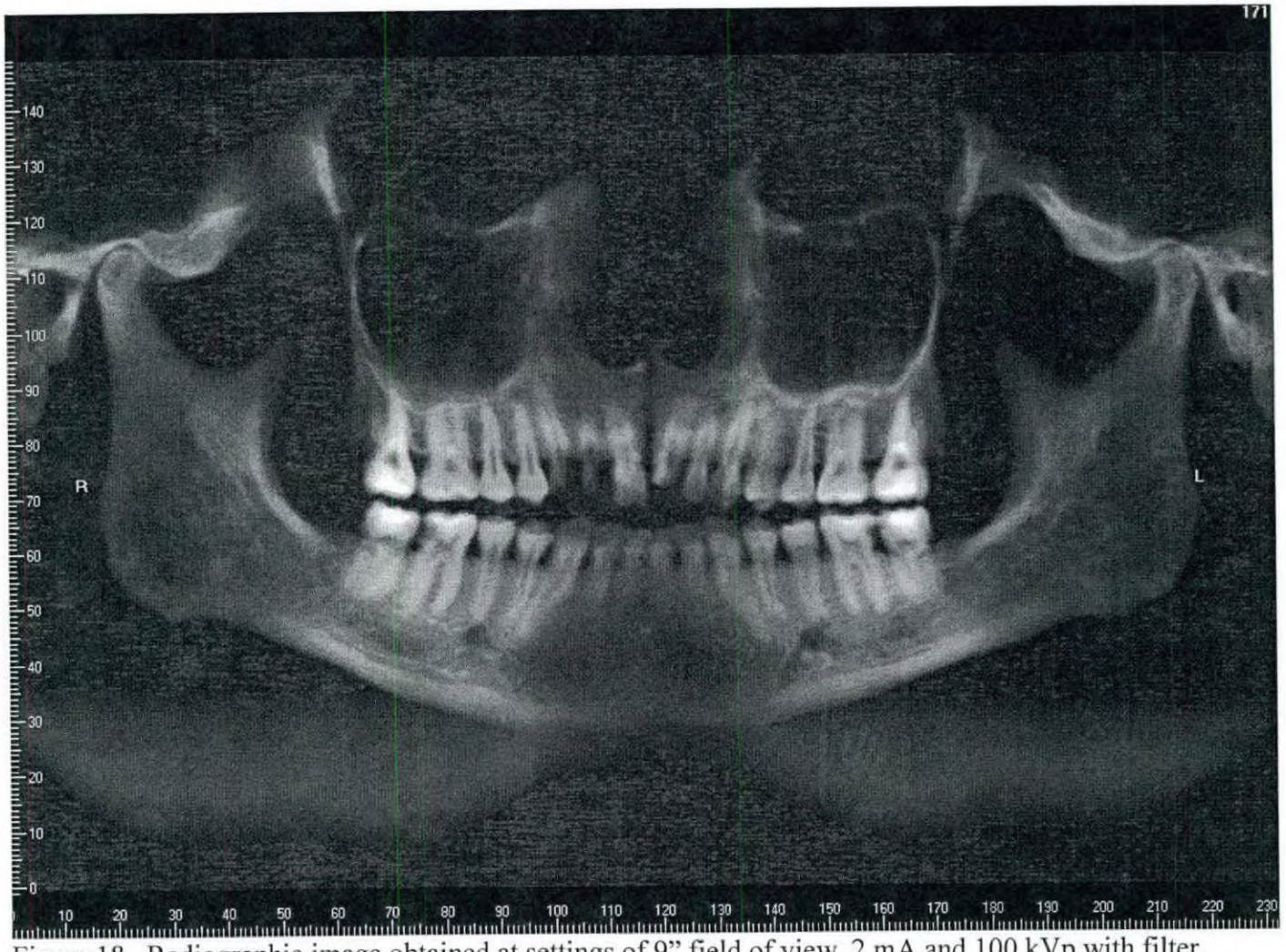


Figure 18. Radiographic image obtained at settings of 9" field of view, 2 mA and 100 kVp with filter.

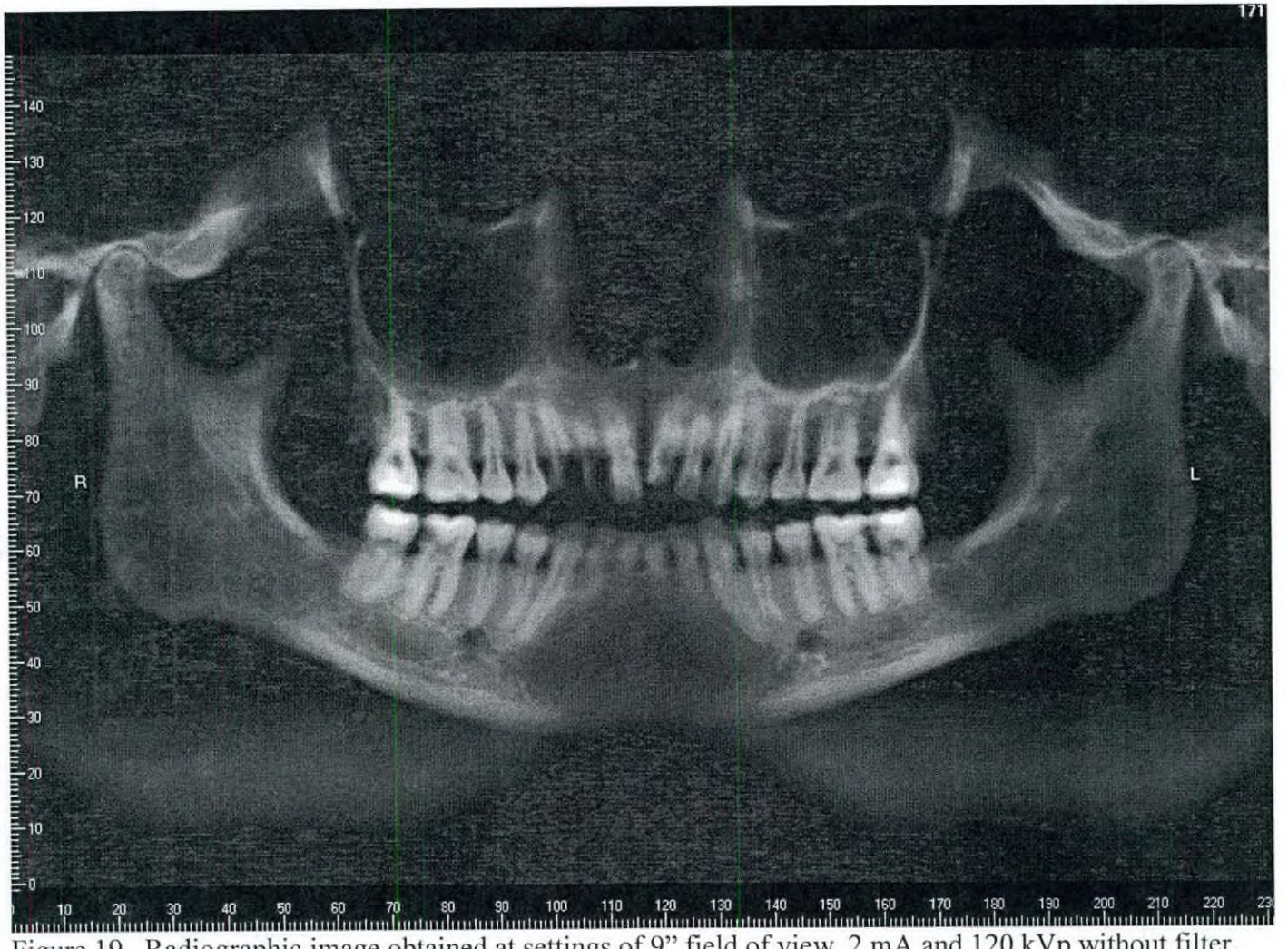


Figure 19. Radiographic image obtained at settings of 9" field of view, 2 mA and 120 kVp without filter.

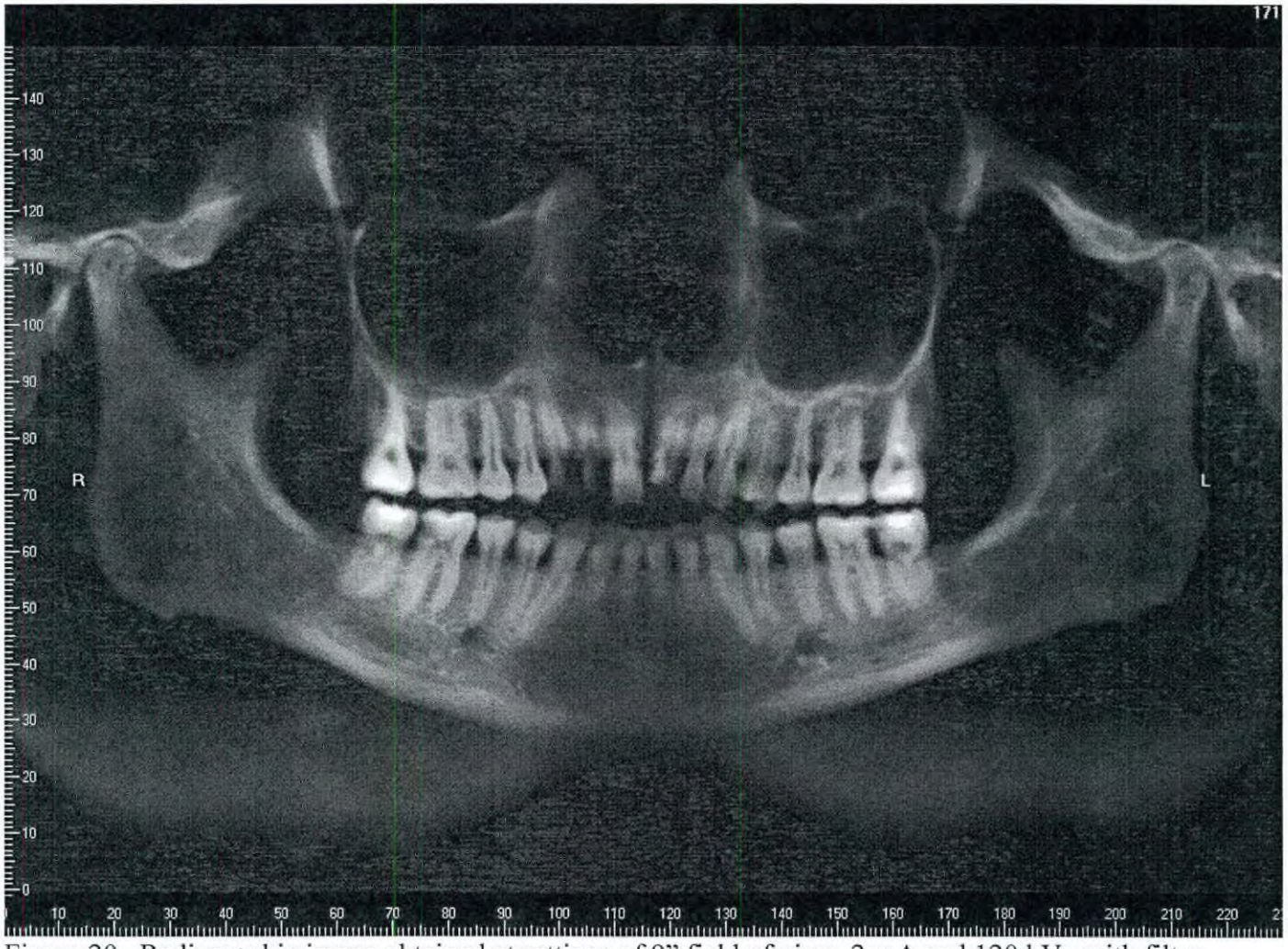


Figure 20. Radiographic image obtained at settings of 9" field of view, 2 mA and 120 kVp with filter.

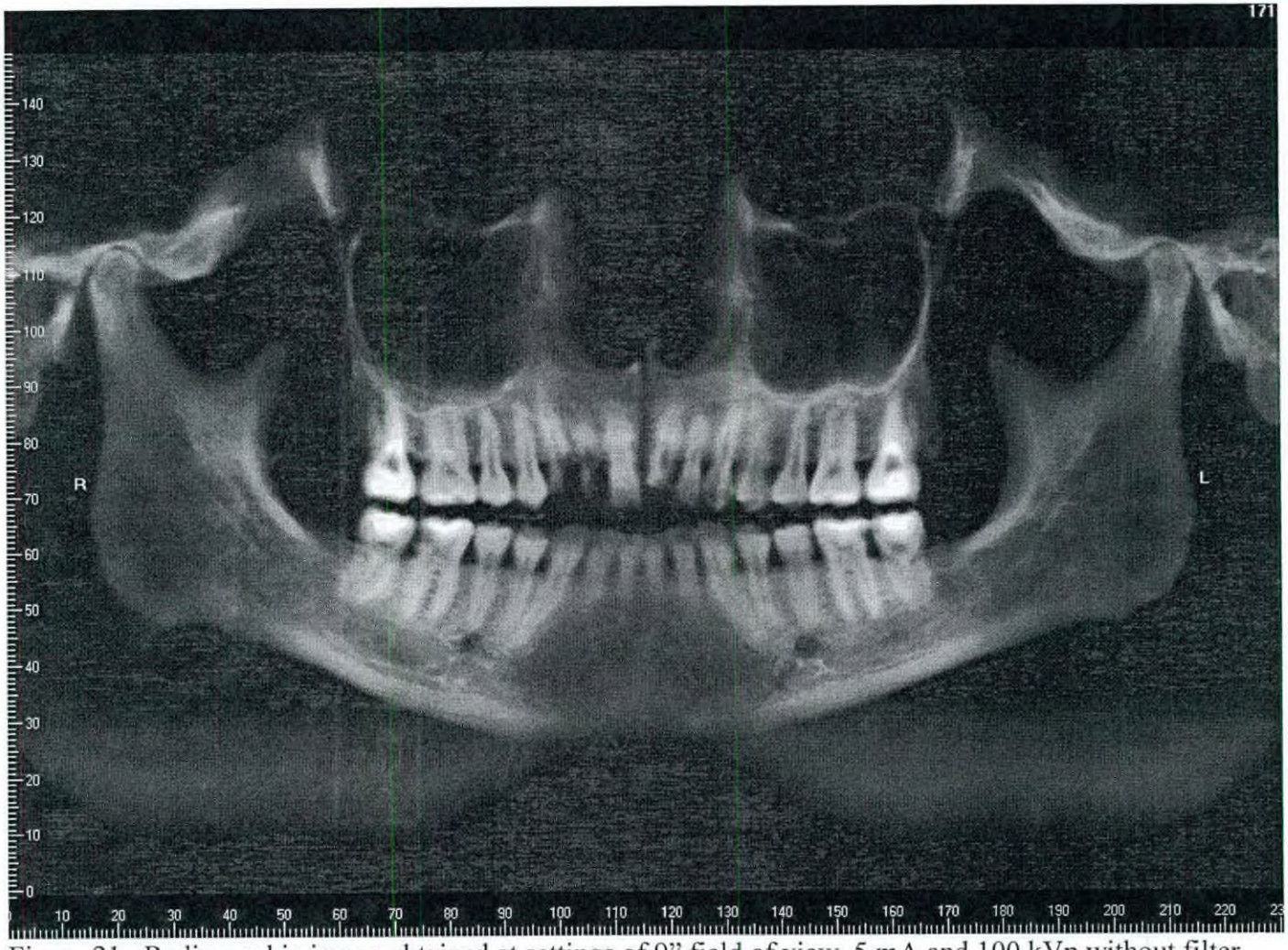


Figure 21. Radiographic image obtained at settings of 9" field of view, 5 mA and 100 kVp without filter.

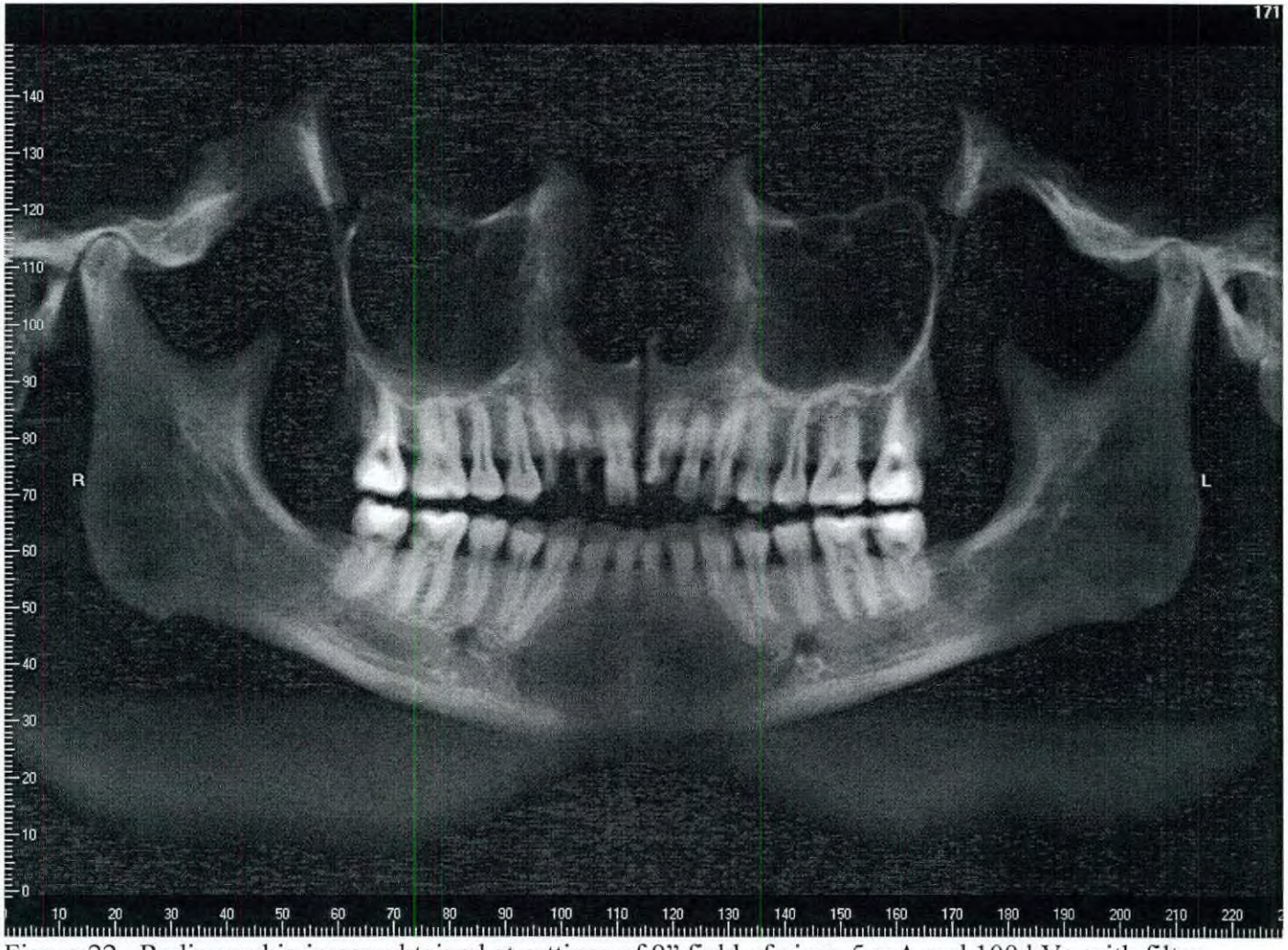


Figure 22. Radiographic image obtained at settings of 9" field of view, 5 mA and 100 kVp with filter.

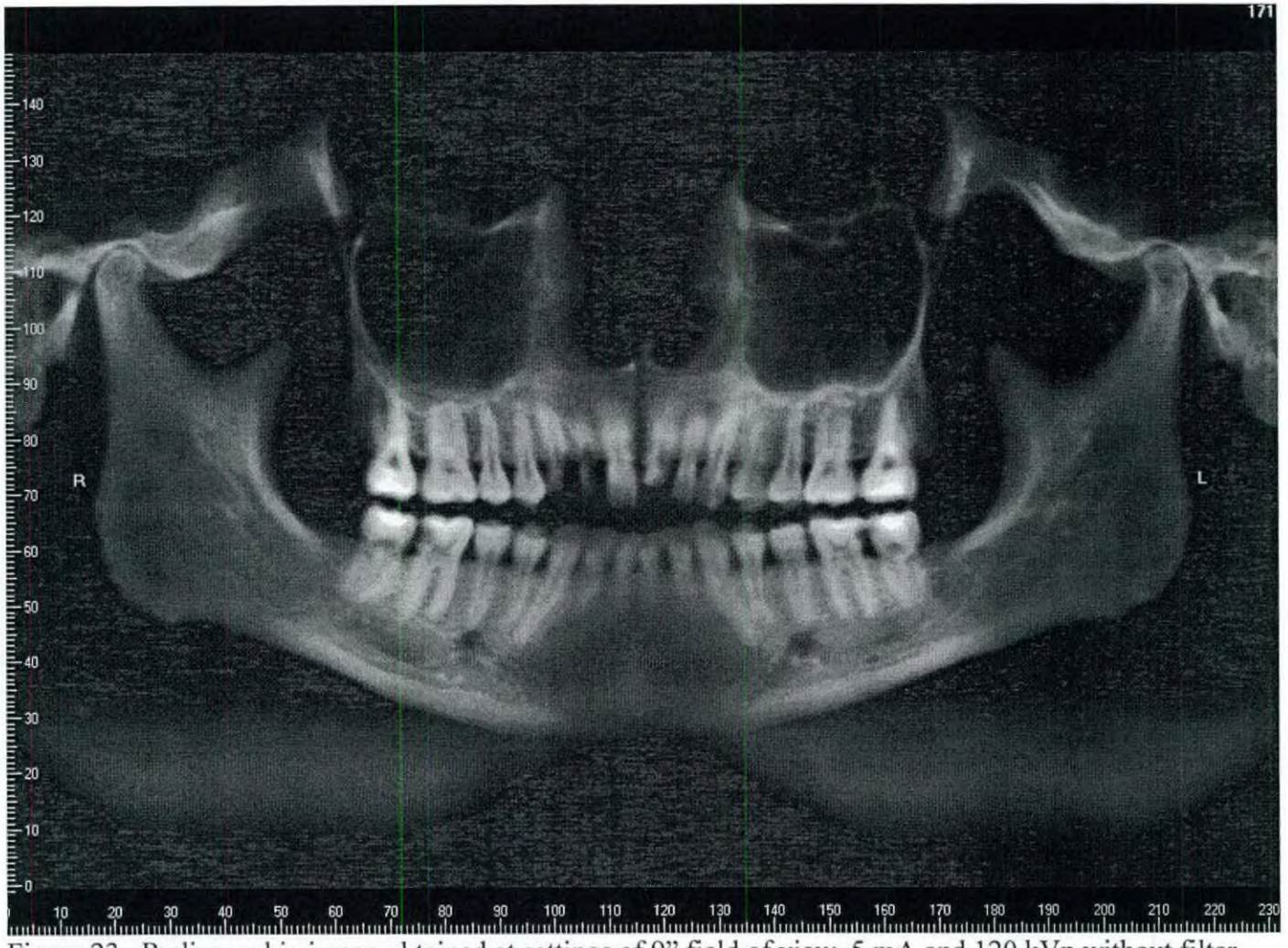


Figure 23. Radiographic image obtained at settings of 9" field of view, 5 mA and 120 kVp without filter.

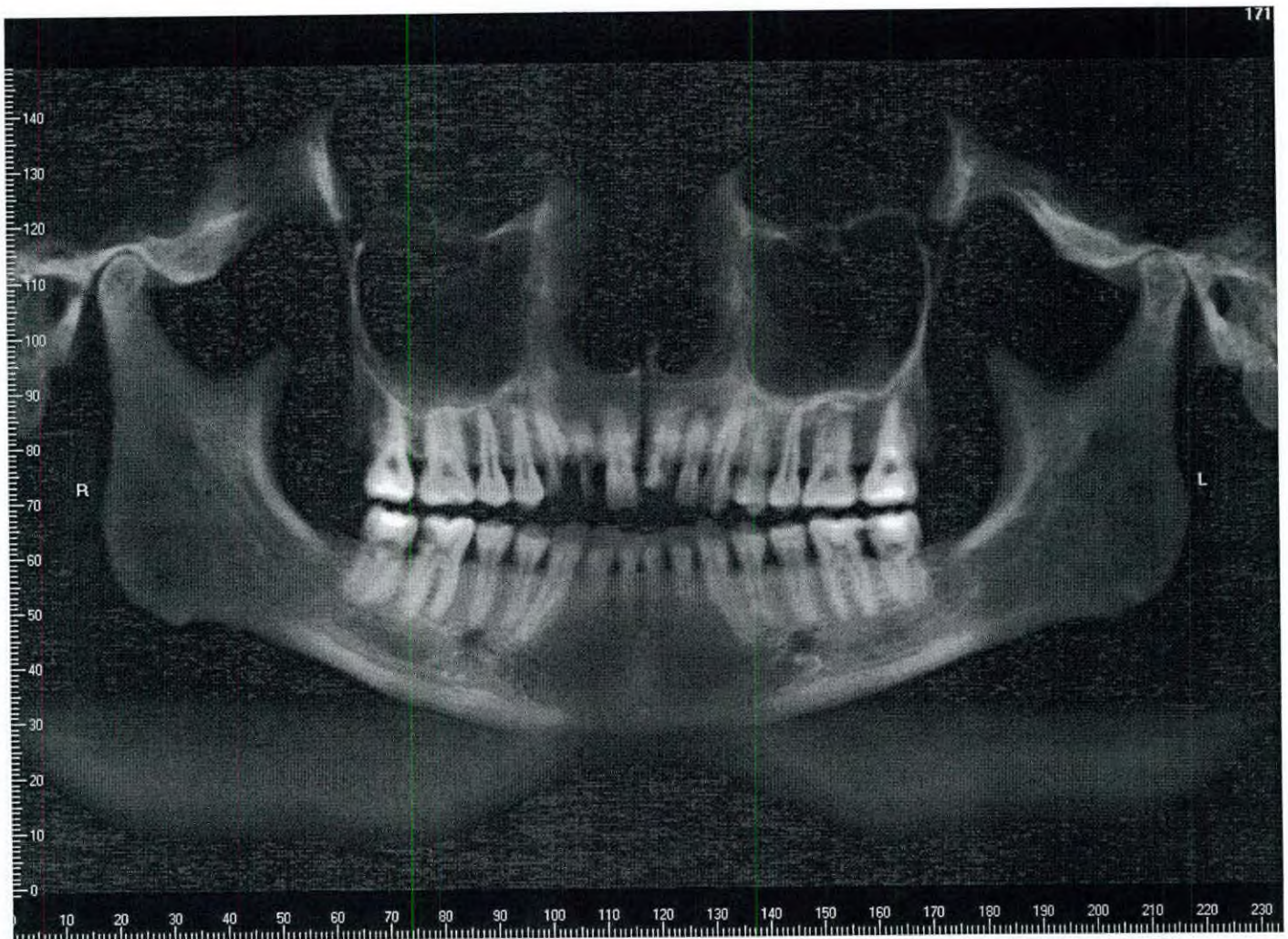


Figure 24. Radiographic image obtained at settings of 9" field of view, 5 mA and 120 kVp with filter.

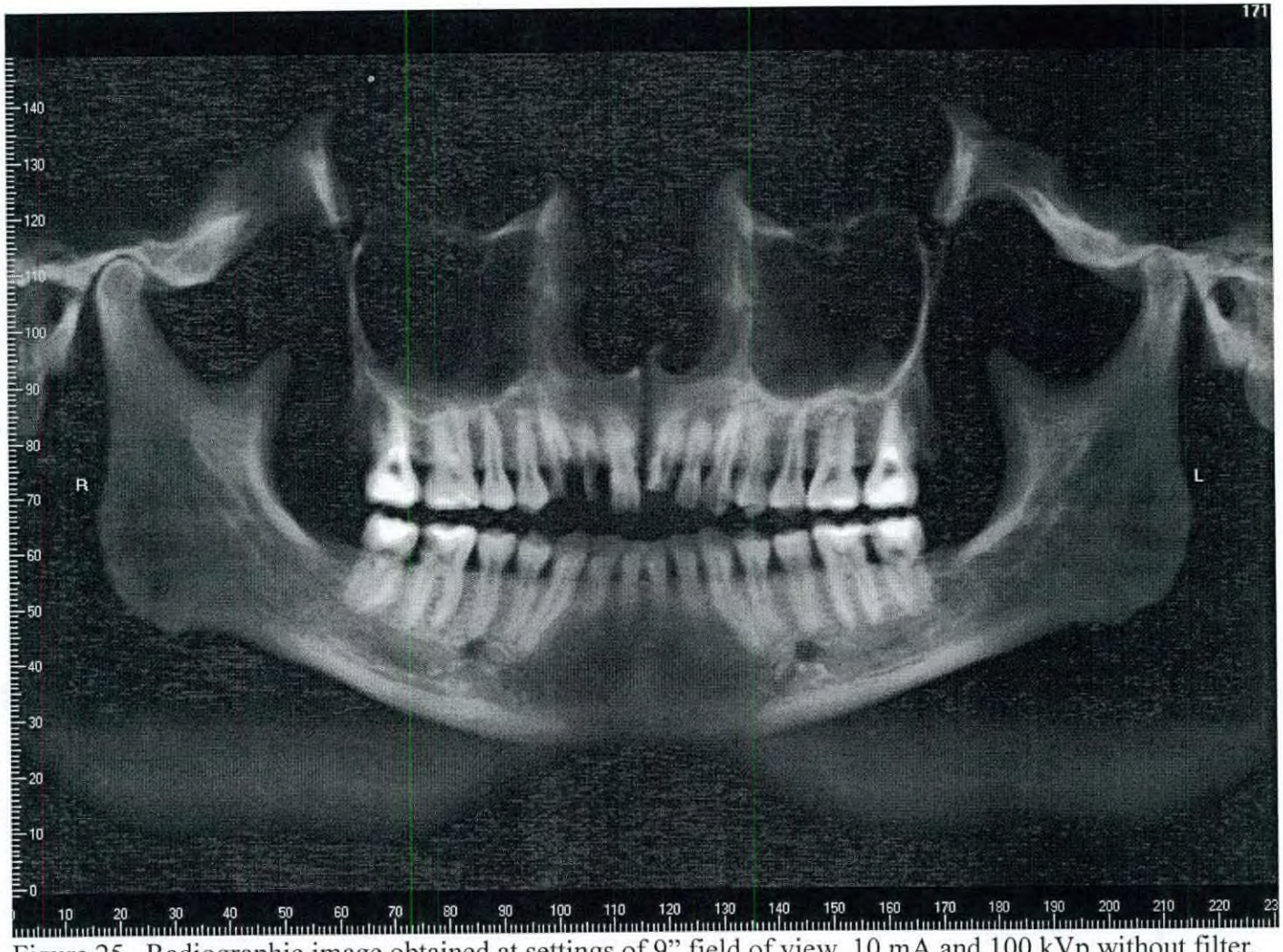


Figure 25. Radiographic image obtained at settings of 9" field of view, 10 mA and 100 kVp without filter.

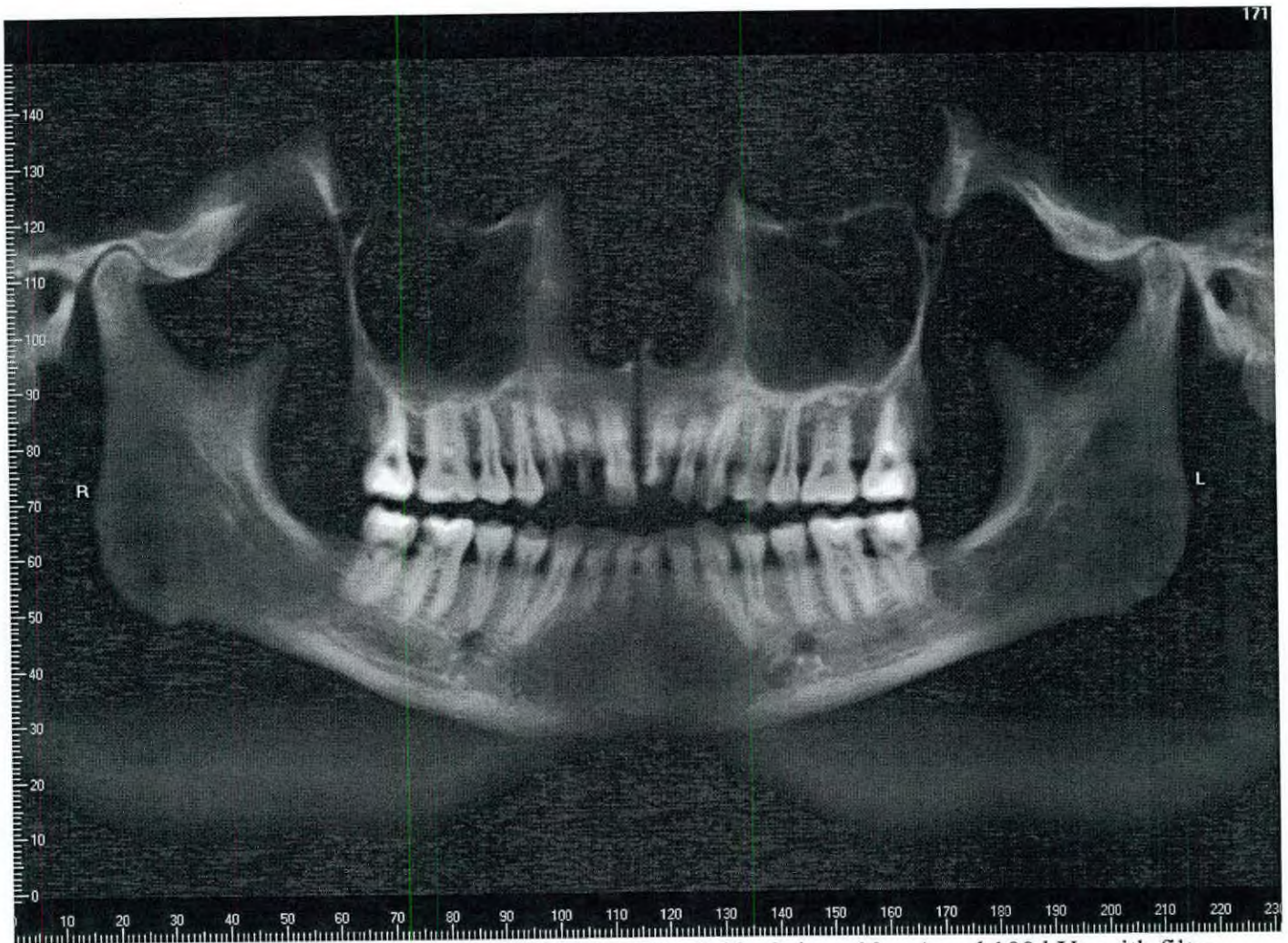


Figure 26. Radiographic image obtained at settings of 9" field of view, 10 mA and 100 kVp with filter.

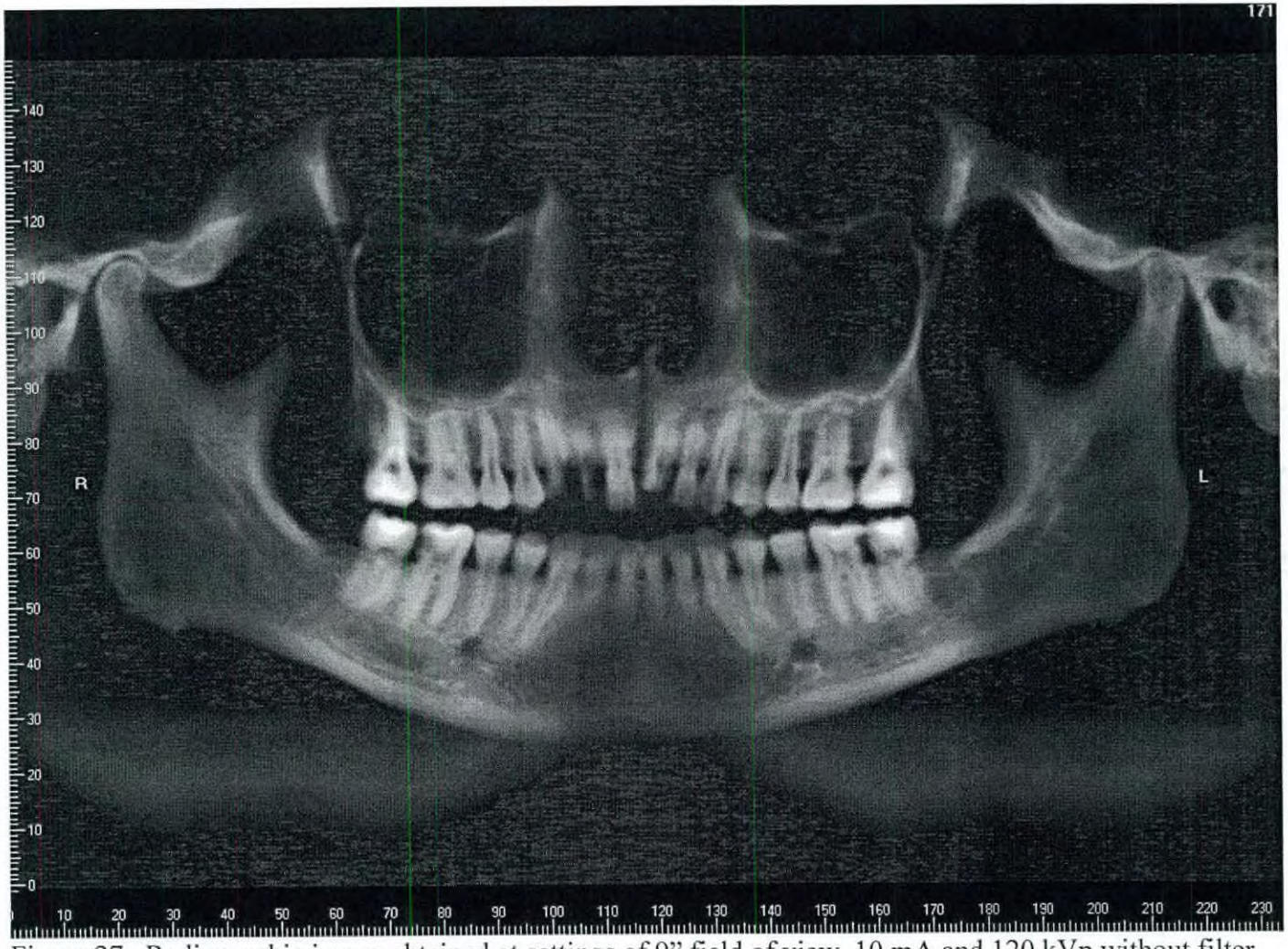


Figure 27. Radiographic image obtained at settings of 9" field of view, 10 mA and 120 kVp without filter.

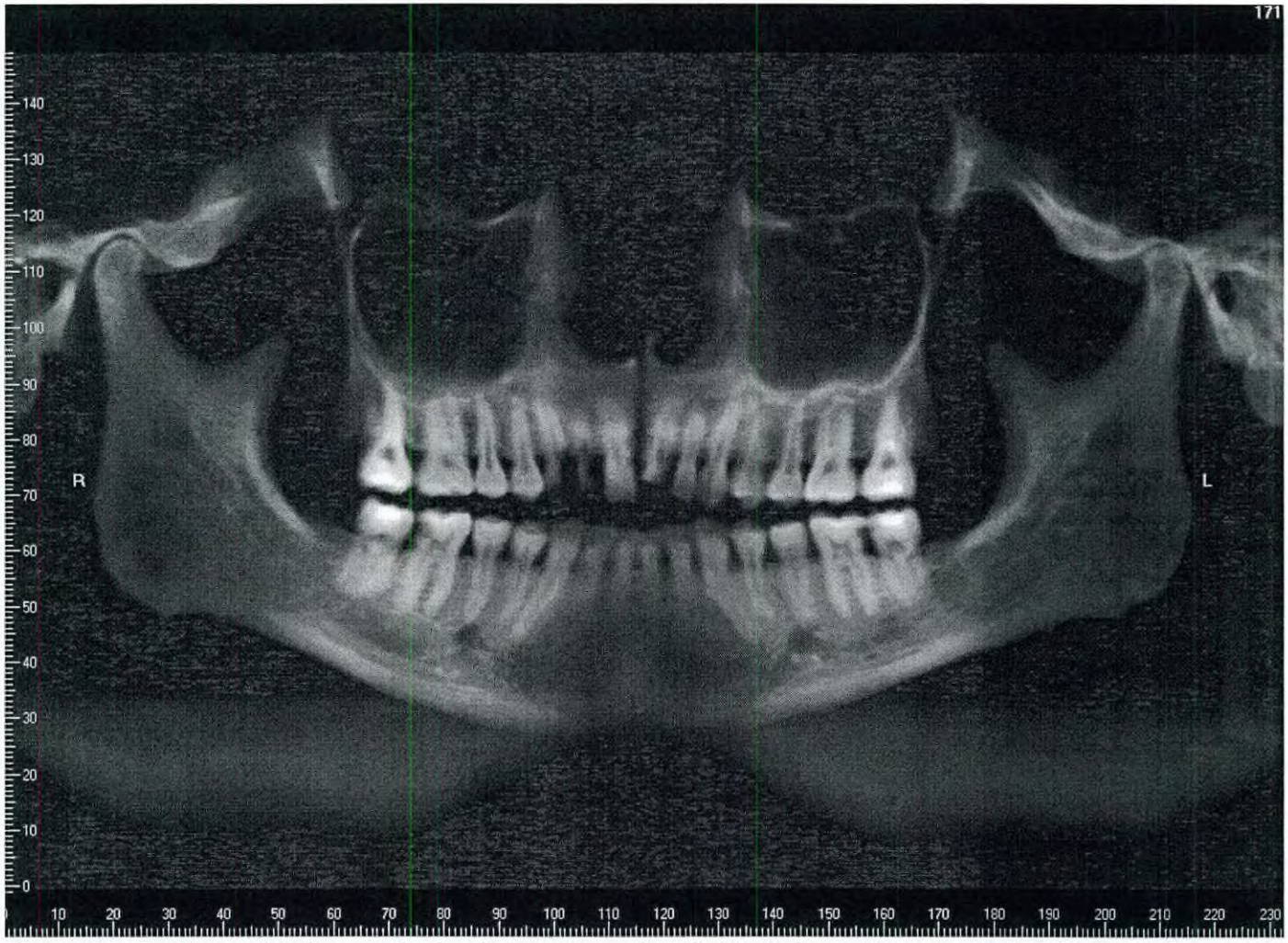


Figure 28. Radiographic image obtained at settings of 9" field of view, 10 mA and 120 kVp with filter.

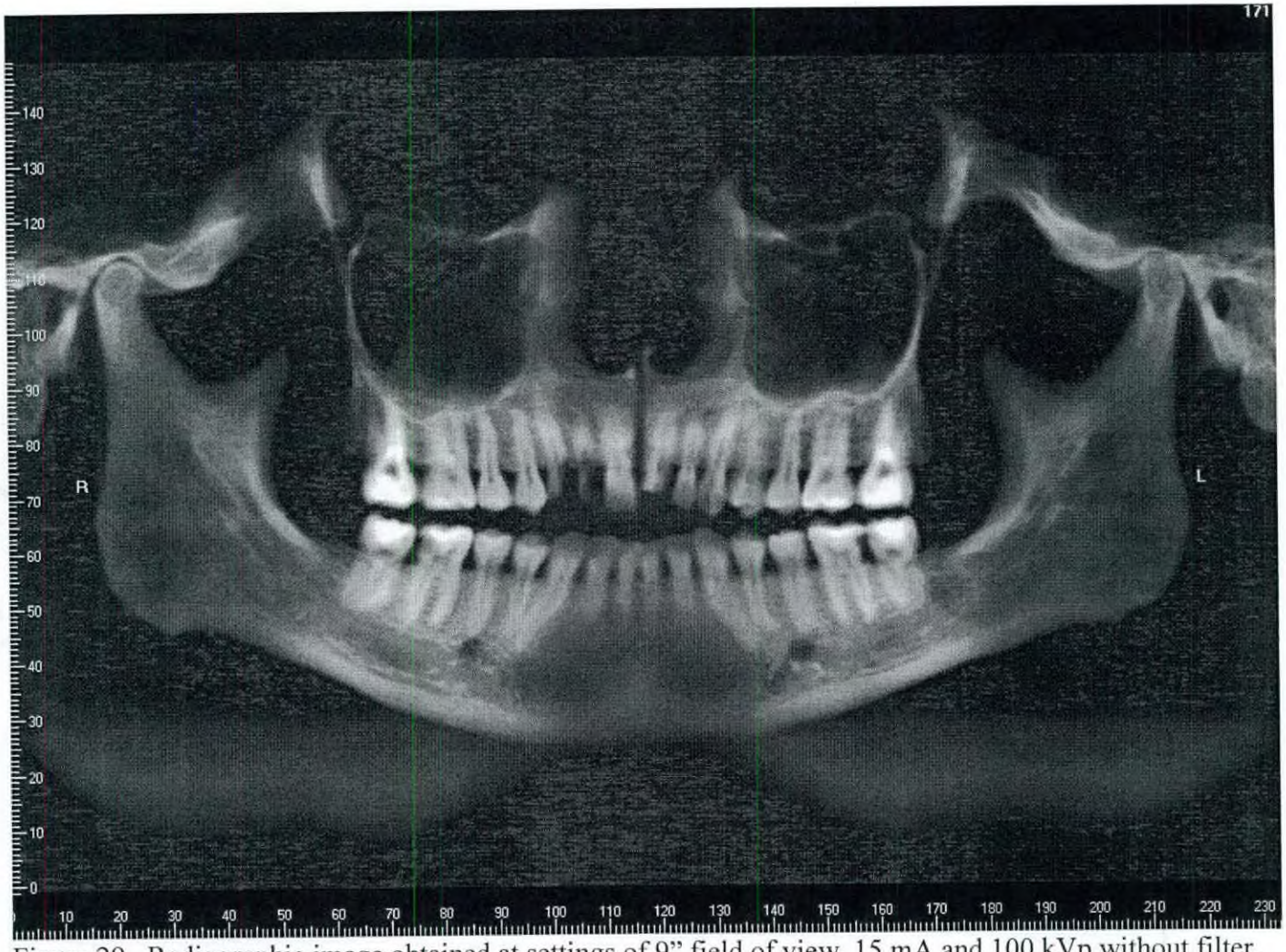


Figure 29. Radiographic image obtained at settings of 9" field of view, 15 mA and 100 kVp without filter.

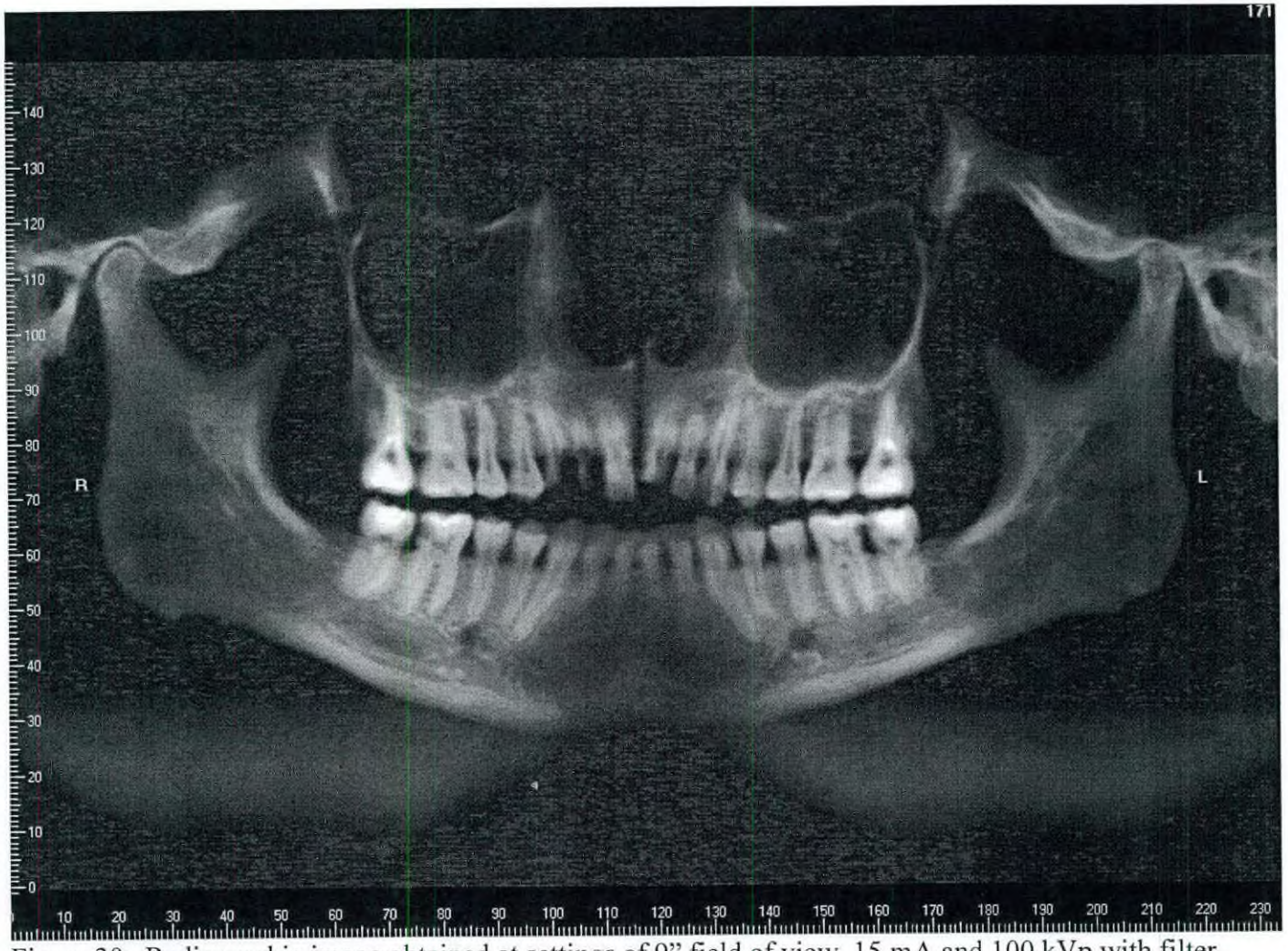


Figure 30. Radiographic image obtained at settings of 9" field of view, 15 mA and 100 kVp with filter.

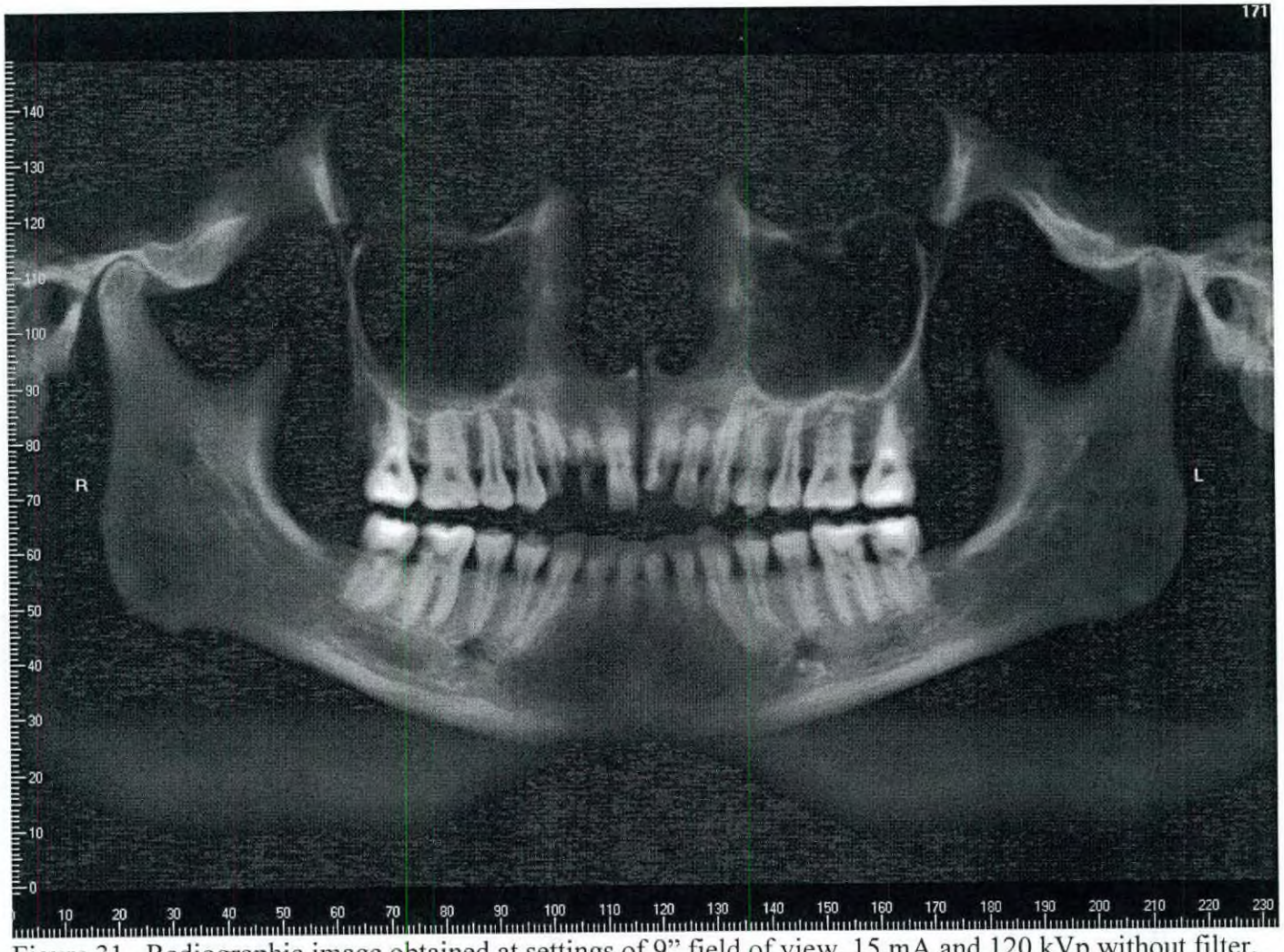


Figure 31. Radiographic image obtained at settings of 9" field of view, 15 mA and 120 kVp without filter.

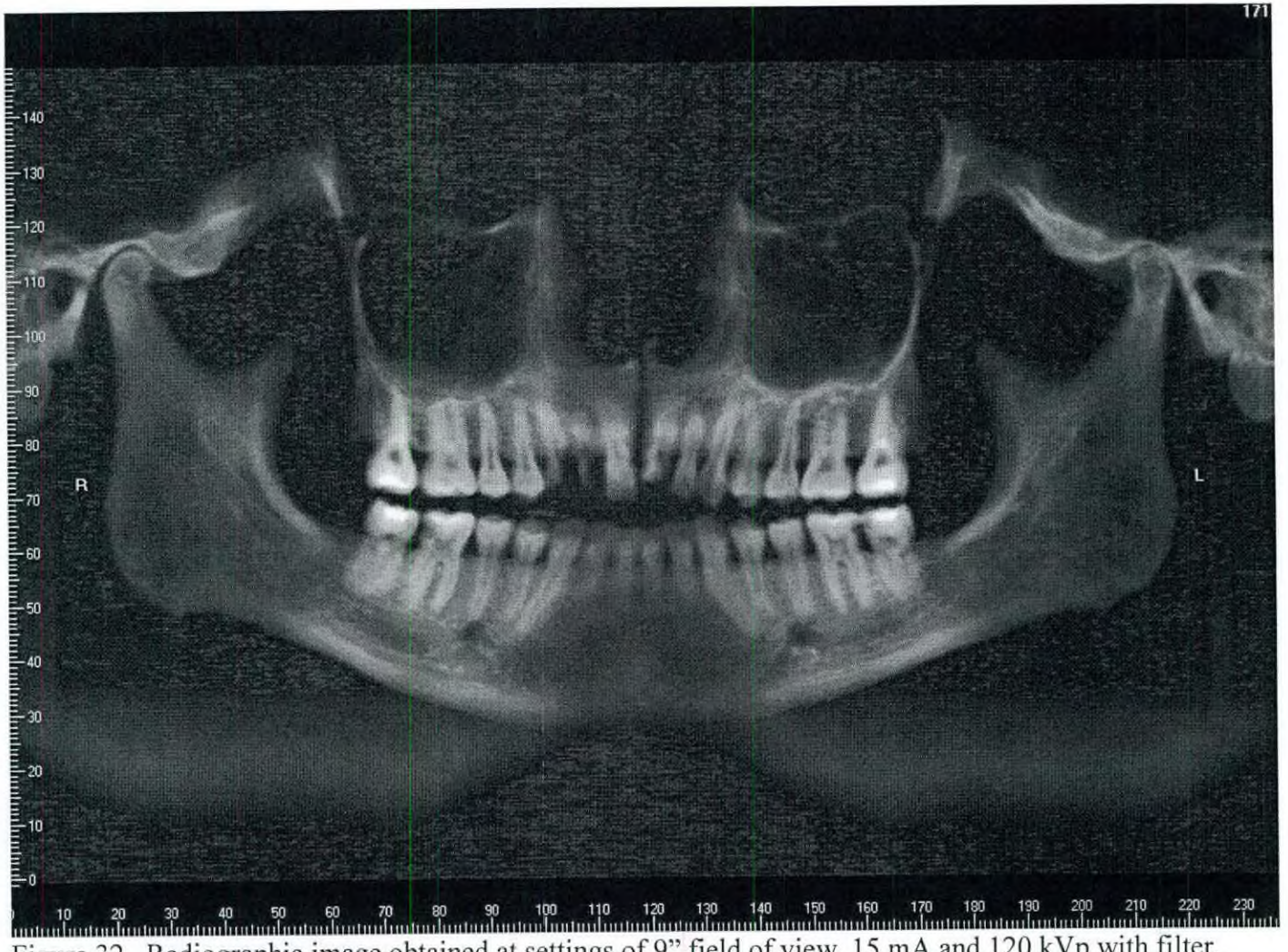


Figure 32. Radiographic image obtained at settings of 9" field of view, 15 mA and 120 kVp with filter.

APPENDIX 5

Twelve Inch Lateral Cephalogram Images

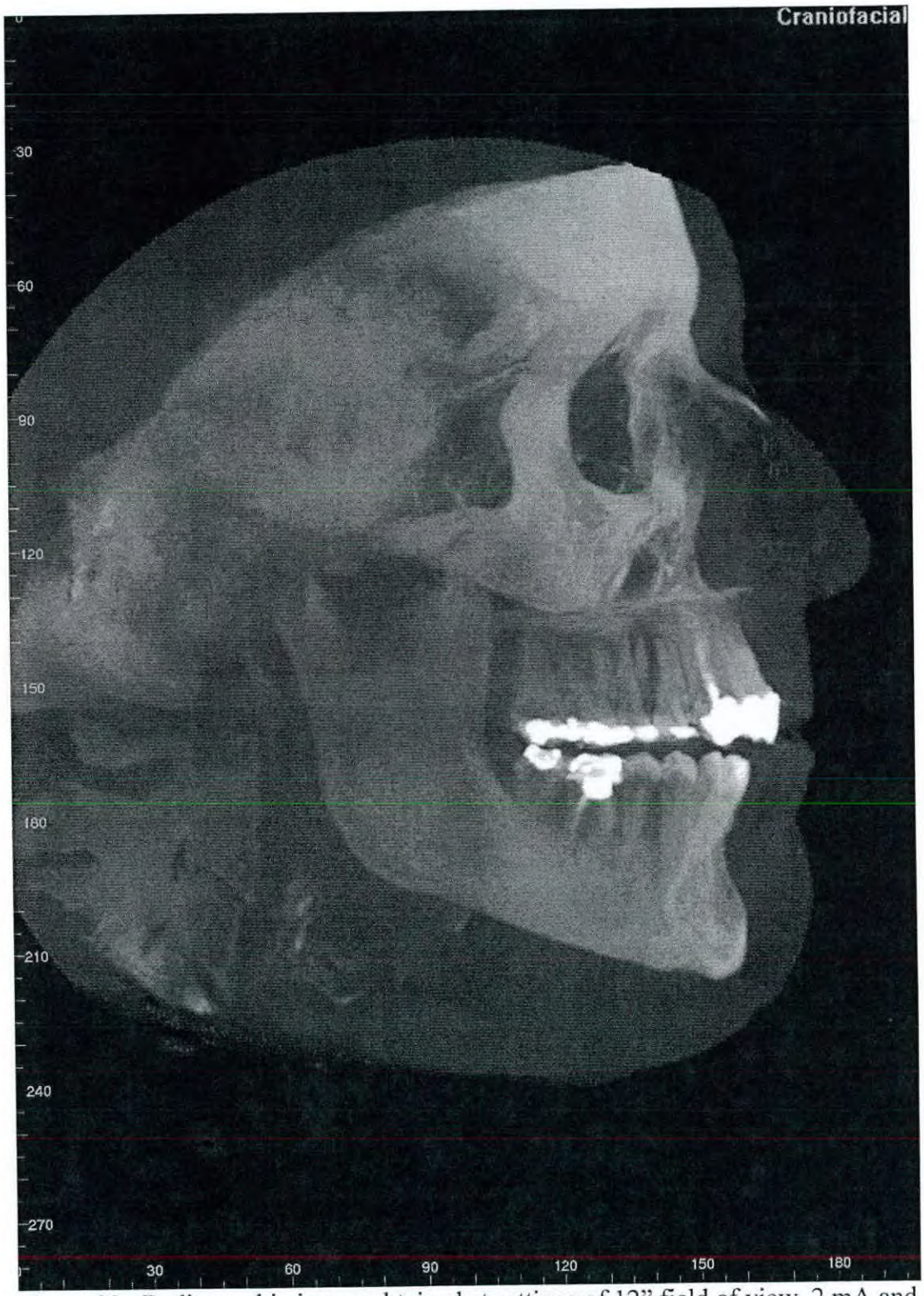


Figure 33. Radiographic image obtained at settings of 12" field of view, 2 mA and 100 kVp without filter.

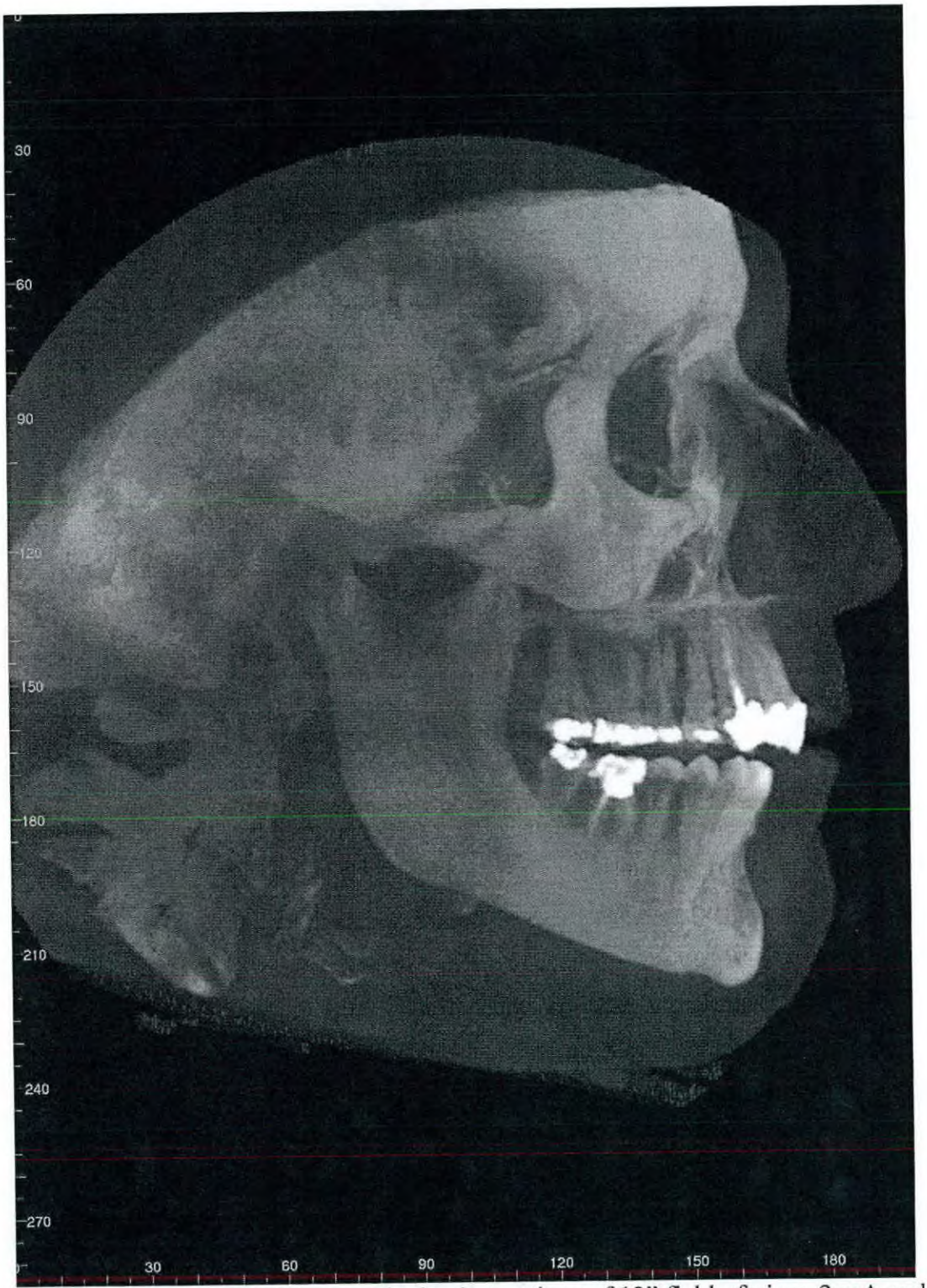


Figure 34. Radiographic image obtained at settings of 12" field of view, 2 mA and 100 kVp with filter.

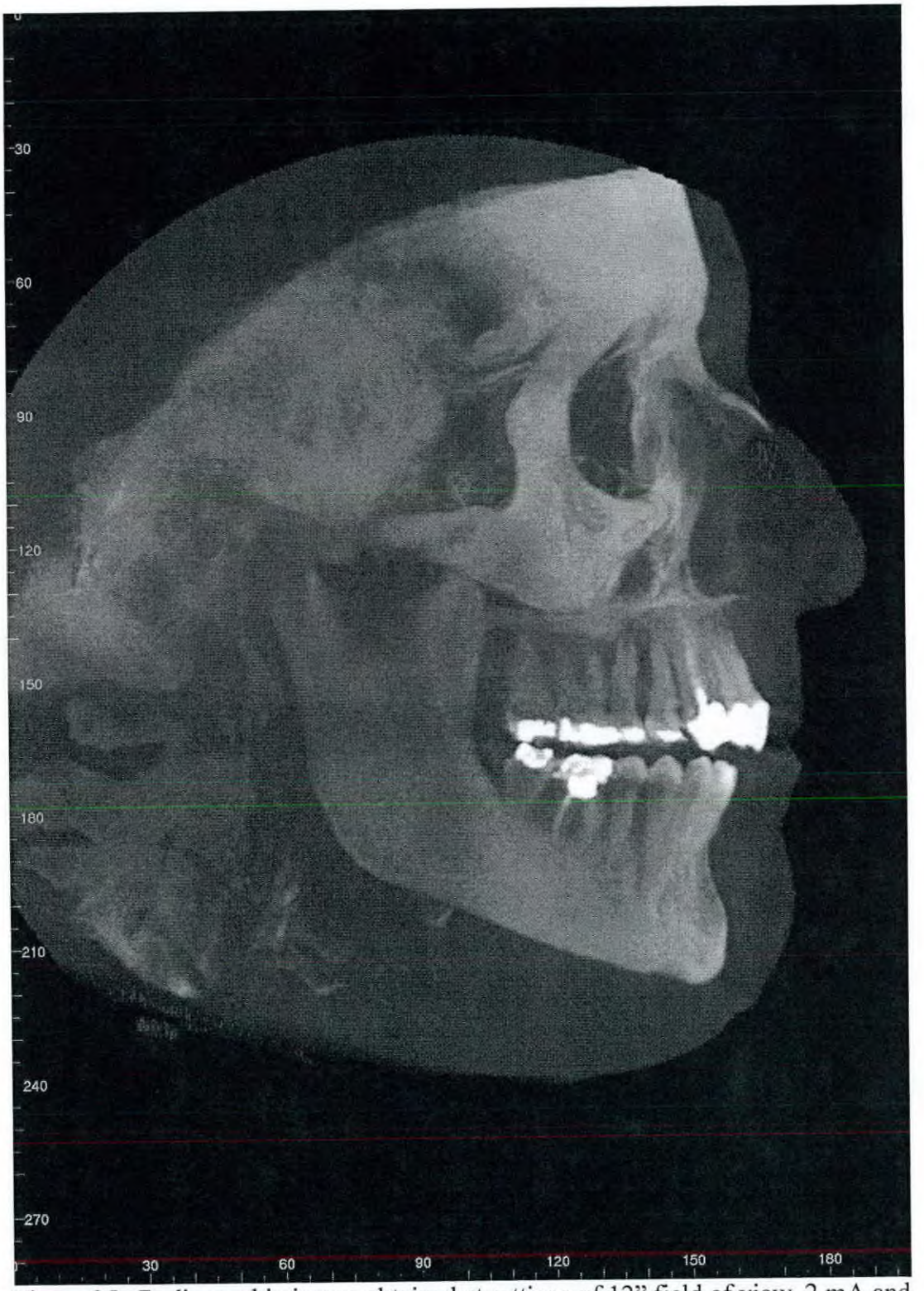


Figure 35. Radiographic image obtained at settings of 12" field of view, 2 mA and 120 kVp without filter.

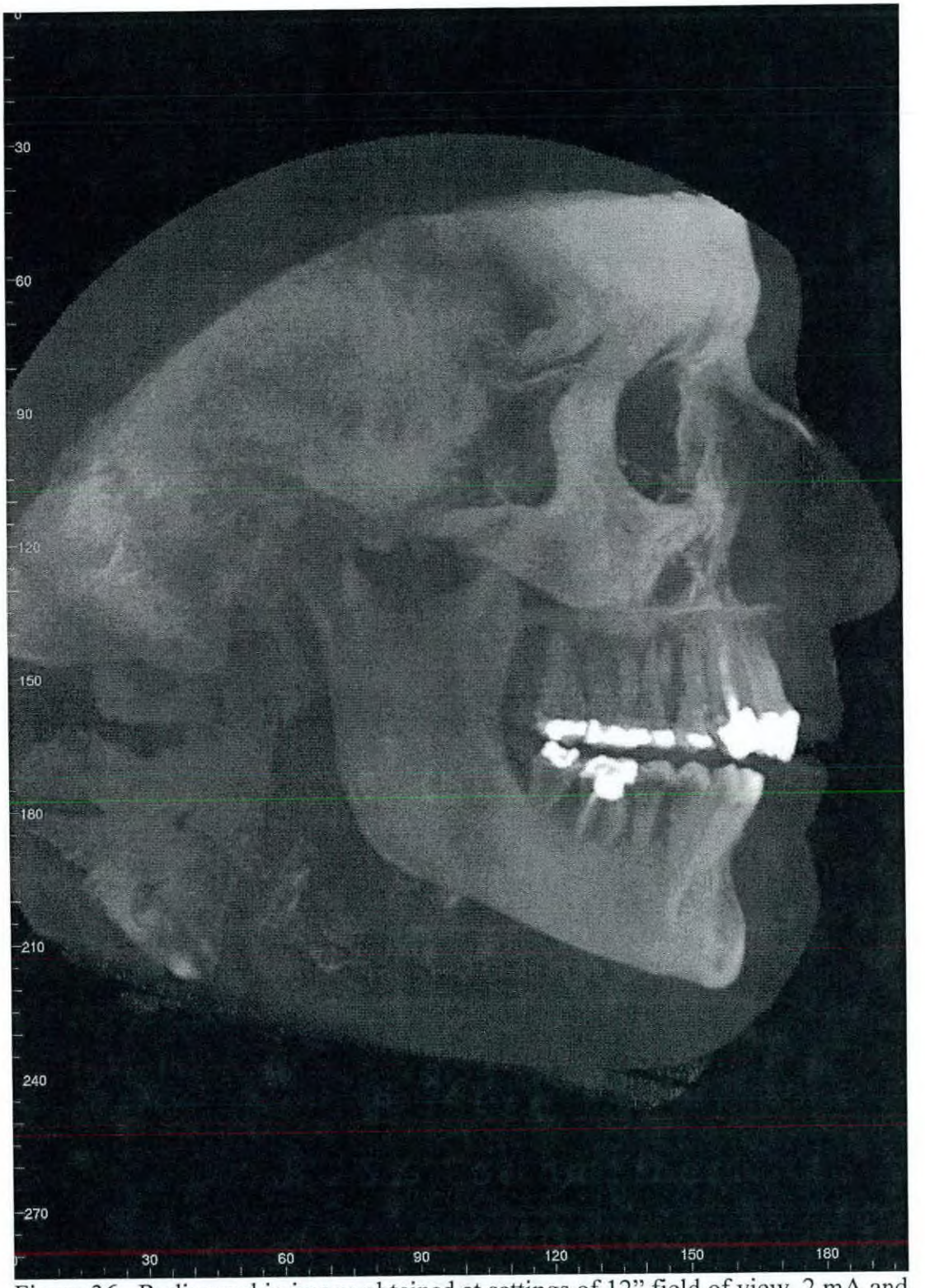


Figure 36. Radiographic image obtained at settings of 12" field of view, 2 mA and 120 kVp with filter.

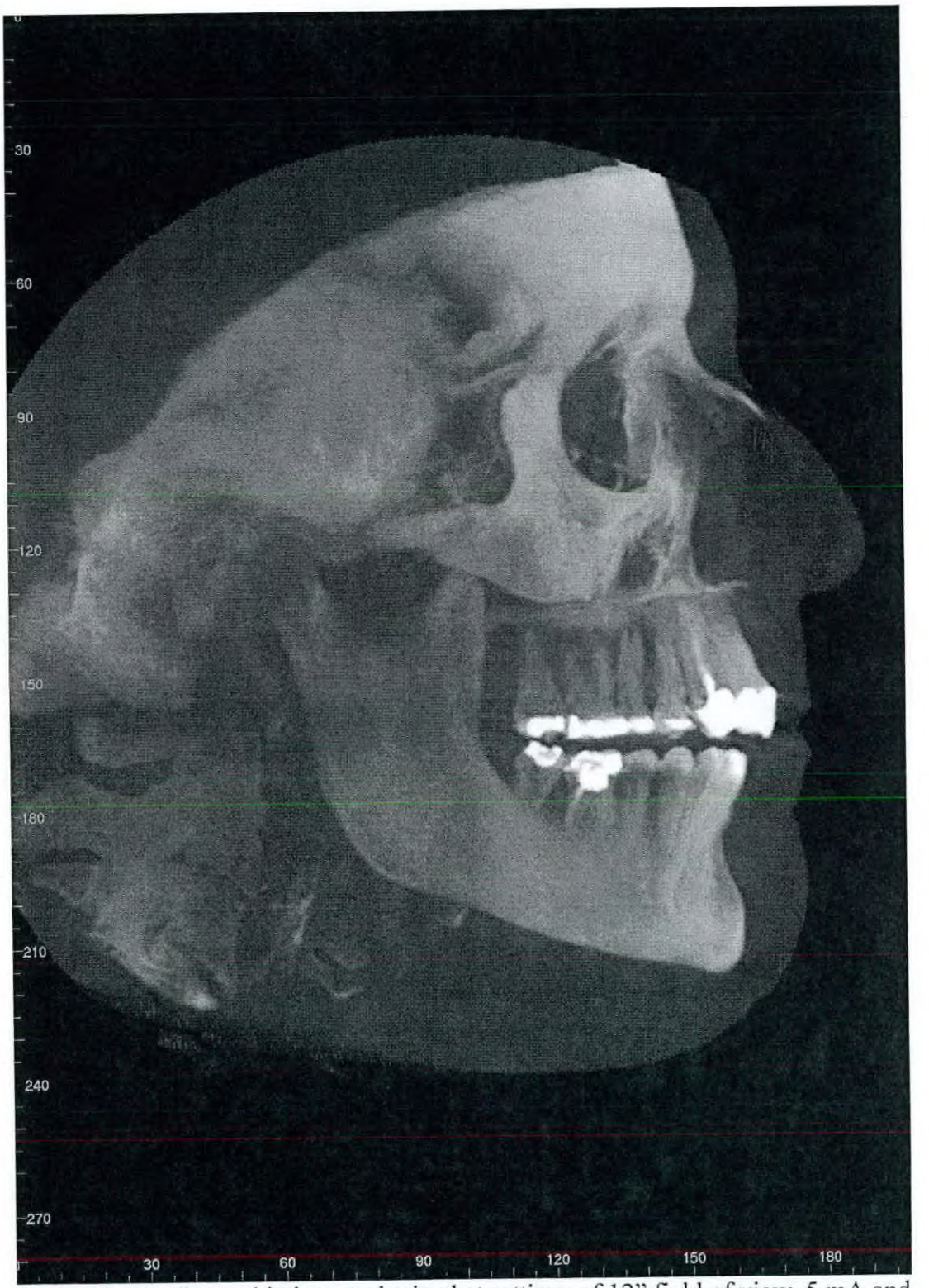


Figure 37. Radiographic image obtained at settings of 12" field of view, 5 mA and 100 kVp without filter.

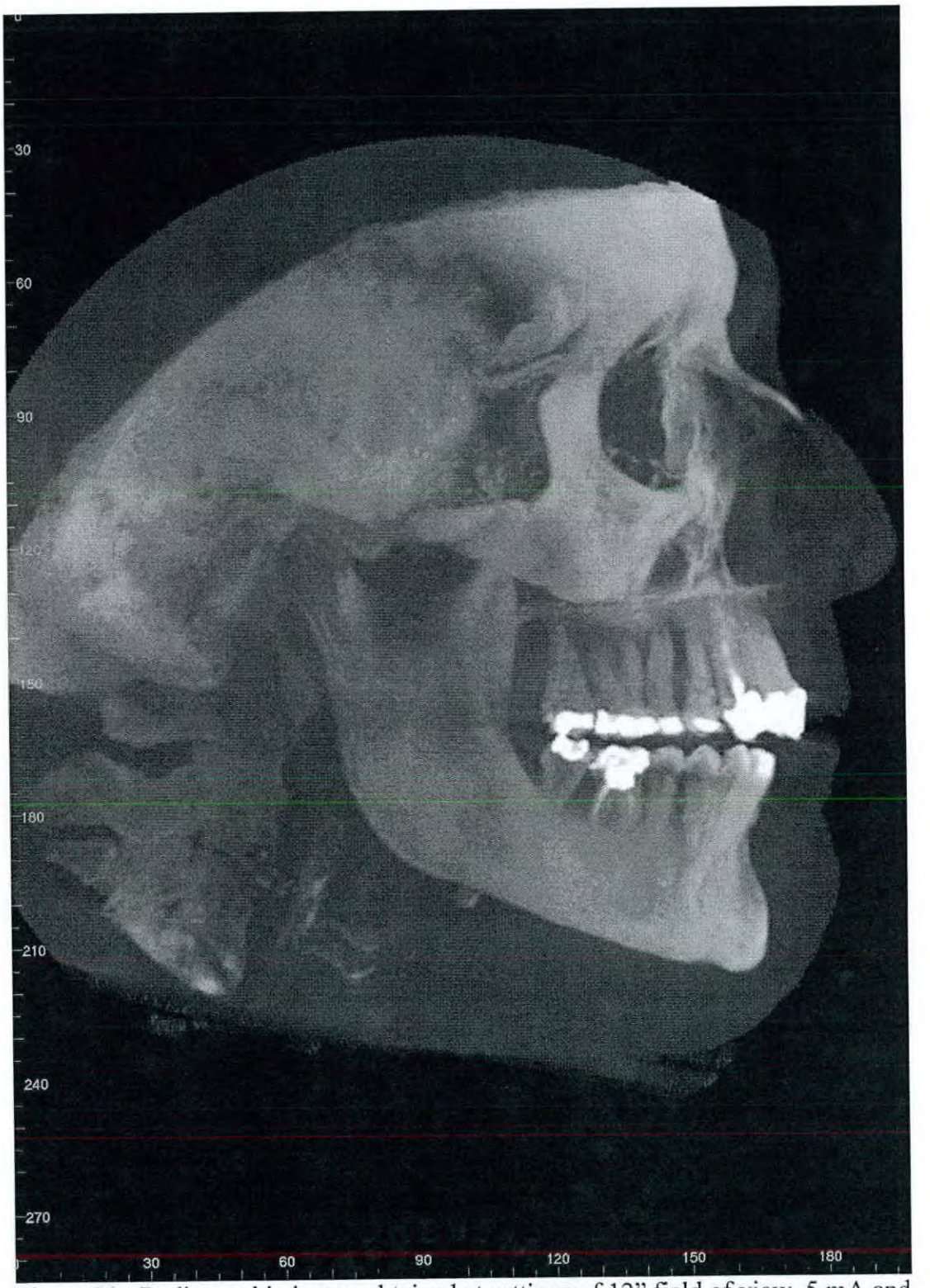


Figure 38. Radiographic image obtained at settings of 12" field of view, 5 mA and 100 kVp with filter.

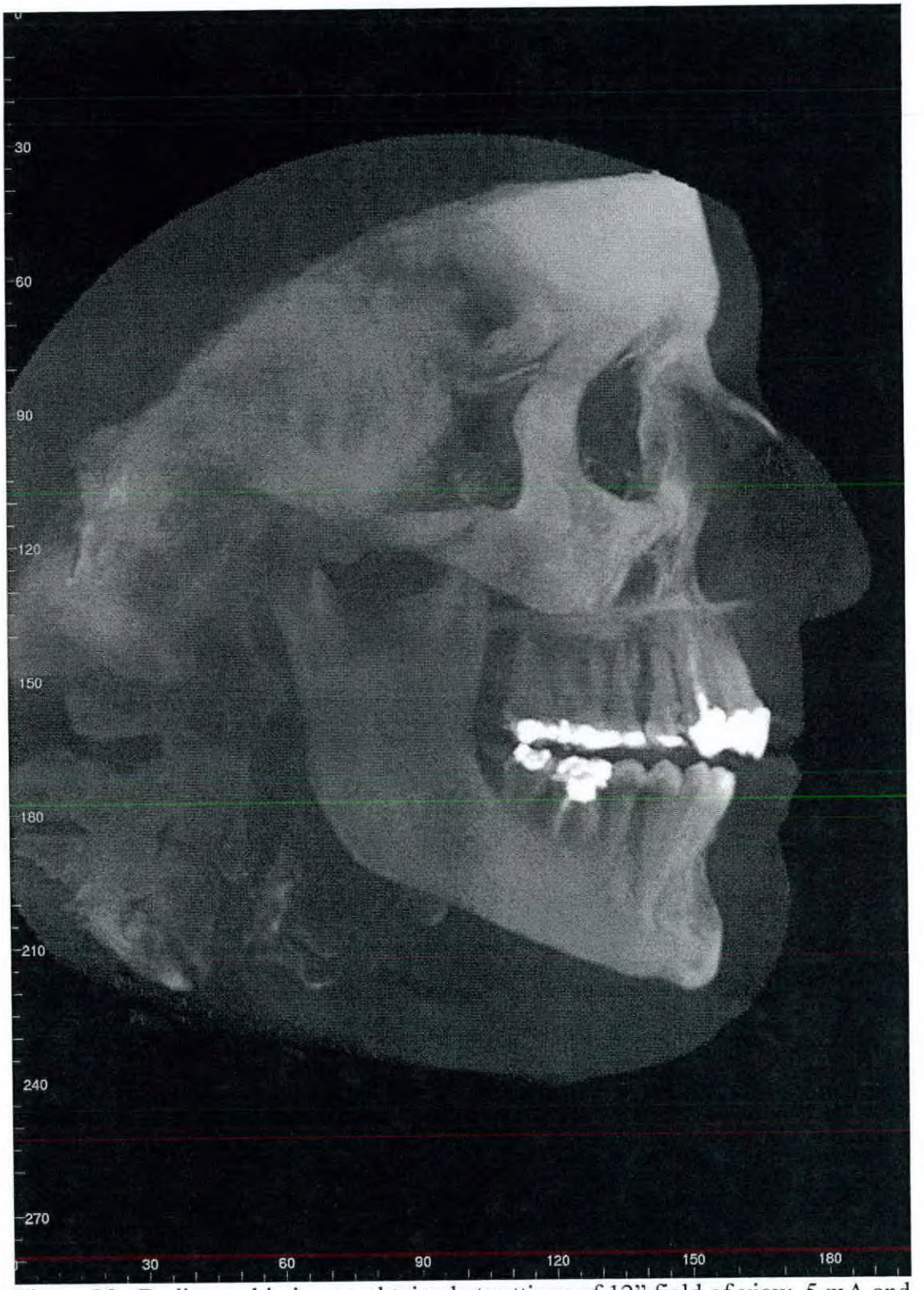


Figure 39. Radiographic image obtained at settings of 12" field of view, 5 mA and 120 kVp without filter.

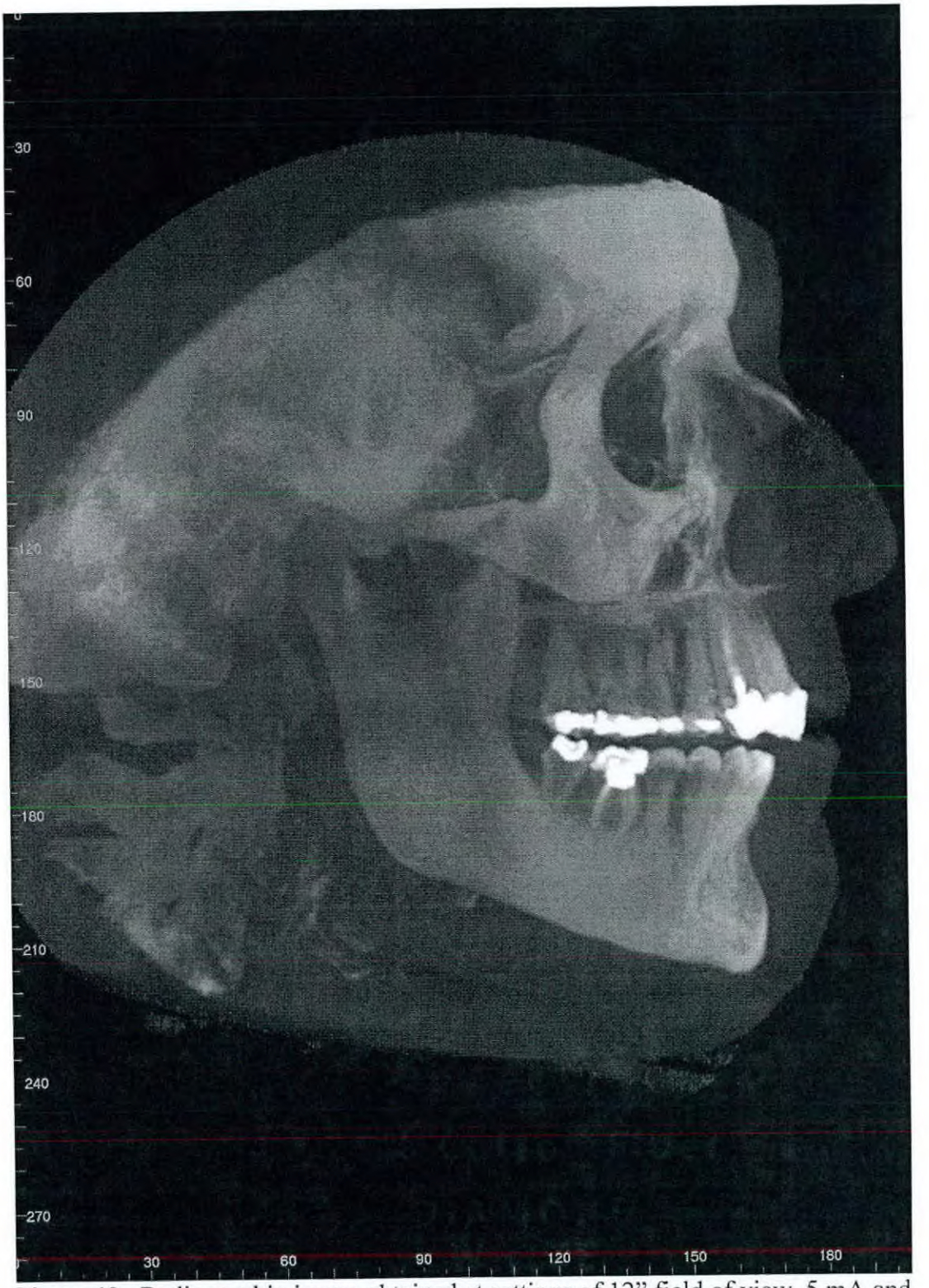


Figure 40. Radiographic image obtained at settings of 12" field of view, 5 mA and 120 kVp with filter.

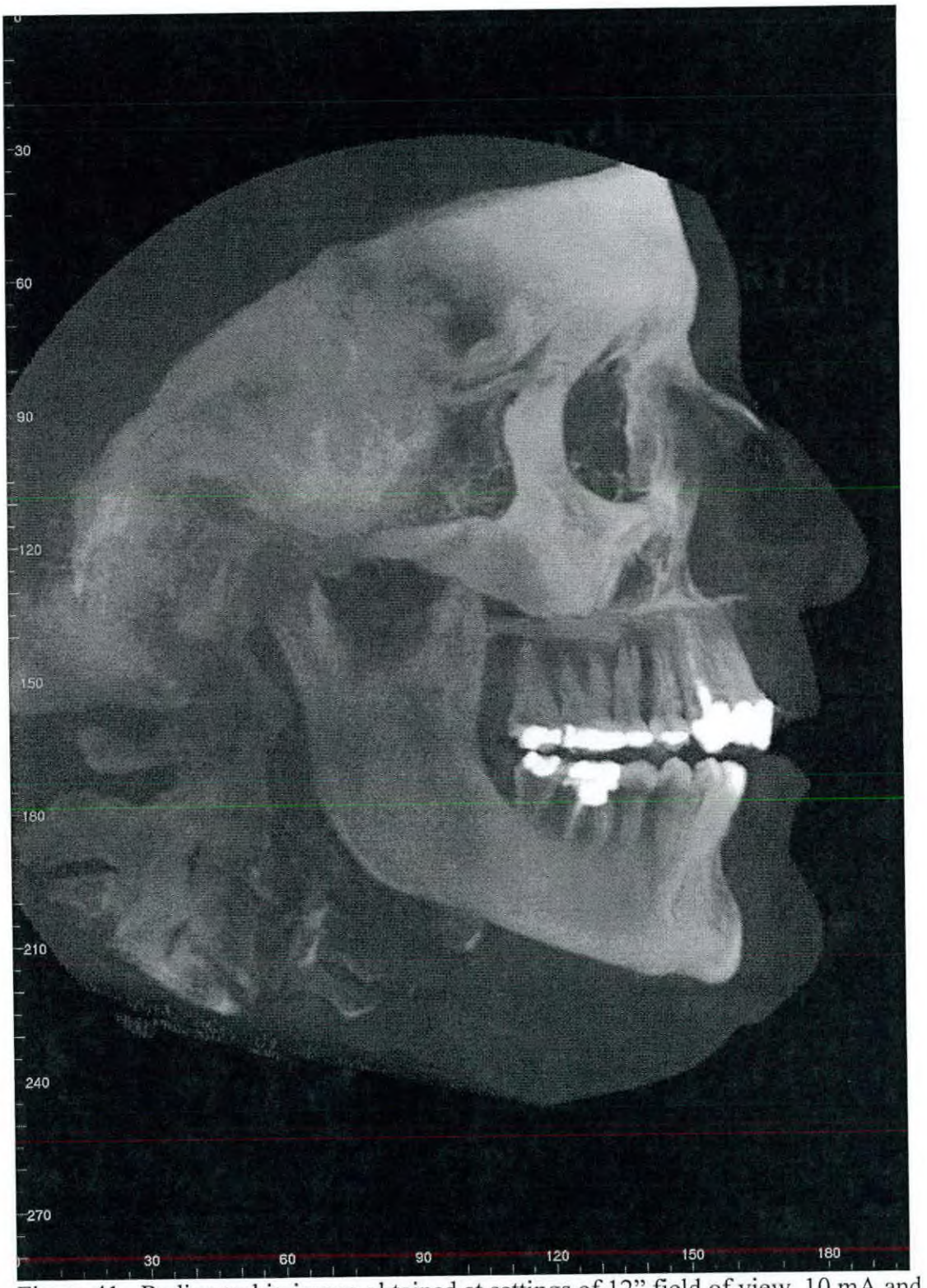


Figure 41. Radiographic image obtained at settings of 12" field of view, 10 mA and 100 kVp without filter.

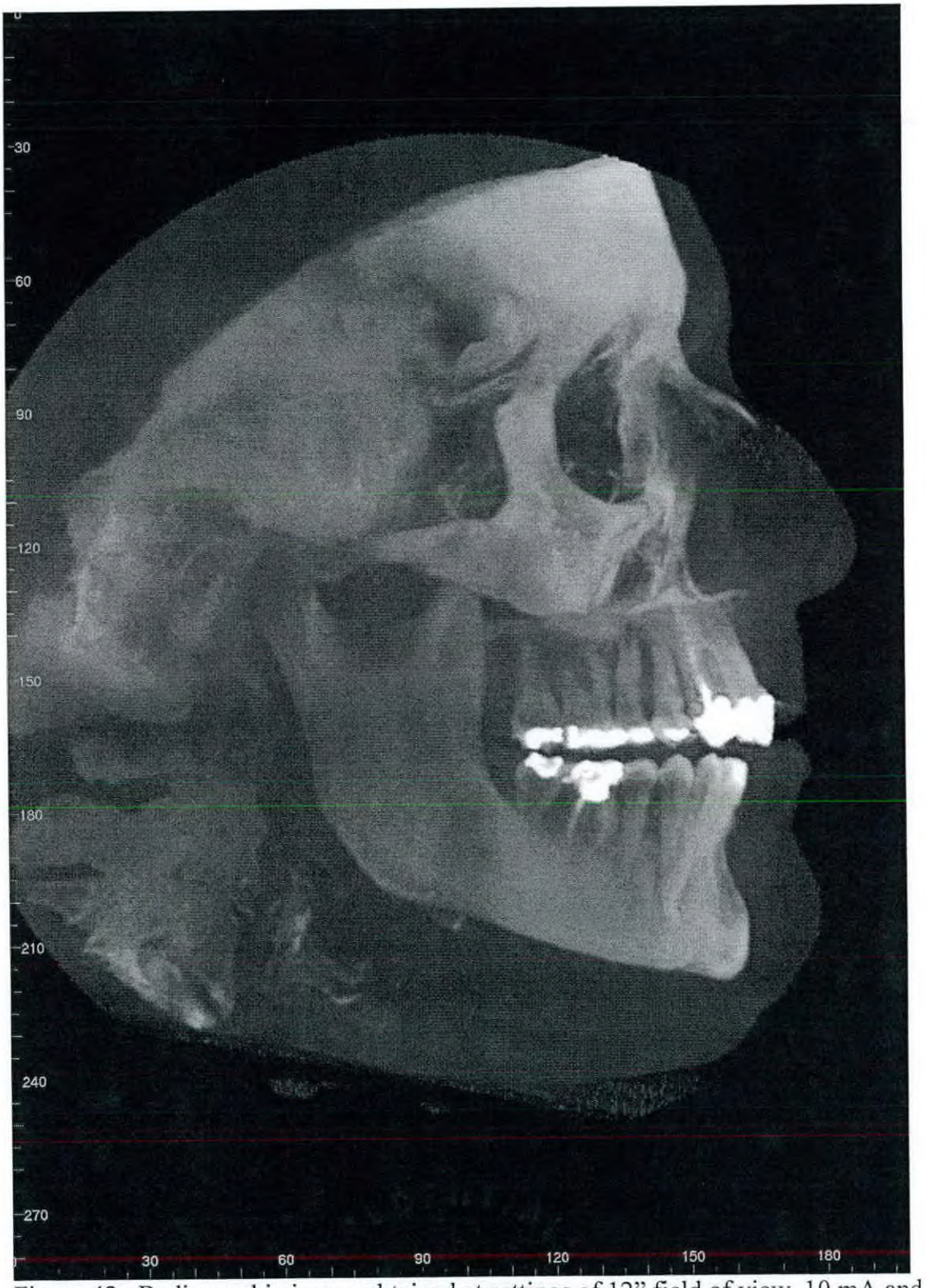


Figure 42. Radiographic image obtained at settings of 12" field of view, 10 mA and 100 kVp with filter.

Department of Commerce

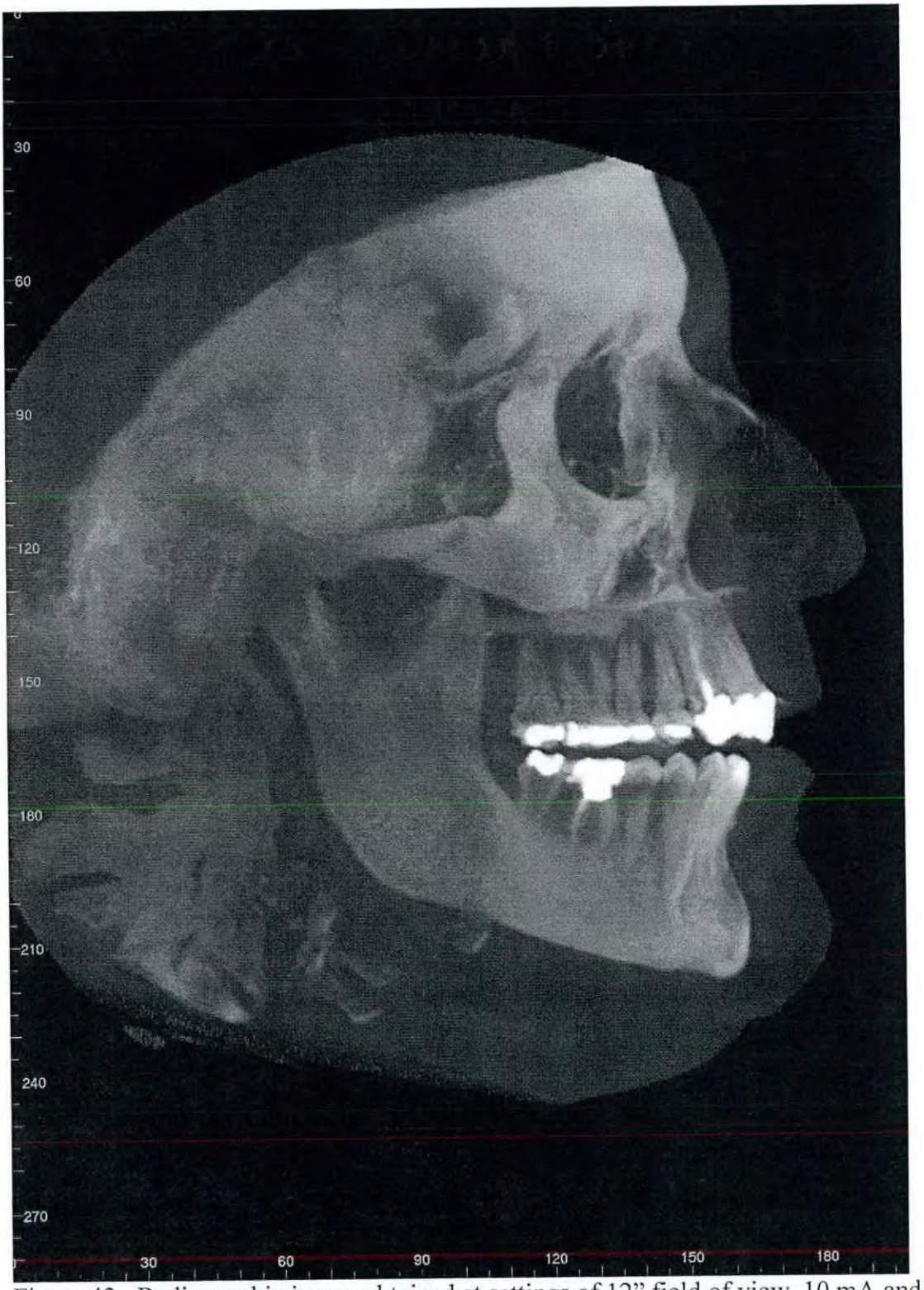


Figure 43. Radiographic image obtained at settings of 12" field of view, 10 mA and 120 kVp without filter.

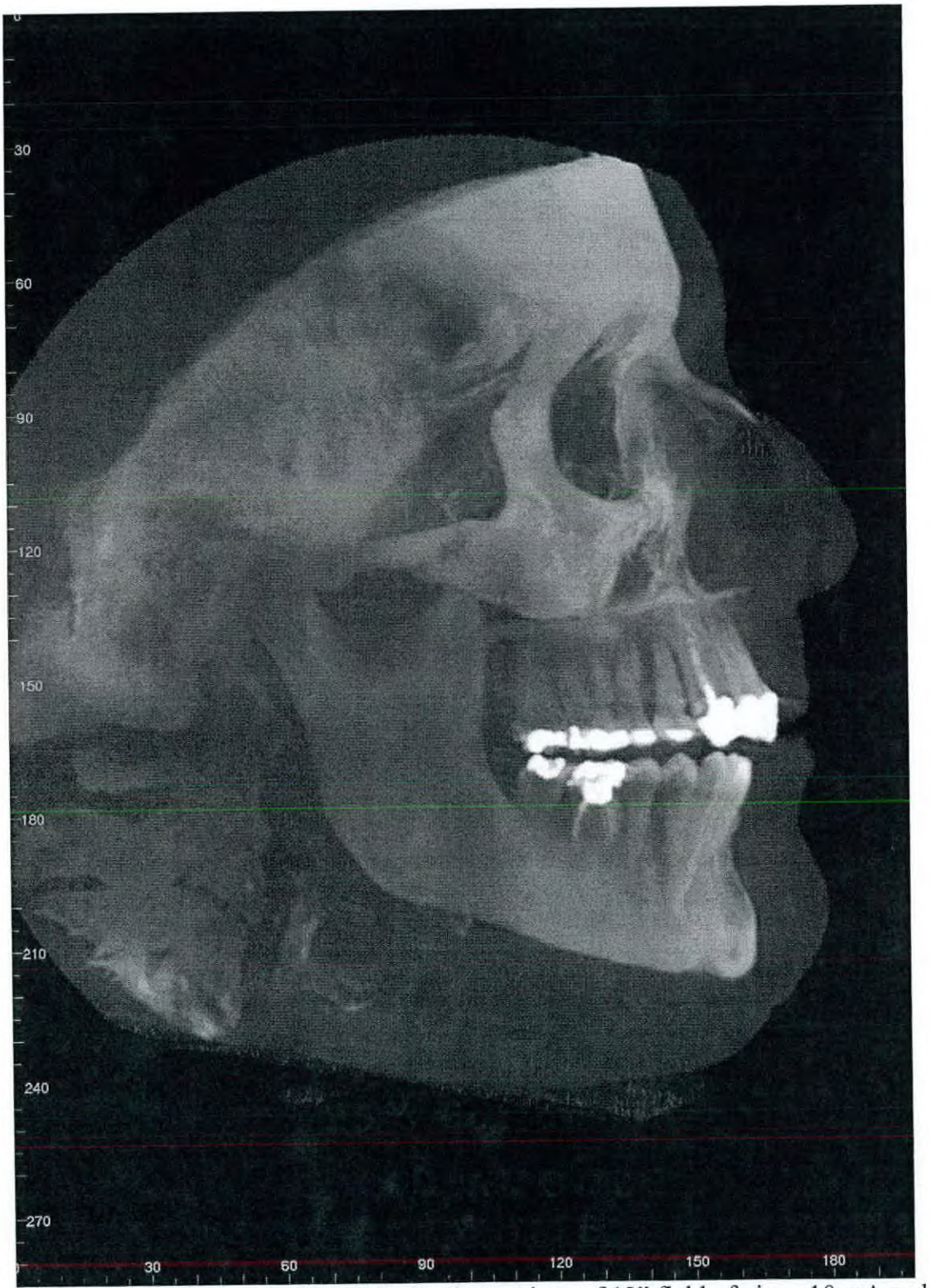


Figure 44. Radiographic image obtained at settings of 12" field of view, 10 mA and 120 kVp with filter.

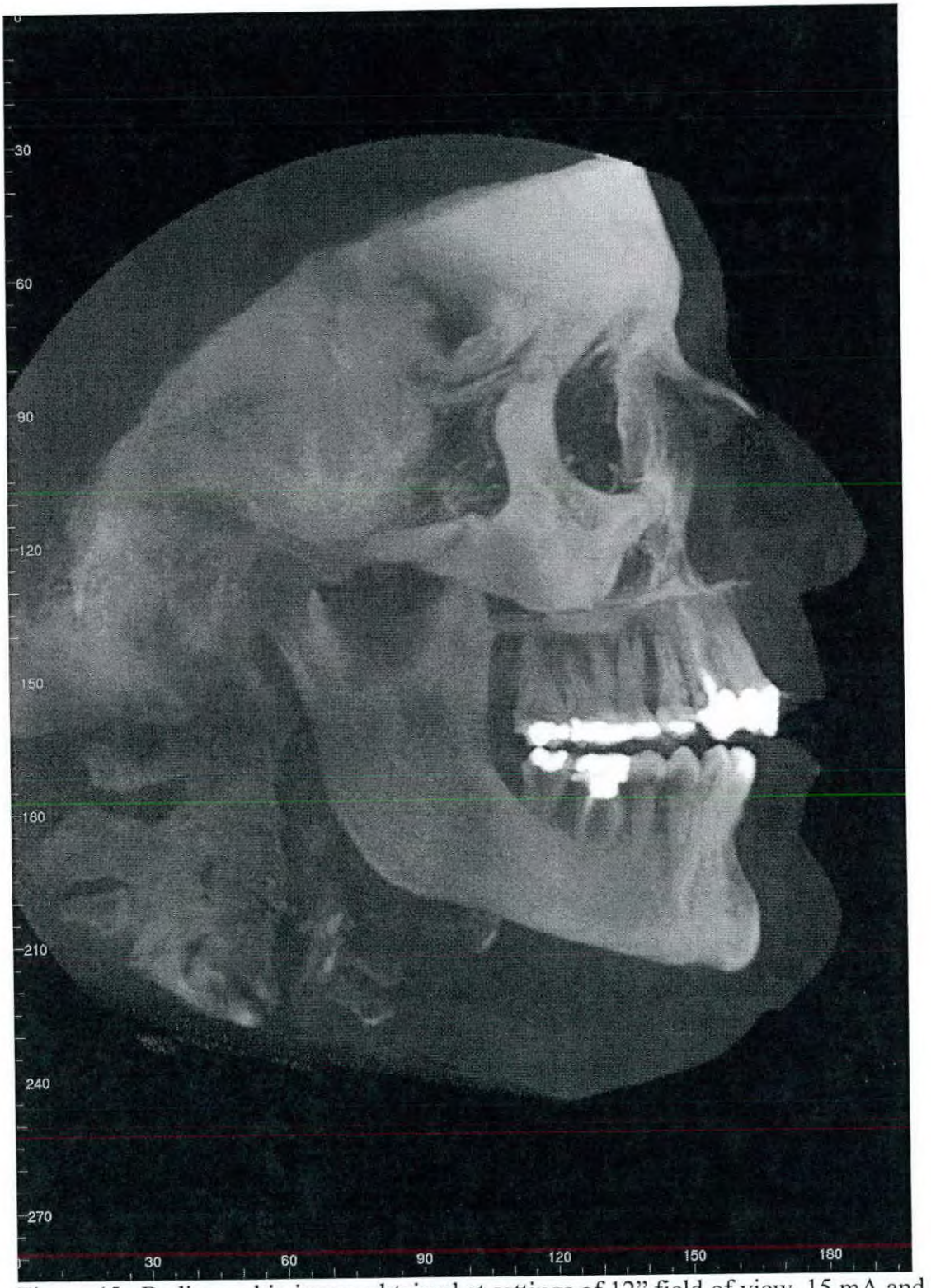


Figure 45. Radiographic image obtained at settings of 12" field of view, 15 mA and 100 kVp without filter.

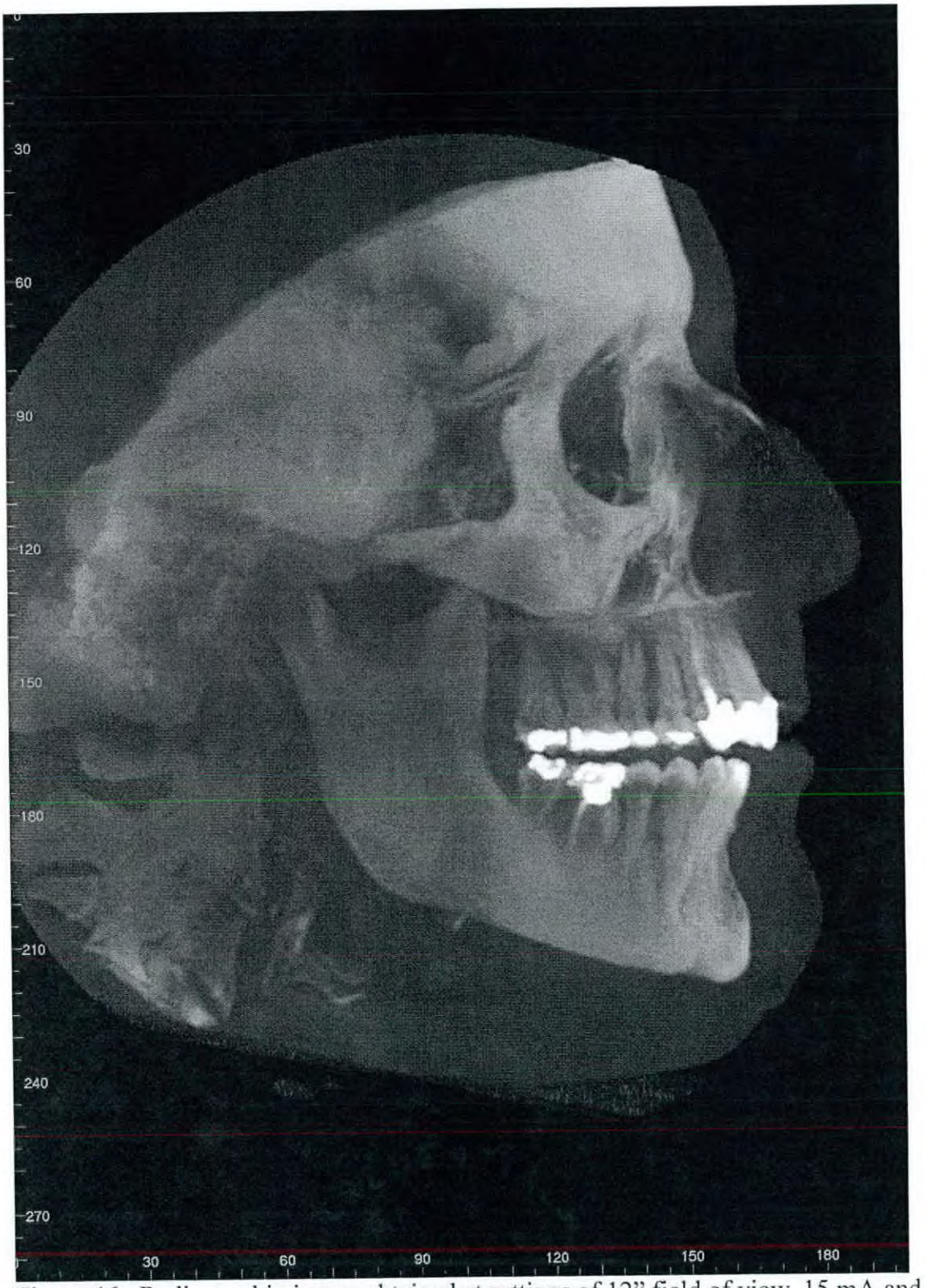


Figure 46. Radiographic image obtained at settings of 12" field of view, 15 mA and 100 kVp with filter.

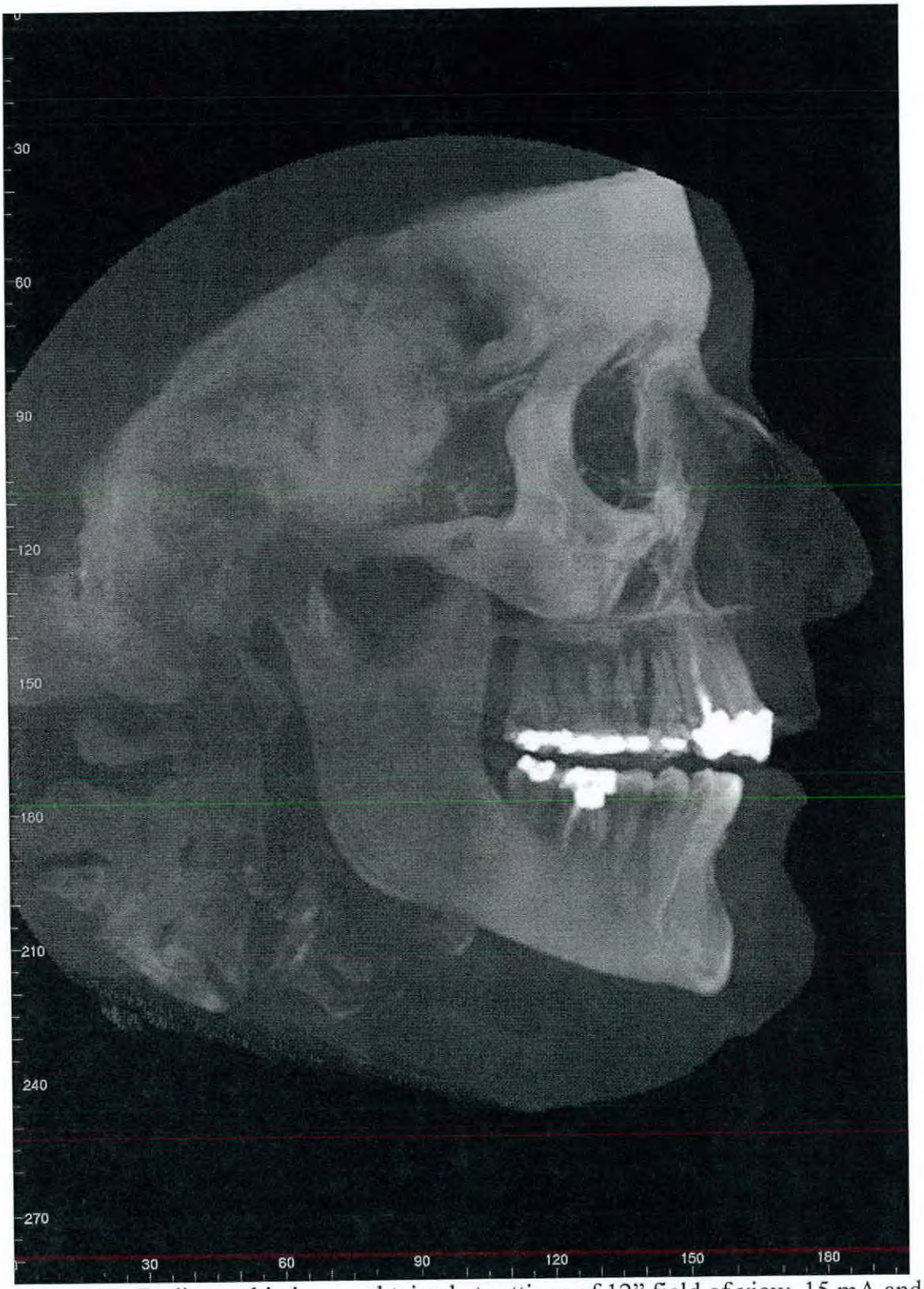


Figure 47. Radiographic image obtained at settings of 12" field of view, 15 mA and 120 kVp without filter.

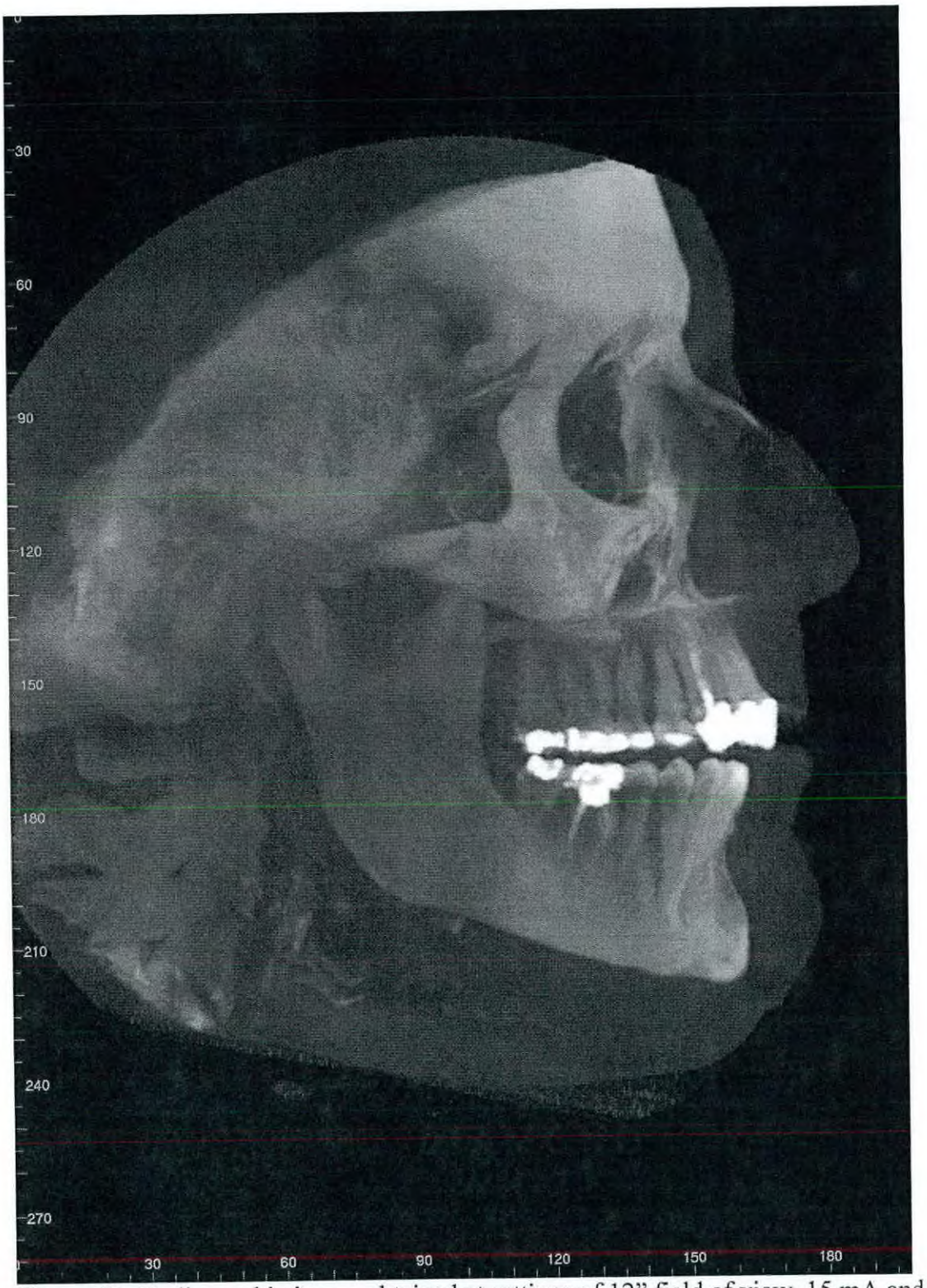


Figure 48. Radiographic image obtained at settings of 12" field of view, 15 mA and 120 kVp with filter.

APPENDIX 6

Raw Data: Six Inch

TABLE 3.--Six Inch Ranking Raw Data and Descriptive Statistics

	VV	JJ	QQ	CC	MM	DD	SS	GG	RR	HH	LL	TT	KK	BB	NN	WW
Operator	02100 06N	0210006Y	0212006N	0212006Y	0510006N	0510006Y	0512006N	0512006Y	1010006N	1010006Y	1012006N	1012006Y	1510006N	1510006Y	1512006N	1512006Y
1	-7	-6	-5	6	-8	1	3	8	-4	-2	-3	2	4	7	-1	5
2	-6	-8	-5	-7	-4	1	2	4	6	3	8	-2	7	-1	5	-3
3	-7	-8	-5	-6	-1	1	-2	3	-3	2	-4	5	8	6	4	7
4	-8	-5	-7	-6	-4	-1	-3	4	-2	3	8	1	6	2	7	5
5	-8	-6	-5	-7	-2	3	-3	-4	7	4	5	-1	8	2	6	1
6	-3	-8	-6	-5	8	-7	-1	2	-4	7	-2	1	5	6	3	4
7	-8	-7	-6	-5	-3	-1	6	-4	-2	1	2	8	3	5	4	7
8	-5	-6	-7	-8	-4	-3	4	-1	6	8	5	-2	7	3	1	2
9	-3	-7	-6	-8	4	1	-1	6	-4	2	5	3	-2	8	-5	7
10	-5	-6	-7	-8	5	-4	4	7	2	-1	-3	3	1	8	-2	6
11	-7	-6	-4	-8	1	-3	-2	-5	4	6	-1	2	3	7	8	5
12	-7	-8	-5	-6	-4	-3	3	4	2	1	-1	5	7	6	-2	8
13	-8	-5	-6	-7	-4	-3	7	1	8	-2	5	-1	3	6	2	4
14	-6	-7	-4	-5	-2	-3	8	2	-8	4	-1	3	7	5	1	6
15	-4	-5	-8	-7	-1	-2	6	8	-3	1	5	-6	7	4	2	3
16	-5	-6	-8	-7	-1	-4	7	2	3	-2	6	4	8	1	5	-3
17	6	-7	1	-6	-1	4	8	-2	3	2	-5	-3	7	5	-8	-4
18	-6	-7	-5	-8	-2	-4	4	-3	1	-1	2	7	8	5	3	6
19	-6	-8	-7	-5	5	-4	2	-3	3	6	7	4	8	1	-1	-2
20	-7	-6	-5	-4	2	5	3	8	1	7	-1	-2	-3	6	-8	4
22	-8	-6	-4	-7	-2	-5	-3	-1	7	2	1	4	8	5	6	3
23	-7	-6	-4	-8	3	-3	-5	7	1	-1	5	4	8	6	2	-2
24	-6	-8	1	-7	-2	-5	4	-4	3	8	-1	2	5	7	-3	6
25	-6	-7	-8	-5	-3	-2	-4	-1	1	6	2	7	3	5	4	8
26	-2	2	1	-5	-1	6	-3	3	-6	8	-7	7	-8	4	-4	5
27	-7	-8	-5	-6	-1	-4	5	7	-3	6	-2	3	2	8	1	4
29	-8	1	2	-2	-5	-1	3	5	-6	7	8	4	-7	-4	-3	6
30	6	3	2	-8	-6	5	-5	-4	7	8	4	1	-7	-2	-1	-3
31	-8	-7	-3	-6	2	-4	-1	1	-5	5	3	6	-2	7	4	8
32	-5	-7	-6	-8	3	-4	6	4	-1	8	-2	5	2	1	-3	7
33	-8	-7	-6	-3	-1	-2	1	4	-5	8	-4	6	7	5	2	3
34	-7	-8	-6	-4	-2	-3	6	2	-5	-1	7	5	3	1	4	8
35	-8	-5	-6	-7	-3	-4	5	8	2	1	-1	7	-2	6	3	4
37	-7	-8	-5	-4	-3	-2	4	7	8	1	3	-6	5	-1	6	2
Mean Rank	-5.62	-5.97	-4.62	-5.79	-1.09	-1.59	2.00	2.21	0.41	3.38	1.56	2.53	3.50	4.12	1.24	3.74
SD	3.35	2.71	2.81	2.61	3.43	3.20	3.98	4.18	4.62	3.47	4.20	3.65	4.73	3.08	4.09	3.59
Median	-7	-7	-5	-6	-2	-3	3	2.5	1	3	2	3	5	5	2	4.5
Max	6	3	2	6	8	6	8	8	8	8	8	8	8	8	8	8
Min	-8	-8	-8	-8	-8	-7	-5	-5	-8	-2	-7	-6	-8	-4	-8	-4
Overall Rank	14	16	13	15	11	12	7	6	10	4	8	5	3	1	9	2

TABLE 4.--Six Inch Diagnosis* Raw Data and Descriptive Statistics

	VV	JJ	QQ	CC	MM	DD	SS	GG	RR	HH	LL	TT	KK	BB	NN	WW
Operator	0210006N	0210006Y	0212006N	0212006Y	0510006N	0510006Y	0512006N	0512006Y	1010006N	1010006Y	1012006N	1012006Y	1510006N	1510006Y	1512006N	1512006Y
1	1	1	1	1	1	1	1	1	1	1	1	1	1	1	1	1
2	0	0	0	0	1	1	1	1	1	1	1	1	1	1	1	1
3	0	0	0	0	1	1	1	1	1	1	0	1	1	1	1	1
4	0	0	0	0	0	1	1	1	1	1	1	1	1	1	1	1
5	1	1	1	1	1	1	1	1	1	1	1	1	1	1	1	1
6	0	0	0	0	0	0	0	0	0	0	0	0	0	0	0	0
7	1	1	1	1	1	1	1	1	1	1	1	1	1	1	1	1
8	0	0	0	0	0	0	1	0	1	1	1	0	1	1	0	1
9	1	0	0	0	1	1	1	1	1	1	1	1	1	1	1	1
10	1	1	1	1	1	1	1	1	1	1	1	1	1	1	1	1
11	1	1	1	1	1	1	1	1	1	1	1	1	1	1	1	1
12	0	0	0	0	0	0	1	1	1	1	1	1	1	1	1	1
13	0	0	0	0	0	0	1	0	1	0	1	0	1	1	1	1
14	0	0	0	0	0	1	1	1	1	1	1	0	1	1	1	0
15	0	0	0	0	1	1	1	1	0	1	1	0	1	1	1	1
16	0	0	0	0	0	0	1	0	0	0	1	0	1	0	1	0
17	0	0	1	0	0	0	0	0	1	1	0	0	1	1	1	0
18	0	0	0	0	1	0	1	1	1	1	1	1	1	1	1	1
19	1	1	1	1	1	1	1	1	1	1	1	1	1	1	1	1
20	0	0	1	0	1	1	0	1	1	1	1	1	1	1	1	0
22	0	0	0	0	0	0	0	0	1	0	0	0	1	0	1	0
23	0	0	0	0	1	0	0	1	1	1	1	1	1	1	1	1
24	0	0	0	0	0	0	0	0	0	0	0	0	0	0	0	0
25	0	0	0	0	0	0	0	0	0	1	0	1	0	0	0	1
26	1	1	1	1	1	1	1	1	1	1	1	1	1	1	1	1
27	1	1	1	1	1	1	1	1	1	1	1	1	1	1	1	1
29	1	1	1	0	1	1	1	1	1	1	1	1	1	1	1	1
30	1	1	1	1	1	1	1	1	1	1	1	1	1	1	1	1
31	1	1	1	1	1	1	1	1	1	1	1	1	1	1	1	1
32	0	0	0	0	0	0	0	0	0	0	0	0	0	0	0	0
33	0	0	0	0	0	0	1	1	1	1	1	1	1	1	1	1
34	0	0	0	0	1	0	1	1	0	1	1	1	1	1	1	1
35	0	1	0	0	1	1	1	1	1	1	1	1	1	1	1	1
37	1	1	1	1	1	1	1	1	1	1	1	1	1	1	1	1
% Yes	38.24	38.24	41.18	32.35	61.76	58.82	76.47	73.53	79.41	82.35	79.41	70.59	88.24	82.35	85.29	76.47
Rank	14	14	13	16	11	12	7	9	5	3	5	10	1	3	2	7

*Images were graded as a 0 or 1 if non-diagnostic or diagnostic, respectively

TABLE 5.--Six Inch Ranking Reliability Raw Data

Time 1	VV	JJ	QQ	CC	MM	DD	SS	GG	RR	HH	LL	TT	KK	BB	NN	WW
Operator	**0210006N**	**0210006Y**	**0212006N**	**0212006Y**	**0510006N**	**0510006Y**	**0512006N**	**0512006Y**	**1010006N**	**1010006Y**	**1012006N**	**1012006Y**	**1510006N**	**1510006Y**	**1512006N**	**1512006Y**
6	-3	-8	-6	-5	8	-7	-1	2	-4	7	-2	1	5	6	3	4
12	-7	-8	-5	-6	-4	-3	3	4	2	1	-1	5	7	6	-2	8
14	-6	-7	-4	-5	-2	-3	8	2	-8	4	-1	3	7	5	1	6
32	-5	-7	-6	-8	3	-4	6	4	-1	8	-2	5	2	1	-3	7
33	-8	-7	-6	-3	-1	-2	1	4	-5	8	-4	6	7	5	2	3
7	-8	-7	-6	-5	-3	-1	6	-4	-2	1	2	8	3	5	4	7
22	-8	-6	-4	-7	-2	-5	-3	-1	7	2	1	4	8	5	6	3
9	-3	-7	-6	-8	4	1	-1	6	-4	2	5	3	-2	8	-5	7
27	-7	-8	-5	-6	-1	-4	5	7	-3	6	-2	3	2	8	1	4
34	-7	-8	-6	-4	-2	-3	6	2	-5	-1	7	5	3	1	4	8
Mean Rank	-6.20	-7.30	-5.40	-5.70	0.00	-3.10	3.00	2.60	-2.30	3.80	0.30	4.30	4.20	5.00	1.10	5.70
SD	1.93	0.67	0.84	1.64	3.77	2.18	3.77	3.24	4.22	3.26	3.47	1.95	3.16	2.40	3.48	2.00
Median	-7	-7	-6	-5.5	-1.5	-3	4	3	-3.5	3	-1	4.5	4	5	1.5	6.5
Max	-3	-6	-4	-3	8	1	8	7	7	8	7	8	8	8	6	8
Min	-8	-8	-6	-8	-4	-7	-3	-4	-8	-1	-4	1	-2	1	-5	3
Overall Rank	15	16	13	14	10	12	6	7	11	5	9	3	4	2	8	1

Time 2	VV	JJ	QQ	CC	MM	DD	SS	GG	RR	HH	LL	TT	KK	BB	NN	WW
Operator	**0210006N**	**0210006Y**	**0212006N**	**0212006Y**	**0510006N**	**0510006Y**	**0512006N**	**0512006Y**	**1010006N**	**1010006Y**	**1012006N**	**1012006Y**	**1510006N**	**1510006Y**	**1512006N**	**1512006Y**
6	-3	-7	-8	-5	6	-6	5	-4	-1	8	4	-2	7	1	3	2
12	-6	-7	-5	-8	-4	-2	3	4	-3	2	1	8	6	7	-1	5
14	-8	-7	-5	-6	-3	-2	-1	3	-4	7	5	1	6	2	8	4
32	-8	-7	3	-6	-2	-4	4	6	-1	8	-3	-5	1	5	2	7
33	-5	-8	-7	-6	3	-4	-3	4	-1	8	5	1	7	-2	2	6
7	-8	-7	-3	-6	-4	-5	-2	2	-1	3	6	8	1	5	4	7
22	-7	-8	-5	-6	-3	-4	2	8	4	1	-1	-2	6	5	7	3
9	-7	-5	-8	-6	6	-3	-4	3	4	8	7	1	-1	5	-2	2
27	-6	-7	-5	-8	1	-4	4	3	-3	7	-1	6	-2	2	5	8
34	-7	-6	-8	-5	-1	-4	1	-2	4	2	7	3	6	5	-3	8
Mean Rank	-6.50	-6.90	-5.10	-6.20	-0.10	-3.80	0.90	2.70	-0.20	5.40	3.00	1.90	3.70	3.50	2.50	5.20
SD	1.58	0.88	3.31	1.03	3.90	1.23	3.21	3.50	3.08	2.99	3.68	4.38	3.53	2.68	3.69	2.35
Median	-7	-7	-5	-6	-1.5	-4	1.5	3	-1	7	4.5	1	6	5	2.5	5.5
Max	-3	-5	3	-5	6	-2	5	8	4	8	7	8	7	7	8	8
Min	-8	-8	-8	-8	-4	-6	-4	-4	-4	1	-3	-5	-2	-2	-3	2
Overall Rank	15	16	13	14	10	12	9	6	11	1	5	8	3	4	7	2

TABLE 6.--Six Inch Diagnosis* Reliability Raw Data

Time 1	VV	JJ	QQ	CC	MM	DD	SS	GG	RR	HH	LL	TT	KK	BB	NN	WW
Operator	0210006N	0210006Y	0212006N	0212006Y	0510006N	0510006Y	0512006N	0512006Y	1010006N	1010006Y	1012006N	1012006Y	1510006N	1510006Y	1512006N	1512006Y
6	0	0	0	0	0	0	0	0	0	0	0	0	0	0	0	0
12	0	0	0	0	0	0	1	1	1	1	1	1	1	1	1	1
14	0	0	0	0	0	1	1	1	1	1	1	0	1	1	1	0
32	0	0	0	0	0	0	0	0	0	0	0	0	0	0	0	0
33	0	0	0	0	0	0	1	1	1	1	1	1	1	1	1	1
7	1	1	1	1	1	1	1	1	1	1	1	1	1	1	1	1
22	0	0	0	0	0	0	0	0	1	0	0	0	1	0	1	0
9	1	1	1	1	1	1	1	1	1	1	1	1	1	1	1	1
27	1	1	1	1	1	1	1	1	1	1	1	1	1	1	1	1
34	0	0	0	0	1	0	1	1	0	1	1	1	1	1	1	1
% Yes	30	30	30	30	40	40	70	70	70	70	70	60	80	70	80	60
Rank	13	13	13	13	11	11	3	3	3	3	3	9	1	3	1	9

Time 2	VV	JJ	QQ	CC	MM	DD	SS	GG	RR	HH	LL	TT	KK	BB	NN	WW
Operator	0210006N	0210006Y	0212006N	0212006Y	0510006N	0510006Y	0512006N	0512006Y	1010006N	1010006Y	1012006N	1012006Y	1510006N	1510006Y	1512006N	1512006Y
6	1	1	1	1	1	1	1	1	1	1	1	1	1	1	1	1
12	0	0	0	1	1	1	1	1	1	1	1	1	1	1	1	1
14	0	1	1	1	1	1	1	1	1	1	1	1	1	1	1	1
32	0	0	0	1	1	1	1	1	1	1	1	1	1	1	1	1
33	0	0	0	0	0	1	1	1	1	1	1	1	1	1	1	1
7	1	1	1	1	1	1	1	1	1	1	1	1	1	1	1	1
22	0	0	0	0	0	0	1	1	1	1	1	1	1	1	1	1
9	1	1	1	1	1	1	1	1	1	1	1	1	1	1	1	1
27	1	1	1	1	1	1	1	1	1	1	1	1	1	1	1	1
34	0	0	0	0	1	0	1	1	1	1	1	1	1	1	1	1
% Yes	40	50	50	70	80	80	100	100	100	100	100	100	100	100	100	100
Rank	16	14	14	13	11	11	1	1	1	1	1	1	1	1	1	1

*Images were graded as a 0 or 1 if non-diagnostic or diagnostic, respectively

APPENDIX 7

Raw Data: Nine Inch

TABLE 7.--Nine Inch Ranking Raw Data and Descriptive Statistics

	V	J	Q	C	M	D	S	G	R	H	L	T	K	B	N	W
Operator	0210009N	0210009Y	0212009N	0212009Y	0510009N	0510009Y	0512009N	0512009Y	1010009N	1010009Y	1012009N	1012009Y	1510009N	1510009Y	1512009N	1512009Y
1	-8	1	3	-7	8	-2	6	4	2	5	-3	-6	-1	7	-4	-5
2	-6	4	-5	5	8	6	-2	1	3	-8	2	-3	7	-4	-7	-1
3	-8	-1	-7	4	3	7	-3	6	-2	-6	5	-4	8	2	-5	1
4	-7	-2	-5	-3	-6	3	-4	6	-8	1	4	2	7	-1	8	5
5	-8	-3	2	-4	-6	5	-5	-2	7	-1	6	4	-7	8	3	1
6	-5	3	-7	-8	-4	-2	-6	-3	6	-1	4	1	5	8	7	2
7	-6	5	-7	-3	2	-4	3	-1	-5	-8	-2	4	6	1	7	8
8	-1	2	-7	4	-2	6	-8	-6	-3	-5	7	3	8	1	5	-4
9	-3	1	3	4	2	-6	-8	5	-1	-4	6	-7	8	-5	-2	7
10	-3	-6	-1	-4	-7	6	-2	8	5	-8	1	-5	2	4	7	3
12	-8	3	-7	1	-6	2	-3	8	-4	5	-1	4	-5	6	-2	7
13	-7	2	-1	-6	-4	-3	3	6	8	-8	-2	1	7	4	-5	5
14	1	5	-2	7	-8	-4	2	6	-6	-1	-3	3	-5	-7	4	8
16	-6	1	-1	-2	6	-8	-7	4	5	-4	7	3	-3	8	2	-5
17	-8	8	-1	-4	-5	-6	-2	4	3	-3	-7	6	7	1	5	2
18	-5	6	1	8	-6	-4	2	7	-8	-1	-7	-3	-2	4	3	5
19	8	-4	-2	4	-7	3	-3	7	-8	-1	2	6	1	-5	-6	5
21	1	3	-5	-6	-4	-3	-8	8	-7	5	6	4	-2	2	-1	7
22	-1	6	2	7	-7	4	-3	5	8	-2	-5	1	3	-4	-6	-8
23	-1	2	-6	-8	-2	-3	5	1	7	4	3	-4	-7	8	6	-5
24	8	-5	-6	-7	4	2	7	-2	-1	-3	3	-4	-8	1	6	5
25	-2	4	1	-3	7	5	8	-7	-6	2	-5	3	-4	-1	-8	6
26	-8	-2	2	-5	1	-1	-6	5	-3	-7	7	6	8	-4	4	3
27	-6	-1	4	2	-8	5	-7	-5	7	-3	-2	3	-4	1	6	8
28	-7	1	-3	7	4	-1	6	8	-4	-8	-2	-6	3	-5	2	5
30	-8	-7	1	6	-6	8	-4	-2	3	7	-3	-5	4	5	-1	2
31	-8	7	4	-4	5	6	-7	8	-2	-6	3	1	-5	-3	2	-1
32	-2	-8	-4	2	8	6	1	3	5	7	-5	4	-7	-6	-3	-1
33	-6	-1	-2	-8	-7	-5	1	8	6	7	-3	5	-4	3	2	4
34	4	-8	3	2	1	-2	-1	-7	8	5	6	-4	7	-6	-5	-3
Mean Rank	-3.87	0.53	-1.77	-0.63	-1.20	0.67	-1.50	2.77	0.50	-1.33	0.73	0.43	0.90	0.77	0.80	2.20
SD	4.61	4.45	3.78	5.31	5.55	4.72	4.87	4.95	5.59	5.08	4.53	4.21	5.66	4.82	4.95	4.53
Median	-6	1	-1.5	-2.5	-3	0.5	-2.5	4.5	0.5	-1.5	1.5	1.5	1.5	1	2	3
Max	8	8	4	8	8	8	8	8	8	7	7	6	8	8	8	8
Min	-8	-8	-7	-8	-8	-8	-8	-7	-8	-8	-7	-7	-8	-7	-8	-8
Overall Rank	16	8	15	11	12	7	14	1	9	13	6	10	3	5	4	2

TABLE 8.--Nine Inch Diagnosis* Raw Data and Descriptive Statistics

	V	J	Q	C	M	D	S	G	R	H	L	T	K	B	N	W
Operator	0210009N	0210009Y	0212009N	0212009Y	0510009N	0510009Y	0512009N	0512009Y	1010009N	1010009Y	1012009N	1012009Y	1510009N	1510009Y	1512009N	1512009Y
1	1	1	1	1	1	1	1	1	1	1	1	1	1	1	1	1
2	1	1	1	1	1	1	1	1	1	1	1	1	1	1	1	1
3	1	1	1	1	1	1	1	1	1	1	1	1	1	1	1	1
4	1	1	1	1	1	1	1	1	1	1	1	1	1	1	1	1
5	1	1	1	1	1	1	1	1	1	1	1	1	1	1	1	1
6	1	1	1	1	1	1	1	1	1	1	1	1	1	1	1	1
7	1	1	1	1	1	1	1	1	1	1	1	1	1	1	1	1
8	0	0	0	1	0	1	0	0	0	0	1	1	1	0	1	0
9	1	1	1	1	1	1	1	1	1	1	1	1	1	1	1	1
10	1	1	1	1	1	1	1	1	1	1	1	1	1	1	1	1
12	1	1	1	1	1	1	1	1	1	1	1	1	1	1	1	1
13	1	1	1	0	1	1	1	1	1	0	1	1	1	1	1	1
14	1	1	1	1	0	1	1	1	0	1	1	1	1	0	1	1
16	1	1	1	1	1	1	1	1	1	1	1	1	1	1	1	1
17	0	1	0	0	0	0	0	1	0	0	0	1	1	0	1	0
18	1	1	1	1	1	1	1	1	1	1	1	1	1	1	1	1
19	1	1	1	1	1	1	1	1	1	1	1	1	1	1	1	1
21	1	1	1	1	1	1	1	1	1	1	1	1	1	1	1	1
22	1	1	1	1	1	1	1	1	1	1	1	1	1	1	1	1
23	1	1	1	1	1	1	1	1	1	1	1	1	1	1	1	1
24	1	1	1	1	1	1	1	1	1	1	1	1	1	1	1	1
25	1	1	1	1	1	1	1	1	1	1	1	1	1	1	1	1
26	1	1	1	1	1	1	1	1	1	1	1	1	1	1	1	1
27	1	1	1	1	1	1	1	1	1	1	1	1	1	1	1	1
28	1	1	1	1	1	1	1	1	1	1	1	1	1	1	1	1
30	1	1	1	1	1	1	1	1	1	1	1	1	1	1	1	1
31	1	1	1	1	1	1	1	1	1	1	1	1	1	1	1	1
32	0	0	1	1	0	0	1	0	1	1	0	0	0	0	1	1
33	1	1	1	1	1	1	1	1	1	1	1	1	1	1	1	1
34	1	1	1	1	1	1	1	1	1	1	1	1	1	1	1	1
% Yes	90	93.33333	93.33333	93.33333	86.66667	93.33333	93.33333	93.33333	90	90	93.33333	96.66667	96.66667	86.66667	100	93.33333
Rank	12	4	4	4	15	4	4	4	12	12	4	2	2	15	1	4

*Images were graded as a 0 or 1 if non-diagnostic or diagnostic, respectively

TABLE 9.--Nine Inch Ranking Reliability Raw Data

Time 1	V	J	Q	C	M	D	S	G	R	H	L	T	K	B	N	W
Operator	0210009N	0210009Y	0212009N	0212009Y	0510009N	0510009Y	0512009N	0512009Y	1010009N	1010009Y	1012009N	1012009Y	1510009N	1510009Y	1512009N	1512009Y
1	-8	1	3	-7	8	-2	6	4	2	5	-3	-6	-1	7	-4	-5
6	-5	3	-7	-8	-4	-2	-6	-3	6	-1	4	1	5	8	7	2
24	8	-5	-6	-7	4	2	7	-2	-1	-3	3	-4	-8	1	6	5
28	-7	1	-3	7	4	-1	6	8	-4	-8	-2	-6	3	-5	2	5
31	-8	7	4	-4	5	6	-7	8	-2	-6	3	1	-5	-3	2	-1
13	-7	2	-1	-6	-4	-3	3	6	8	-8	-2	1	7	4	-5	5
26	-8	-2	2	-5	1	-1	-6	5	-3	-7	7	6	8	-4	4	3
25	-2	4	1	-3	7	5	8	-7	-6	2	-5	3	-4	-1	-8	6
19	8	-4	-2	4	-7	3	-3	7	-8	-1	2	6	1	-5	-6	5
21	1	3	-5	-6	-4	-3	-8	8	-7	5	6	4	-2	2	-1	7
Mean Rank	-2.80	1.00	-1.40	-3.50	1.00	0.40	0.00	3.40	-1.50	-2.20	1.30	0.60	0.40	0.40	-0.30	3.20
SD	6.41	3.71	3.86	5.02	5.35	3.34	6.57	5.42	5.38	5.05	4.06	4.53	5.34	4.81	5.27	3.68
Median	-6	1.5	-1.5	-5.5	2.5	-1	0	5.5	-2.5	-2	2.5	1	0	0	0.5	5
Max	8	7	4	7	8	6	8	8	8	5	7	6	8	8	7	7
Min	-8	-5	-7	-8	-7	-3	-8	-7	-8	-8	-5	-6	-8	-5	-8	-5
Overall Rank	15	4	12	16	4	7	10	1	13	14	3	6	7	7	11	2

Time 2	V	J	Q	C	M	D	S	G	R	H	L	T	K	B	N	W
Operator	0210009N	0210009Y	0212009N	0212009Y	0510009N	0510009Y	0512009N	0512009Y	1010009N	1010009Y	1012009N	1012009Y	1510009N	1510009Y	1512009N	1512009Y
1	-8	-5	-2	-7	5	1	-6	6	-3	8	-4	3	2	7	4	-1
6	-8	6	-4	-3	-7	-5	3	8	4	7	1	-6	-1	5	2	-2
24	-6	-1	3	2	-4	4	-3	5	-8	-5	-7	-2	6	8	7	1
28	2	6	5	4	-1	-2	-4	-3	8	-7	-8	-5	-6	3	7	1
31	8	7	-1	-4	-8	-7	3	5	-6	-5	-3	4	1	2	-2	6
13	2	-3	6	-7	-6	-5	3	-1	-4	-8	-2	7	5	4	8	1
26	-7	-1	-3	-4	-8	1	6	3	4	-6	8	-2	7	2	5	-5
25	-1	2	-8	-7	-6	-2	-4	6	5	3	-5	4	-3	8	1	7
19	8	-4	7	3	-6	1	6	-1	-8	5	-3	-5	-2	2	4	-7
21	-2	7	-1	-5	8	5	3	1	-7	-8	-4	-3	-6	4	6	2
Mean Rank	-1.20	1.40	0.20	-2.80	-3.30	-0.90	0.70	2.90	-1.50	-1.60	-2.70	-0.50	0.30	4.50	4.20	0.30
SD	6.14	4.79	4.87	4.26	5.60	3.98	4.47	3.70	6.11	6.54	4.52	4.60	4.72	2.42	3.12	4.35
Median	-1.5	0.5	-1	-4	-6	-0.5	3	4	-3.5	-5	-3.5	-2	0	4	4.5	1
Max	8	7	7	4	8	5	6	8	8	8	8	7	7	8	8	7
Min	-8	-5	-8	-7	-8	-7	-6	-3	-8	-8	-8	-6	-6	2	-2	-7
Overall Rank	11	4	8	15	16	10	5	3	12	13	14	9	6	1	2	6

TABLE 10.--Nine Inch Diagnosis* Reliability Raw Data

Time 1	V	J	Q	C	M	D	S	G	R	H	L	T	K	B	N	W
Operator	0210009N	0210009Y	0212009N	0212009Y	0510009N	0510009Y	0512009N	0512009Y	1010009N	1010009Y	1012009N	1012009Y	1510009N	1510009Y	1512009N	1512009Y
1	1	1	1	1	1	1	1	1	1	1	1	1	1	1	1	1
6	1	1	1	1	1	1	1	1	1	1	1	1	1	1	1	1
24	1	1	1	1	1	1	1	1	1	1	1	1	1	1	1	1
28	1	1	1	1	1	1	1	1	1	1	1	1	1	1	1	1
31	1	1	1	1	1	1	1	1	1	1	1	1	1	1	1	1
13	1	1	1	0	1	1	1	1	1	0	1	1	1	1	1	1
26	1	1	1	1	1	1	1	1	1	1	1	1	1	1	1	1
25	1	1	1	1	1	1	1	1	1	1	1	1	1	1	1	1
19	1	1	1	1	1	1	1	1	1	1	1	1	1	1	1	1
21	1	1	1	1	1	1	1	1	1	1	1	1	1	1	1	1
% Yes	100	100	100	90	100	100	100	100	100	90	100	100	100	100	100	100
Rank	1	1	1	15	1	1	1	1	1	15	1	1	1	1	1	1

Time 2	V	J	Q	C	M	D	S	G	R	H	L	T	K	B	N	W
Operator	0210009N	0210009Y	0212009N	0212009Y	0510009N	0510009Y	0512009N	0512009Y	1010009N	1010009Y	1012009N	1012009Y	1510009N	1510009Y	1512009N	1512009Y
1	1	1	1	1	1	1	1	1	1	1	1	1	1	1	1	1
6	1	1	1	1	1	1	1	1	1	1	1	1	1	1	1	1
24	0	0	0	0	0	1	1	1	1	1	1	1	1	1	1	1
28	1	1	1	1	1	1	1	1	1	1	1	1	1	1	1	1
31	1	1	1	1	1	1	1	1	1	1	1	1	1	1	1	1
13	0	1	1	1	1	1	1	1	1	1	1	1	1	1	1	1
26	1	1	1	1	1	1	1	1	1	1	1	1	1	1	1	1
25	1	1	1	1	1	1	1	1	1	1	1	1	1	1	1	1
19	1	1	1	1	1	1	1	1	1	1	1	1	1	1	1	1
21	1	1	1	1	1	1	1	1	1	1	1	1	1	1	1	1
% Yes	80	90	90	90	90	100	100	100	100	100	100	100	100	100	100	100
Rank	16	12	12	12	12	1	1	1	1	1	1	1	1	1	1	1

*Images were graded as a 0 or 1 if non-diagnostic or diagnostic, respectively.

APPENDIX 8

Raw Data: Twelve Inch

TABLE 11.--Twelve Inch Ranking Raw Data and Descriptive Statistics

	V	J	Q	C	M	D	S	G	R	H	L	T	K	B	N	W
Operator	0210012N	0210012Y	0212012N	0212012Y	0510012N	0510012Y	0512012N	0512012Y	1010012N	1010012Y	1012012N	1012012Y	1510012N	1510012Y	1512012N	1512012Y
1	-6	-4	-8	-3	8	-2	-7	1	7	6	3	4	5	2	-1	-5
2	-5	-3	6	-8	-2	-7	-1	-4	7	8	5	1	3	2	-6	4
3	-8	-7	-1	2	6	4	-3	-2	-4	3	-5	1	-6	5	8	7
4	-4	-6	4	5	7	1	-3	3	-1	-7	6	-2	-8	-5	8	2
5	6	-2	-4	-7	5	-8	2	-1	3	1	4	-5	8	-3	7	-6
6	4	2	3	-2	-4	-5	-3	5	-7	-1	1	8	-6	6	7	-8
7	3	-4	6	-7	4	-5	7	-8	5	-3	8	-1	2	1	-2	-6
8	-7	-6	-4	-8	6	-2	5	-1	-5	8	2	7	-3	4	3	1
9	-2	-5	-3	-8	2	7	-1	-7	3	5	6	4	1	-4	-6	8
10	-8	-5	5	-4	3	-3	-7	2	8	4	-2	6	-6	-1	7	1
11	-5	-2	-4	-6	4	6	-3	-7	7	2	3	1	8	5	-8	-1
12	-8	-5	-4	1	-1	4	-2	-7	2	3	6	-6	8	-3	5	7
13	-6	-5	-8	-2	1	2	-7	-3	8	4	-1	6	7	-4	3	5
14	6	-7	-6	-4	4	7	-3	-8	3	5	-1	2	8	1	-2	-5
15	4	1	-3	7	-4	-6	6	-1	-8	3	-5	2	-7	5	8	-2
16	-1	-2	5	8	-4	4	7	1	-5	3	-6	2	-7	6	-8	-3
17	-7	1	-6	-4	2	-5	5	-8	4	7	3	8	-3	6	-2	-1
18	-8	5	-2	-5	-3	-7	-4	1	8	2	-6	3	6	7	4	-1
19	-8	5	3	6	-6	-5	1	7	-2	-1	-7	4	-4	-3	2	8
20	-5	-6	-3	-8	1	6	-1	-4	7	8	-2	2	5	4	-7	3
21	-8	-7	-3	-6	1	-5	2	-4	-1	3	4	-2	5	7	8	6
22	-4	-3	6	-7	1	5	-1	-2	3	7	8	2	4	-5	-6	-8
23	6	-1	2	4	-3	-7	3	1	-6	-4	8	5	-8	7	-2	-5
24	3	-5	-8	-6	2	4	-4	-7	6	5	1	-2	8	7	-1	-3
25	-8	-6	-3	-7	-2	-4	1	-5	5	4	6	-1	7	2	8	3
26	-8	-7	-2	-6	1	6	-5	-4	7	4	8	-1	3	2	5	-3
27	-7	-3	-8	-5	4	-2	-6	-4	8	-1	5	6	7	1	3	2
28	6	-4	-8	-2	-1	-3	5	-5	1	-7	-6	2	7	3	8	4
29	3	-8	4	-6	-2	-3	1	-7	8	2	6	-1	7	-5	5	-4
30	-8	-7	-3	-6	-4	-2	2	-5	8	1	7	5	4	-1	6	3
Mean Rank	-3.00	-3.53	-1.57	-3.13	0.87	-0.83	-0.47	-2.77	2.63	2.47	1.97	2.00	1.83	1.63	1.80	0.10
SD	5.38	3.46	4.76	4.87	3.76	4.95	4.23	4.04	5.20	4.01	4.92	3.60	5.87	4.13	5.55	4.84
Median	-5	-4.5	-3	-5	1	-2	-1	-4	3.5	3	3	2	4	2	3	0
Max	6	5	6	8	8	7	7	7	8	8	8	8	8	7	8	8
Min	-8	-8	-8	-8	-6	-8	-7	-8	-8	-7	-7	-6	-8	-5	-8	-8
Overall Rank	14	16	12	15	8	11	10	13	1	2	4	3	5	7	6	9

TABLE 12.--Twelve Inch Diagnosis* Raw Data and Descriptive Statistics

	V	J	Q	C	M	D	S	G	R	H	L	T	K	B	N	W
Operator	0210012N	0210012Y	0212012N	0212012Y	0510012N	0510012Y	0512012N	0512012Y	1010012N	1010012Y	1012012N	1012012Y	1510012N	1510012Y	1512012N	1512012Y
1	1	1	1	1	1	1	1	1	1	1	1	1	1	1	1	1
2	1	1	1	1	1	1	1	1	1	1	1	1	1	1	1	1
3	1	1	1	1	1	1	1	1	1	1	1	1	1	1	1	1
4	1	1	1	1	1	1	1	1	1	1	1	1	1	1	1	1
5	1	1	1	1	1	1	1	1	1	1	1	1	1	1	1	1
6	1	1	1	1	1	1	1	1	1	1	1	1	1	1	1	1
7	1	1	1	1	1	1	1	1	1	1	1	1	1	1	1	1
8	1	1	1	1	1	1	1	1	1	1	1	1	1	1	1	1
9	1	0	1	0	1	1	1	0	1	1	1	1	1	1	0	1
10	1	1	1	1	1	1	1	1	1	1	1	1	1	1	1	1
11	1	1	1	1	1	1	1	1	1	1	1	1	1	1	1	1
12	1	1	1	1	1	1	1	1	1	1	1	1	1	1	1	1
13	1	1	1	1	1	1	1	1	1	1	1	1	1	1	0	1
14	1	1	1	1	1	1	1	1	1	1	1	1	1	1	1	1
15	1	1	1	1	1	1	1	1	1	1	1	1	1	1	1	1
16	1	1	1	1	1	1	1	1	1	1	1	1	1	1	1	1
17	1	1	1	1	1	1	1	1	1	1	1	1	1	1	1	1
18	1	1	1	1	1	1	1	1	1	1	1	1	1	1	1	1
19	1	1	1	1	1	1	1	1	1	1	1	1	1	1	1	1
20	1	1	1	1	1	1	1	1	1	1	1	1	1	1	1	1
21	1	1	1	1	1	1	1	1	1	1	1	1	1	1	1	1
22	1	1	1	1	1	1	1	1	1	1	1	1	1	1	1	1
23	1	1	1	1	1	1	1	1	1	1	1	1	1	1	1	1
24	1	1	1	1	1	1	1	1	1	1	1	1	1	1	1	1
25	1	1	1	1	1	1	1	1	1	1	1	1	1	1	1	1
26	1	1	1	1	1	1	1	1	1	1	1	1	1	1	1	1
27	1	1	1	1	1	1	1	1	1	1	1	1	1	1	1	1
28	1	1	1	1	1	1	1	1	1	1	1	1	1	1	1	1
29	1	1	1	1	1	1	1	1	1	1	1	1	1	1	1	1
30	1	1	1	1	1	1	1	1	1	1	1	1	1	1	1	1
% Yes	100	96.66667	100	96.66667	100	100	100	96.66667	100	100	100	100	100	100	93.33333	100
Rank	1	13	1	13	1	1	1	13	1	1	1	1	1	1	16	1

*Images were graded as a 0 or 1 if non-diagnostic or diagnostic, respectively.

TABLE 13.--Twelve Inch Ranking Reliability Raw Data

Time 1	V	J	Q	C	M	D	S	G	R	H	L	T	K	B	N	W
Operator	**0210012N**	**0210012Y**	**0212012N**	**0212012Y**	**0510012N**	**0510012Y**	**0512012N**	**0512012Y**	**1010012N**	**1010012Y**	**1012012N**	**1012012Y**	**1510012N**	**1510012Y**	**1512012N**	**1512012Y**
2	-5	-3	6	-8	-2	-7	-1	-4	7	8	5	1	3	2	-6	4
3	-8	-7	-1	2	6	4	-3	-2	-4	3	-5	1	-6	5	8	7
5	6	-2	-4	-7	5	-8	2	-1	3	1	4	-5	8	-3	7	-6
6	4	2	3	-2	-4	-5	-3	5	-7	-1	1	8	-6	6	7	-8
7	3	-4	6	-7	4	-5	7	-8	5	-3	8	-1	2	1	-2	-6
12	-8	-5	-4	1	-1	4	-2	-7	2	3	6	-6	8	-3	5	7
13	-6	-5	-8	-2	1	2	-7	-3	8	4	-1	6	7	-4	3	5
10	-8	-5	5	-4	3	-3	-7	2	8	4	-2	6	-6	-1	7	1
1	-6	-4	-8	-3	8	-2	-7	1	7	6	3	4	5	2	-1	-5
14	-8	-5	-4	1	-1	4	-2	-7	2	3	6	-6	8	-3	5	7
Mean Rank	-3.60	-3.80	-0.90	-2.90	1.90	-1.60	-2.30	-2.40	3.10	2.80	2.50	0.80	2.30	0.20	3.30	0.60
SD	5.62	2.44	5.53	3.60	3.90	4.74	4.40	4.27	5.13	3.19	4.14	5.22	6.09	3.55	4.74	6.20
Median	-6	-4.5	-2.5	-2.5	2	-2.5	-2.5	-2.5	4	3	3.5	1	4	0	5	2.5
Max	6	2	6	2	8	4	7	5	8	8	8	8	8	6	8	7
Min	-8	-7	-8	-8	-4	-8	-7	-8	-7	-3	-5	-6	-6	-4	-6	-8
Overall Rank	15	16	10	14	6	11	12	13	2	3	4	7	5	9	1	8

Time 2	V	J	Q	C	M	D	S	G	R	H	L	T	K	B	N	W
Operator	**0210012N**	**0210012Y**	**0212012N**	**0212012Y**	**0510012N**	**0510012Y**	**0512012N**	**0512012Y**	**1010012N**	**1010012Y**	**1012012N**	**1012012Y**	**1510012N**	**1510012Y**	**1512012N**	**1512012Y**
2	-2	-7	5	-8	-6	-3	7	-4	6	-1	8	-5	3	2	1	4
3	-8	-4	1	-2	3	-5	7	-1	-6	6	-3	2	-7	5	4	8
5	-5	-8	-3	2	-2	5	-1	1	-7	7	-4	6	-6	4	8	3
6	-8	-4	-7	-6	-5	-1	6	1	-3	2	3	-2	4	8	7	5
7	-6	-4	5	-7	8	-2	-3	-5	4	2	6	-1	-8	1	3	7
12	-7	-5	-6	-3	4	-8	-1	1	-4	6	2	7	-2	8	5	3
13	-8	-6	-4	4	-3	5	-7	-1	3	7	-2	1	6	-5	2	8
10	-7	-4	-5	1	-2	8	4	-1	-8	3	-3	7	-6	6	2	5
1	4	-6	-8	-1	7	-3	-4	-2	-5	3	1	2	8	6	-7	5
14	-3	-7	1	-5	2	6	-1	-4	8	5	3	-2	7	4	-6	-8
Mean Rank	-5.00	-5.50	-2.10	-2.50	0.60	0.20	0.70	-1.50	-1.20	4.00	1.10	1.50	-0.10	3.90	1.90	4.00
SD	3.80	1.51	4.79	4.03	4.90	5.39	4.97	2.22	5.87	2.62	4.07	4.14	6.35	3.87	4.95	4.59
Median	-6.5	-5.5	-3.5	-2.5	0	-1.5	-1	-1	-3.5	4	1.5	1.5	0.5	4.5	2.5	5
Max	4	-4	5	4	8	8	7	1	8	7	8	7	8	8	8	8
Min	-8	-8	-8	-8	-6	-8	-7	-5	-8	-1	-4	-5	-8	-5	-7	-8
Overall Rank	15	16	13	14	8	9	7	12	11	1	6	5	10	3	4	1

TABLE 14.--Twelve Inch Diagnosis* Reliability Raw Data

Time 1	V	J	Q	C	M	D	S	G	R	H	L	T	K	B	N	W
Operator	0210012N	0210012Y	0212012N	0212012Y	0510012N	0510012Y	0512012N	0512012Y	1010012N	1010012Y	1012012N	1012012Y	1510012N	1510012Y	1512012N	1512012Y
2	1	1	1	1	1	1	1	1	1	1	1	1	1	1	1	1
3	1	1	1	1	1	1	1	1	1	1	1	1	1	1	1	1
5	1	1	1	1	1	1	1	1	1	1	1	1	1	1	1	1
6	1	1	1	1	1	1	1	1	1	1	1	1	1	1	1	1
7	1	1	1	1	1	1	1	1	1	1	1	1	1	1	1	1
12	1	1	1	1	1	1	1	1	1	1	1	1	1	1	1	1
13	1	1	1	1	1	1	1	1	1	1	1	1	1	1	0	1
10	1	1	1	1	1	1	1	1	1	1	1	1	1	1	1	1
1	1	1	1	1	1	1	1	1	1	1	1	1	1	1	1	1
14	1	1	1	1	1	1	1	1	1	1	1	1	1	1	1	1
% Yes	100	100	100	100	100	100	100	100	100	100	100	100	100	100	90	100
Rank	1	1	1	1	1	1	1	1	1	1	1	1	1	1	16	1

Time 2	V	J	Q	C	M	D	S	G	R	H	L	T	K	B	N	W
Operator	0210012N	0210012Y	0212012N	0212012Y	0510012N	0510012Y	0512012N	0512012Y	1010012N	1010012Y	1012012N	1012012Y	1510012N	1510012Y	1512012N	1512012Y
2	1	1	1	1	1	1	1	1	1	1	1	1	1	1	1	1
3	1	1	1	1	1	1	1	1	1	1	1	1	1	1	1	1
5	1	1	1	1	1	1	1	1	1	1	1	1	1	1	1	1
6	1	1	1	1	1	1	1	1	1	1	1	1	1	1	1	1
7	1	1	1	1	1	1	1	1	1	1	1	1	1	1	1	1
12	1	1	1	1	1	1	1	1	1	1	1	1	1	1	1	1
13	1	1	1	1	1	1	1	1	1	1	1	1	1	1	1	1
10	1	1	1	1	1	1	1	1	1	1	1	1	1	1	1	1
1	1	1	1	1	1	1	1	1	1	1	1	1	1	1	1	1
14	1	1	1	1	1	1	1	1	1	1	1	1	1	1	1	1
% Yes	100	100	100	100	100	100	100	100	100	100	100	100	100	100	100	100
Rank	1	1	1	1	1	1	1	1	1	1	1	1	1	1	1	1

*Images were graded as a 0 or 1 if non-diagnostic or diagnostic, respectively.

APPENDIX 9

Friedman and Wilcoxon Signed Ranks Tests for 6" Images

TABLE 15.--Ranks for 6" Image Pairs Comparing Filter

		N	Mean Rank	Sum of Ranks
0210006Y - 0210006N	Negative Ranks	20(a)	16.70	334.00
	Positive Ranks	14(b)	18.64	261.00
	Ties	0(c)		
	Total	34		
0212006Y - 0212006N	Negative Ranks	22(d)	19.09	420.00
	Positive Ranks	12(e)	14.58	175.00
	Ties	0(f)		
	Total	34		
0510006Y - 0510006N	Negative Ranks	18(g)	17.97	323.50
	Positive Ranks	16(h)	16.97	271.50
	Ties	0(i)		
	Total	34		
0512006Y - 0512006N	Negative Ranks	13(j)	21.73	282.50
	Positive Ranks	21(k)	14.88	312.50
	Ties	0(l)		
	Total	34		
1010006Y - 1010006N	Negative Ranks	12(m)	12.50	150.00
	Positive Ranks	22(n)	20.23	445.00
	Ties	0(o)		
	Total	34		
1012006Y - 1012006N	Negative Ranks	15(p)	16.07	241.00
	Positive Ranks	19(q)	18.63	354.00
	Ties	0(r)		
	Total	34		
1510006Y - 1510006N	Negative Ranks	18(s)	15.00	270.00
	Positive Ranks	16(t)	20.31	325.00
	Ties	0(u)		
	Total	34		
1512006Y - 1512006N	Negative Ranks	10(v)	15.60	156.00
	Positive Ranks	24(w)	18.29	439.00
	Ties	0(x)		
	Total	34		

a 0510006N < 0210006N
b 0510006N > 0210006N
c 0510006N = 0210006N
d 1010006N < 0210006N
e 1010006N > 0210006N
f 1010006N = 0210006N
g 1510006N < 0210006N
h 1510006N > 0210006N
i 1510006N = 0210006N
j 1010006N < 0510006N
k 1010006N > 0510006N
l 1010006N = 0510006N
m 1510006N < 0510006N
n 1510006N > 0510006N
o 1510006N = 0510006N
p 1510006N < 1010006N
q 1510006N > 1010006N
r 1510006N = 1010006N

TABLE 16.--Wilcoxon Signed Rank Test Comparing Effect of Filter on 6" Images

	0210006Y - 0210006N	0212006Y - 0212006N	0510006Y - 0510006N	0512006Y - 0512006N	1010006Y - 1010006N	1012006Y - 1012006N	1510006Y - 1510006N	1512006Y - 1512006N
Z	-.638(a)	-2.118(a)	-.446(a)	-.257(b)	-2.526(b)	-.968(b)	-.472(b)	-2.424(b)
Asymp. Sig. (2-tailed)	.523	.034	.655	.797	.012	.333	.637	.015

a Based on positive ranks.
b Based on negative ranks.
Bonferroni Correction: 0.05/8 = 0.00625

TABLE 17.--Ranks for 6" Image Pairs Comparing kVp

		N	Mean Rank	Sum of Ranks
0212006N - 0210006N	Negative Ranks	11(a)	19.00	209.00
	Positive Ranks	23(b)	16.78	386.00
	Ties	0(c)		
	Total	34		
0212006Y - 0210006Y	Negative Ranks	17(d)	15.50	263.50
	Positive Ranks	17(e)	19.50	331.50
	Ties	0(f)		
	Total	34		
0512006N - 0510006N	Negative Ranks	12(g)	11.67	140.00
	Positive Ranks	22(h)	20.68	455.00
	Ties	0(i)		
	Total	34		
0512006Y - 0510006Y	Negative Ranks	6(j)	16.25	97.50
	Positive Ranks	28(k)	17.77	497.50
	Ties	0(l)		
	Total	34		
1012006N - 1010006N	Negative Ranks	16(m)	15.91	254.50
	Positive Ranks	18(n)	18.92	340.50
	Ties	0(o)		
	Total	34		
1012006Y - 1010006Y	Negative Ranks	19(p)	18.61	353.50
	Positive Ranks	15(q)	16.10	241.50
	Ties	0(r)		
	Total	34		
1512006N - 1510006N	Negative Ranks	23(s)	19.30	444.00
	Positive Ranks	11(t)	13.73	151.00
	Ties	0(u)		
	Total	34		
1512006Y - 1510006Y	Negative Ranks	21(v)	17.07	358.50
	Positive Ranks	13(w)	18.19	236.50
	Ties	0(x)		
	Total	34		

a 0212006N < 0210006N
b 0212006N > 0210006N
c 0212006N = 0210006N
d 0212006Y < 0210006Y
e 0212006Y > 0210006Y
f 0212006Y = 0210006Y
g 0512006N < 0510006N
h 0512006N > 0510006N
i 0512006N = 0510006N
j 0512006Y < 0510006Y
k 0512006Y > 0510006Y
l 0512006Y = 0510006Y
m 1012006N < 1010006N
n 1012006N > 1010006N
o 1012006N = 1010006N
p 1012006Y < 1010006Y
q 1012006Y > 1010006Y
r 1012006Y = 1010006Y
s 1512006N < 1510006N
t 1512006N > 1510006N
u 1512006N = 1510006N
v 1512006Y < 1510006Y
w 1512006Y > 1510006Y
x 1512006Y = 1510006Y

TABLE 18.--Wilcoxon Signed Rank Test Comparing kVp on 6" Images

	0212006N - 0210006N	0212006Y- 0210006Y	0512006N - 0510006N	0512006Y- 0510006Y	1012006N - 1010006N	1012006Y- 1010006Y	1512006N - 1510006N	1512006Y- 1510006Y
Z	-1.529(a)	-.589(a)	-2.700(a)	-3.423(a)	-.737(a)	-.959(b)	-2.513(b)	-1.053(b)
Asymp. Sig. (2-tailed)	.126	.556	.007	**.001†**	.461	.337	.012	.292

a Based on negative ranks.
b Based on positive ranks.
† p < 0.00625

TABLE. 19--Friedman Test for 6" 100 kVp Without Filter Images

N	34
Chi-Square	47.506
Df	3
Asymp. Sig.	**.000 †**

† p < 0.05

TABLE 20.--Ranks for 6" 100 kVp Without Filter Images

		N	Mean Rank	Sum of Ranks
0510006N - 0210006N	Negative Ranks	3(a)	20.00	60.00
	Positive Ranks	31(b)	17.26	535.00
	Ties	0(c)		
	Total	34		
1010006N - 0210006N	Negative Ranks	5(d)	6.80	34.00
	Positive Ranks	29(e)	19.34	561.00
	Ties	0(f)		
	Total	34		
1510006N - 0210006N	Negative Ranks	2(g)	15.00	30.00
	Positive Ranks	32(h)	17.66	565.00
	Ties	0(i)		
	Total	34		
1010006N - 0510006N	Negative Ranks	16(j)	13.78	220.50
	Positive Ranks	18(k)	20.81	374.50
	Ties	0(l)		
	Total	34		
1510006N - 0510006N	Negative Ranks	9(m)	8.83	79.50
	Positive Ranks	25(n)	20.62	515.50
	Ties	0(o)		
	Total	34		
1510006N - 1010006N	Negative Ranks	9(p)	13.33	120.00
	Positive Ranks	25(q)	19.00	475.00
	Ties	0(r)		
	Total	34		

a 0510006N < 0210006N
b 0510006N > 0210006N
c 0510006N = 0210006N
d 1010006N < 0210006N
e 1010006N > 0210006N
f 1010006N = 0210006N
g 1510006N < 0210006N
h 1510006N > 0210006N
i 1510006N = 0210006N
j 1010006N < 0510006N
k 1010006N > 0510006N
l 1010006N = 0510006N
m 1510006N < 0510006N
n 1510006N > 0510006N
o 1510006N = 0510006N
p 1510006N < 1010006N
q 1510006N > 1010006N
r 1510006N = 1010006N

TABLE 21.--Wilcoxon Signed Rank Test Comparing mA on 6" 100 kVp Without Filter

	0510006N - 0210006N	1010006N - 0210006N	1510006N - 0210006N	1010006N - 0510006N	1510006N - 0510006N	1510006N - 1010006N
Z	-4.067(a)	-4.509(a)	-4.579(a)	-1.319(a)	-3.730(a)	-3.041(a)
Asymp. Sig. (2-tailed)	.000 †	.000 †	.000 †	.187	.000 †	.002 †

a Based on negative ranks.
† p < 0.00833

TABLE 22.--Friedman Test for 6" 100 kVp With Filter Images

N	34
Chi-Square	73.518
df	3
Asymp. Sig.	.000

† p < 0.05

TABLE 23.--Ranks for 6" 100 kVp With Filter Images

		N	Mean Rank	Sum of Ranks
0510006Y - 0210006Y	Negative Ranks	1(a)	6.00	6.00
	Positive Ranks	33(b)	17.85	589.00
	Ties	0(c)		
	Total	34		
1010006Y - 0210006Y	Negative Ranks	0(d)	.00	.00
	Positive Ranks	34(e)	17.50	595.00
	Ties	0(f)		
	Total	34		
1510006Y - 0210006Y	Negative Ranks	2(g)	2.50	5.00
	Positive Ranks	32(h)	18.44	590.00
	Ties	0(i)		
	Total	34		
1010006Y - 0510006Y	Negative Ranks	2(j)	12.00	24.00
	Positive Ranks	32(k)	17.84	571.00
	Ties	0(l)		
	Total	34		
1510006Y - 0510006Y	Negative Ranks	5(m)	8.10	40.50
	Positive Ranks	29(n)	19.12	554.50
	Ties	0(o)		
	Total	34		
1510006Y - 1010006Y	Negative Ranks	15(p)	15.77	236.50
	Positive Ranks	19(q)	18.87	358.50
	Ties	0(r)		
	Total	34		

a 0510006Y < 0210006Y
b 0510006Y > 0210006Y
c 0510006Y = 0210006Y
d 1010006Y < 0210006Y
e 1010006Y > 0210006Y
f 1010006Y = 0210006Y
g 1510006Y < 0210006Y
h 1510006Y > 0210006Y
i 1510006Y = 0210006Y
j 1010006Y < 0510006Y
k 1010006Y > 0510006Y
l 1010006Y = 0510006Y
m 1510006Y < 0510006Y
n 1510006Y > 0510006Y
o 1510006Y = 0510006Y
p 1510006Y < 1010006Y
q 1510006Y > 1010006Y
r 1510006Y = 1010006Y

TABLE 24.--Wilcoxon Signed Rank Test Comparing mA on 6" 100 kVp With Filter

	0510006Y - 0210006Y	1010006Y - 0210006Y	1510006Y - 0210006Y	1010006Y - 0510006Y	1510006Y - 0510006Y	1510006Y - 1010006Y
Z	-4.997(a)	-5.091(a)	-5.013(a)	-4.688(a)	-4.399(a)	-1.045(a)
Asymp. Sig. (2-tailed)	.000 †	.000 †	.000 †	.000 †	.000 †	.296

a Based on negative ranks.
† p < 0.00833

TABLE 25.--Friedman Test for 6" 120 kVp Without Filter Images

N	34
Chi-Square	37.624
df	3
Asymp. Sig.	.000 †

† p < 0.05

TABLE 26.--Ranks for 6" 120 kVp Without Filter Images

		N	Mean Rank	Sum of Ranks
0512006N - 0212006N	Negative Ranks	3(a)	9.17	27.50
	Positive Ranks	31(b)	18.31	567.50
	Ties	0(c)		
	Total	34		
1012006N - 0212006N	Negative Ranks	3(d)	13.83	41.50
	Positive Ranks	31(e)	17.85	553.50
	Ties	0(f)		
	Total	34		
1512006N - 0212006N	Negative Ranks	6(g)	9.00	54.00
	Positive Ranks	28(h)	19.32	541.00
	Ties	0(i)		
	Total	34		
1012006N - 0512006N	Negative Ranks	20(j)	16.30	326.00
	Positive Ranks	14(k)	19.21	269.00
	Ties	0(l)		
	Total	34		
1512006N - 0512006N	Negative Ranks	21(m)	15.90	334.00
	Positive Ranks	13(n)	20.08	261.00
	Ties	0(o)		
	Total	34		
1512006N - 1012006N	Negative Ranks	17(p)	18.41	313.00
	Positive Ranks	17(q)	16.59	282.00
	Ties	0(r)		
	Total	34		

a 0512006N < 0212006N
b 0512006N > 0212006N
c 0512006N = 0212006N
d 1012006N < 0212006N
e 1012006N > 0212006N
f 1012006N = 0212006N
g 1512006N < 0212006N
h 1512006N > 0212006N
i 1512006N = 0212006N
j 1012006N < 0512006N
k 1012006N > 0512006N
l 1012006N = 0512006N
m 1512006N < 0512006N
n 1512006N > 0512006N
o 1512006N = 0512006N
p 1512006N < 1012006N
q 1512006N > 1012006N
r 1512006N = 1012006N

TABLE 27.--Wilcoxon Signed Rank Test Comparing mA on 6" 120 kVp Without Filter

	0512006N - 0212006N	1012006N - 0212006N	1512006N - 0212006N	1012006N - 0512006N	1512006N - 0512006N	1512006N - 1012006N
Z	-4.620(a)	-4.381(a)	-4.168(a)	-.488(b)	-.625(b)	-.266(b)
Asymp. Sig. (2-tailed)	.000 †	.000 †	.000 †	.625	.532	.790

a Based on negative ranks.
b Based on positive ranks.
† p < 0.00833

TABLE 28.--Friedman Test for 6" 120 kVp With Filter Images

N	34
Chi-Square	56.859
df	3
Asymp. Sig.	.000 †

† p < 0.05

TABLE 29.--Ranks for 6" 120 kVp With Filter Images

		N	Mean Rank	Sum of Ranks
0512006Y - 0212006Y	Negative Ranks	0(a)	.00	.00
	Positive Ranks	34(b)	17.50	595.00
	Ties	0(c)		
	Total	34		
1012006Y - 0212006Y	Negative Ranks	2(d)	3.75	7.50
	Positive Ranks	32(e)	18.36	587.50
	Ties	0(f)		
	Total	34		
1512006Y - 0212006Y	Negative Ranks	1(g)	1.00	1.00
	Positive Ranks	33(h)	18.00	594.00
	Ties	0(i)		
	Total	34		
1012006Y - 0512006Y	Negative Ranks	16(j)	16.47	263.50
	Positive Ranks	18(k)	18.42	331.50
	Ties	0(l)		
	Total	34		
1512006Y - 0512006Y	Negative Ranks	12(m)	17.33	208.00
	Positive Ranks	22(n)	17.59	387.00
	Ties	0(o)		
	Total	34		
1512006Y - 1012006Y	Negative Ranks	12(p)	15.29	183.50
	Positive Ranks	22(q)	18.70	411.50
	Ties	0(r)		
	Total	34		

a 0512006Y < 0212006Y
b 0512006Y > 0212006Y
c 0512006Y = 0212006Y
d 1012006Y < 0212006Y
e 1012006Y > 0212006Y
f 1012006Y = 0212006Y
g 1512006Y < 0212006Y
h 1512006Y > 0212006Y
i 1512006Y = 0212006Y
j 1012006Y < 0512006Y
k 1012006Y > 0512006Y
l 1012006Y = 0512006Y
m 1512006Y < 0512006Y
n 1512006Y > 0512006Y
o 1512006Y = 0512006Y
p 1512006Y < 1012006Y
q 1512006Y > 1012006Y
r 1512006Y = 1012006Y

TABLE 30.--Wilcoxon Signed Rank Test Comparing mA on 6" 120 kVp With Filter

	0512006Y - 0212006Y	1012006Y - 0212006Y	1512006Y - 0212006Y	1012006Y - 0512006Y	1512006Y - 0512006Y	1512006Y - 1012006Y
Z	-5.092(a)	-4.967(a)	-5.075(a)	-.583(a)	-1.534(a)	-1.957(a)
Asymp. Sig. (2-tailed)	**.000** †	**.000** †	**.000** †	.560	.125	.050

a Based on negative ranks.
† $p < 0.00833$

APPENDIX 10

Friedman and Wilcoxon Signed Ranks Tests for 9" Images

TABLE 31.--Ranks for 9" Image Pairs Comparing Filter

		N	Mean Rank	Sum of Ranks
0210009Y - 0210009N	Negative Ranks	5(a)	19.60	98.00
	Positive Ranks	25(b)	14.68	367.00
	Ties	0(c)		
	Total	30		
0212009Y - 0212009N	Negative Ranks	16(d)	11.94	191.00
	Positive Ranks	14(e)	19.57	274.00
	Ties	0(f)		
	Total	30		
0510009Y - 0510009N	Negative Ranks	13(g)	13.50	175.50
	Positive Ranks	17(h)	17.03	289.50
	Ties	0(i)		
	Total	30		
0512009Y - 0512009N	Negative Ranks	6(j)	15.17	91.00
	Positive Ranks	24(k)	15.58	374.00
	Ties	0(l)		
	Total	30		
1010009Y - 1010009N	Negative Ranks	19(m)	15.61	296.50
	Positive Ranks	11(n)	15.32	168.50
	Ties	0(o)		
	Total	30		
1012009Y - 1012009N	Negative Ranks	18(p)	13.19	237.50
	Positive Ranks	12(q)	18.96	227.50
	Ties	0(r)		
	Total	30		
1510009Y - 1510009N	Negative Ranks	14(s)	17.21	241.00
	Positive Ranks	16(t)	14.00	224.00
	Ties	0(u)		
	Total	30		
1512009Y - 1512009N	Negative Ranks	13(v)	13.65	177.50
	Positive Ranks	17(w)	16.91	287.50
	Ties	0(x)		
	Total	30		

a 0210009Y < 0210009N
b 0210009Y > 0210009N
c 0210009Y = 0210009N
d 0212009Y < 0212009N
e 0212009Y > 0212009N
f 0212009Y = 0212009N
g 0510009Y < 0510009N
h 0510009Y > 0510009N
i 0510009Y = 0510009N
j 0512009Y < 0512009N
k 0512009Y > 0512009N
l 0512009Y = 0512009N
m 1010009Y < 1010009N
n 1010009Y > 1010009N
o 1010009Y = 1010009N
p 1012009Y < 1012009N
q 1012009Y > 1012009N
r 1012009Y = 1012009N
s 1510009Y < 1510009N
t 1510009Y > 1510009N
u 1510009Y = 1510009N
v 1512009Y < 1512009N
w 1512009Y > 1512009N
x 1512009Y = 1512009N

TABLE 32.--Wilcoxon Signed Rank Test Comparing Effect of Filter on 9" Images

	0210009Y - 0210009N	0212009Y - 0212009N	0510009Y - 0510009N	0512009Y - 0512009N	1010009Y - 1010009N	1012009Y - 1012009N	1510009Y - 1510009N	1512009Y - 1512009N
Z	-2.769(a)	-.855(a)	-1.176(a)	-2.915(a)	-1.318(b)	-.103(b)	-.175(b)	-1.134(a)
Asymp. Sig. (2-tailed)	**.006** †	.393	.240	**.004** †	.187	.918	.861	.257

a Based on negative ranks.
b Based on positive ranks.
† $p < 0.00625$

TABLE 33.--Ranks for 9" Image Pairs Comparing kVp

		N	Mean Rank	Sum of Ranks
0212009N - 0210009N	Negative Ranks	10(a)	14.10	141.00
	Positive Ranks	20(b)	16.20	324.00
	Ties	0(c)		
	Total	30		
0212009Y - 0210009Y	Negative Ranks	16(d)	17.09	273.50
	Positive Ranks	14(e)	13.68	191.50
	Ties	0(f)		
	Total	30		
0512009N - 0510009N	Negative Ranks	12(g)	19.21	230.50
	Positive Ranks	18(h)	13.03	234.50
	Ties	0(i)		
	Total	30		
0512009Y - 0510009Y	Negative Ranks	11(j)	14.73	162.00
	Positive Ranks	19(k)	15.95	303.00
	Ties	0(l)		
	Total	30		
1012009N - 1010009N	Negative Ranks	14(m)	15.75	220.50
	Positive Ranks	16(n)	15.28	244.50
	Ties	0(o)		
	Total	30		
1012009Y - 1010009Y	Negative Ranks	11(p)	13.91	153.00
	Positive Ranks	19(q)	16.42	312.00
	Ties	0(r)		
	Total	30		
1512009N - 1510009N	Negative Ranks	14(s)	16.46	230.50
	Positive Ranks	16(t)	14.66	234.50
	Ties	0(u)		
	Total	30		
1512009Y - 1510009Y	Negative Ranks	10(v)	16.75	167.50
	Positive Ranks	20(w)	14.88	297.50
	Ties	0(x)		
	Total	30		

a 0212009N < 0210009N
b 0212009N > 0210009N
c 0212009N = 0210009N
d 0212009Y < 0210009Y
e 0212009Y > 0210009Y
f 0212009Y = 0210009Y
g 0512009N < 0510009N
h 0512009N > 0510009N
i 0512009N = 0510009N
j 0512009Y < 0510009Y
k 0512009Y > 0510009Y
l 0512009Y = 0510009Y
m 1012009N < 1010009N
n 1012009N > 1010009N
o 1012009N = 1010009N
p 1012009Y < 1010009Y
q 1012009Y > 1010009Y
r 1012009Y = 1010009Y
s 1512009N < 1510009N
t 1512009N > 1510009N
u 1512009N = 1510009N
v 1512009Y < 1510009Y
w 1512009Y > 1510009Y
x 1512009Y = 1510009Y

TABLE 34.--Wilcoxon Signed Rank Test Comparing Effect of kVp on 9" Images[c]

	0212009N - 0210009N	0212009Y - 0210009Y	0512009N - 0510009N	0512009Y - 0510009Y	1012009N - 1010009N	1012009Y - 1010009Y	1512009N - 1510009N	1512009Y - 1510009Y
Z	-1.885(a)	-.845(b)	-.041(a)	-1.451(a)	-.247(a)	-1.638(a)	-.041(a)	-1.340(a)
Asymp. Sig. (2-tailed)	.059	.398	.967	.147	.805	.101	.967	.180

a Based on negative ranks.
b Based on positive ranks.
c Based on Wilcoxon Signed Rank Test, $p < 0.00833$.

TABLE 35.--Friedman Test for 9" 100 kVp Without Filter Images

N	30
Chi-Square	10.360
df	3
Asymp. Sig.	.016 †

† $p < 0.05$

TABLE 36.--Ranks for 9" 100 kVp Without Filter Images

		N	Mean Rank	Sum of Ranks
0510009N - 0210009N	Negative Ranks	12(a)	12.33	148.00
	Positive Ranks	18(b)	17.61	317.00
	Ties	0(c)		
	Total	30		
1010009N - 0210009N	Negative Ranks	8(d)	12.13	97.00
	Positive Ranks	22(e)	16.73	368.00
	Ties	0(f)		
	Total	30		
1510009N - 0210009N	Negative Ranks	7(g)	13.93	97.50
	Positive Ranks	23(h)	15.98	367.50
	Ties	0(i)		
	Total	30		
1010009N - 0510009N	Negative Ranks	17(j)	11.15	189.50
	Positive Ranks	13(k)	21.19	275.50
	Ties	0(l)		
	Total	30		
1510009N - 0510009N	Negative Ranks	10(m)	16.15	161.50
	Positive Ranks	20(n)	15.18	303.50
	Ties	0(o)		
	Total	30		
1510009N - 1010009N	Negative Ranks	15(p)	14.60	219.00
	Positive Ranks	15(q)	16.40	246.00
	Ties	0(r)		
	Total	30		

a 0510009N < 0210009N
b 0510009N > 0210009N
c 0510009N = 0210009N
d 1010009N < 0210009N
e 1010009N > 0210009N
f 1010009N = 0210009N
g 1510009N < 0210009N
h 1510009N > 0210009N
i 1510009N = 0210009N
j 1010009N < 0510009N
k 1010009N > 0510009N
l 1010009N = 0510009N
m 1510009N < 0510009N
n 1510009N > 0510009N
o 1510009N = 0510009N
p 1510009N < 1010009N
q 1510009N > 1010009N
r 1510009N = 1010009N

TABLE 37.--Wilcoxon Signed Rank Test Comparing mA on 9" 100 kVp Without Filter

	0510009N - 0210009N	1010009N - 0210009N	1510009N - 0210009N	1010009N - 0510009N	1510009N - 0510009N	1510009N - 1010009N
Z	-1.741(a)	-2.789(a)	-2.780(a)	-.885(a)	-1.462(a)	-.278(a)
Asymp. Sig. (2-tailed)	.082	**.005** †	**.005** †	.376	.144	.781

a Based on negative ranks.
† $p < 0.00833$

TABLE 38.--Friedman Test for 9" 100 kVp With Filter Images[a]

N	30
Chi-Square	2.160
df	3
Asymp. Sig.	.540

[a] Based on Friedman Test, $p < 0.05$.

TABLE 39.--Friedman Test for 9" 120 kVp Without Filter Images[a]

N	30
Chi-Square	4.120
df	3
Asymp. Sig.	.249

[a] Based on Friedman Test, $p < 0.05$.

TABLE 40.--Friedman Test for 9" 120 kVp With Filter Images

N	30
Chi-Square	10.000
df	3
Asymp. Sig.	**.019** †

† $p < 0.05$

TABLE 41.--Ranks for 9" 120 kVp With Filter Images

		N	Mean Rank	Sum of Ranks
0512009Y - 0212009Y	Negative Ranks	9(a)	12.89	116.00
	Positive Ranks	21(b)	16.62	349.00
	Ties	0(c)		
	Total	30		
1012009Y - 0212009Y	Negative Ranks	11(d)	17.59	193.50
	Positive Ranks	19(e)	14.29	271.50
	Ties	0(f)		
	Total	30		
1512009Y - 0212009Y	Negative Ranks	10(g)	12.85	128.50
	Positive Ranks	20(h)	16.83	336.50
	Ties	0(i)		
	Total	30		
1012009Y - 0512009Y	Negative Ranks	20(j)	16.20	324.00
	Positive Ranks	10(k)	14.10	141.00
	Ties	0(l)		
	Total	30		
1512009Y - 0512009Y	Negative Ranks	19(m)	14.03	266.50
	Positive Ranks	11(n)	18.05	198.50
	Ties	0(o)		
	Total	30		
1512009Y - 1012009Y	Negative Ranks	11(p)	13.77	151.50
	Positive Ranks	19(q)	16.50	313.50
	Ties	0(r)		
	Total	30		

a 0512009Y < 0212009Y
b 0512009Y > 0212009Y
c 0512009Y = 0212009Y
d 1012009Y < 0212009Y
e 1012009Y > 0212009Y
f 1012009Y = 0212009Y
g 1512009Y < 0212009Y
h 1512009Y > 0212009Y
i 1512009Y = 0212009Y
j 1012009Y < 0512009Y
k 1012009Y > 0512009Y
l 1012009Y = 0512009Y
m 1512009Y < 0512009Y
n 1512009Y > 0512009Y
o 1512009Y = 0512009Y
p 1512009Y < 1012009Y
q 1512009Y > 1012009Y
r 1512009Y = 1012009Y

TABLE 42.--Wilcoxon Signed Rank Test Comparing mA on 9" 120 kVp With Filter[c]

	0512009Y - 0212009Y	1012009Y - 0212009Y	1512009Y - 0212009Y	1012009Y - 0512009Y	1512009Y - 0512009Y	1512009Y - 1012009Y
Z	-2.399(a)	-.803(a)	-2.143(a)	-1.885(b)	-.702(b)	-1.670(a)
Asymp. Sig. (2-tailed)	.016	.422	.032	.059	.483	.095

a Based on negative ranks.
b Based on positive ranks.
c Based on Wilcoxon Signed Rank Test, p < 0.00833.

APPENDIX 11

Friedman and Wilcoxon Signed Ranks Tests for 12" Images

TABLE 43.--Ranks for 12" Image Pair Comparing Filter

		N	Mean Rank	Sum of Ranks
0210012Y - 0210012N	Negative Ranks	13(a)	18.54	241.00
	Positive Ranks	17(b)	13.18	224.00
	Ties	0(c)		
	Total	30		
0212012Y - 0212012N	Negative Ranks	16(d)	18.28	292.50
	Positive Ranks	14(e)	12.32	172.50
	Ties	0(f)		
	Total	30		
0510012Y - 0510012N	Negative Ranks	18(g)	17.31	311.50
	Positive Ranks	12(h)	12.79	153.50
	Ties	0(i)		
	Total	30		
0512012Y - 0512012N	Negative Ranks	20(j)	16.00	320.00
	Positive Ranks	10(k)	14.50	145.00
	Ties	0(l)		
	Total	30		
1010012Y - 1010012N	Negative Ranks	15(m)	16.53	248.00
	Positive Ranks	15(n)	14.47	217.00
	Ties	0(o)		
	Total	30		
1012012Y - 1012012N	Negative Ranks	15(p)	15.43	231.50
	Positive Ranks	15(q)	15.57	233.50
	Ties	0(r)		
	Total	30		
1510012Y - 1510012N	Negative Ranks	18(s)	13.83	249.00
	Positive Ranks	12(t)	18.00	216.00
	Ties	0(u)		
	Total	30		
1512012Y - 1512012N	Negative Ranks	21(v)	14.76	310.00
	Positive Ranks	9(w)	17.22	155.00
	Ties	0(x)		
	Total	30		

a 0210012Y < 0210012N
b 0210012Y > 0210012N
c 0210012Y = 0210012N
d 0212012Y < 0212012N
e 0212012Y > 0212012N
f 0212012Y = 0212012N
g 0510012Y < 0510012N
h 0510012Y > 0510012N
i 0510012Y = 0510012N
j 0512012Y < 0512012N
k 0512012Y > 0512012N
l 0512012Y = 0512012N
m 1010012Y < 1010012N
n 1010012Y > 1010012N
o 1010012Y = 1010012N
p 1012012Y < 1012012N
q 1012012Y > 1012012N
r 1012012Y = 1012012N
s 1510012Y < 1510012N
t 1510012Y > 1510012N
u 1510012Y = 1510012N
v 1512012Y < 1512012N
w 1512012Y > 1512012N
x 1512012Y = 1512012N

TABLE 44.--Ranks for 12" Image Pairs Comparing Filter[c]

	0210012Y - 0210012N	0212012Y - 0212012N	0510012Y - 0510012N	0512012Y - 0512012N	1010012Y - 1010012N	1012012Y - 1012012N	1510012Y - 1510012N	1512012Y - 1512012N
Z	-.176(a)	-1.238(a)	-1.629(a)	-1.804(a)	-.320(a)	-.021(b)	-.340(a)	-1.597(a)
Asymp. Sig. (2-tailed)	.861	.216	.103	.071	.749	.984	.734	.110

[a] Based on positive ranks.
[b] Based on negative ranks.
[c] Based on Wilcoxon Signed Rank Test, p < 0.00625.

TABLE 45.--Ranks for 12" Image Pairs Comparing kVp

		N	Mean Rank	Sum of Ranks
0212012N - 0210012N	Negative Ranks	11(a)	15.18	167.00
	Positive Ranks	19(b)	15.68	298.00
	Ties	0(c)		
	Total	30		
0212012Y - 0210012Y	Negative Ranks	14(d)	16.14	226.00
	Positive Ranks	16(e)	14.94	239.00
	Ties	0(f)		
	Total	30		
0512012N - 0510012N	Negative Ranks	17(g)	16.53	281.00
	Positive Ranks	13(h)	14.15	184.00
	Ties	0(i)		
	Total	30		
0512012Y - 0510012Y	Negative Ranks	18(j)	16.53	297.50
	Positive Ranks	12(k)	13.96	167.50
	Ties	0(l)		
	Total	30		
1012012N - 1010012N	Negative Ranks	17(m)	15.50	263.50
	Positive Ranks	13(n)	15.50	201.50
	Ties	0(o)		
	Total	30		
1012012Y - 1010012Y	Negative Ranks	18(p)	14.69	264.50
	Positive Ranks	12(q)	16.71	200.50
	Ties	0(r)		
	Total	30		
1512012N - 1510012N	Negative Ranks	16(s)	15.34	245.50
	Positive Ranks	14(t)	15.68	219.50
	Ties	0(u)		
	Total	30		
1512012Y - 1510012Y	Negative Ranks	17(v)	17.09	290.50
	Positive Ranks	13(w)	13.42	174.50
	Ties	0(x)		
	Total	30		

a 0212012N < 0210012N
b 0212012N > 0210012N
c 0212012N = 0210012N
d 0212012Y < 0210012Y
e 0212012Y > 0210012Y
f 0212012Y = 0210012Y
g 0512012N < 0510012N
h 0512012N > 0510012N
i 0512012N = 0510012N
j 0512012Y < 0510012Y
k 0512012Y > 0510012Y
l 0512012Y = 0510012Y
m 1012012N < 1010012N
n 1012012N > 1010012N
o 1012012N = 1010012N
p 1012012Y < 1010012Y
q 1012012Y > 1010012Y
r 1012012Y = 1010012Y
s 1512012N < 1510012N
t 1512012N > 1510012N
u 1512012N = 1510012N
v 1512012Y < 1510012Y
w 1512012Y > 1510012Y
x 1512012Y = 1510012Y

TABLE 46.--Wilcoxon Signed Rank Test Comparing Effect of kVP on 12" Images[c]

	0212012N - 0210012N	0212012Y - 0210012Y	0512012N - 0510012N	0512012Y - 0510012Y	1012012N - 1010012N	1012012Y - 1010012Y	1512012N - 1510012N	1512012Y - 1510012Y
Z	-1.349(a)	-.134(a)	-1.000(b)	-1.339(b)	-.639(b)	-.660(b)	-.268(b)	-1.195(b)
Asymp. Sig. (2-tailed)	.177	.893	.317	.181	.523	.509	.789	.232

a Based on negative ranks.
b Based on positive ranks.
[c] Based on Wilcoxon Signed Rank Test, $p < 0.00625$.

TABLE 47.--Friedman Test for 12" 100 kVp Without Filter Images[a]

N	30
Chi-Square	16.720
df	3
Asymp. Sig.	.001

[a] Based on Friedman Test, $p < 0.05$.

TABLE 48.--Ranks for 12" 100 kVp Without Filter Images

		N	Mean Rank	Sum of Ranks
0510012N - 0210012N	Negative Ranks	9(a)	11.22	101.00
	Positive Ranks	21(b)	17.33	364.00
	Ties	0(c)		
	Total	30		
1010012N - 0210012N	Negative Ranks	7(d)	11.86	83.00
	Positive Ranks	23(e)	16.61	382.00
	Ties	0(f)		
	Total	30		
1510012N - 0210012N	Negative Ranks	6(g)	15.00	90.00
	Positive Ranks	24(h)	15.63	375.00
	Ties	0(i)		
	Total	30		
1010012N - 0510012N	Negative Ranks	11(j)	13.23	145.50
	Positive Ranks	19(k)	16.82	319.50
	Ties	0(l)		
	Total	30		
1510012N - 0510012N	Negative Ranks	12(m)	14.79	177.50
	Positive Ranks	18(n)	15.97	287.50
	Ties	0(o)		
	Total	30		
1510012N - 1010012N	Negative Ranks	18(p)	15.83	285.00
	Positive Ranks	12(q)	15.00	180.00
	Ties	0(r)		
	Total	30		

a 0510012N < 0210012N
b 0510012N > 0210012N
c 0510012N = 0210012N
d 1010012N < 0210012N
e 1010012N > 0210012N
f 1010012N = 0210012N
g 1510012N < 0210012N
h 1510012N > 0210012N
i 1510012N = 0210012N
j 1010012N < 0510012N
k 1010012N > 0510012N
l 1010012N = 0510012N
m 1510012N < 0510012N
n 1510012N > 0510012N
o 1510012N = 0510012N
p 1510012N < 1010012N
q 1510012N > 1010012N
r 1510012N = 1010012N

TABLE 49.--Wilcoxon Signed Rank Test Comparing mA on 12" 100 kVp Without Filter

	0510012N - 0210012N	1010012N - 0210012N	1510012N - 0210012N	1010012N - 0510012N	1510012N - 0510012N	1510012N - 1010012N
Z	-2.708(a)	-3.079(a)	-2.934(a)	-1.792(a)	-1.134(a)	-1.088(b)
Asymp. Sig. (2-tailed)	**.007** †	**.002** †	**.003** †	.073	.257	.277

a Based on negative ranks.
b Based on positive ranks.
† $p < 0.00833$

TABLE 50.--Friedman Test for 12" 100 kVp With Filter Images

N	30
Chi-Square	25.360
Df	3
Asymp. Sig.	**.000** †

† $p < 0.05$

TABLE 51.--Ranks for 12" 100 kVp With Filter Images

		N	Mean Rank	Sum of Ranks
0510012Y - 0210012Y	Negative Ranks	9(a)	15.22	137.00
	Positive Ranks	21(b)	15.62	328.00
	Ties	0(c)		
	Total	30		
1010012Y - 0210012Y	Negative Ranks	6(d)	7.00	42.00
	Positive Ranks	24(e)	17.63	423.00
	Ties	0(f)		
	Total	30		
1510012Y - 0210012Y	Negative Ranks	3(g)	10.17	30.50
	Positive Ranks	27(h)	16.09	434.50
	Ties	0(i)		
	Total	30		
1010012Y - 0510012Y	Negative Ranks	9(j)	10.17	91.50
	Positive Ranks	21(k)	17.79	373.50
	Ties	0(l)		
	Total	30		
1510012Y - 0510012Y	Negative Ranks	10(m)	14.60	146.00
	Positive Ranks	20(n)	15.95	319.00
	Ties	0(o)		
	Total	30		
1510012Y - 1010012Y	Negative Ranks	17(p)	16.35	278.00
	Positive Ranks	13(q)	14.38	187.00
	Ties	0(r)		
	Total	30		

a 0510012Y < 0210012Y
b 0510012Y > 0210012Y
c 0510012Y = 0210012Y
d 1010012Y < 0210012Y
e 1010012Y > 0210012Y
f 1010012Y = 0210012Y
g 1510012Y < 0210012Y
h 1510012Y > 0210012Y
i 1510012Y = 0210012Y
j 1010012Y < 0510012Y
k 1010012Y > 0510012Y
l 1010012Y = 0510012Y
m 1510012Y < 0510012Y
n 1510012Y > 0510012Y
o 1510012Y = 0510012Y
p 1510012Y < 1010012Y
q 1510012Y > 1010012Y
r 1510012Y = 1010012Y

TABLE 52.--Wilcoxon Signed Rank Test Comparing mA on 12" 100 kVp With Filter

	0510012Y - 0210012Y	1010012Y - 0210012Y	1510012Y - 0210012Y	1010012Y - 0510012Y	1510012Y - 0510012Y	1510012Y - 1010012Y
Z	-1.966(a)	-3.930(a)	-4.161(a)	-2.908(a)	-1.784(a)	-.940(b)
Asymp. Sig. (2-tailed)	.049	**.000** †	**.000** †	**.004** †	.074	.347

a Based on negative ranks.
b Based on positive ranks.
† $p < 0.00833$

TABLE 53.--Friedman Test for 12" 120 kVp Without Filter Images

N	30
Chi-Square	13.320
df	3
Asymp. Sig.	**.004** †

† $p < 0.05$

TABLE 54.--Ranks for 12" 120 kVp Without Filter Images

		N	Mean Rank	Sum of Ranks
0512012N - 0212012N	Negative Ranks	10(a)	18.10	181.00
	Positive Ranks	20(b)	14.20	284.00
	Ties	0(c)		
	Total	30		
1012012N - 0212012N	Negative Ranks	8(d)	13.13	105.00
	Positive Ranks	22(e)	16.36	360.00
	Ties	0(f)		
	Total	30		
1512012N - 0212012N	Negative Ranks	9(g)	14.50	130.50
	Positive Ranks	21(h)	15.93	334.50
	Ties	0(i)		
	Total	30		
1012012N - 0512012N	Negative Ranks	9(j)	14.67	132.00
	Positive Ranks	21(k)	15.86	333.00
	Ties	0(l)		
	Total	30		
1512012N - 0512012N	Negative Ranks	10(m)	14.85	148.50
	Positive Ranks	20(n)	15.83	316.50
	Ties	0(o)		
	Total	30		
1512012N - 1012012N	Negative Ranks	17(p)	14.29	243.00
	Positive Ranks	13(q)	17.08	222.00
	Ties	0(r)		
	Total	30		

a 0512012N < 0212012N
b 0512012N > 0212012N
c 0512012N = 0212012N
d 1012012N < 0212012N
e 1012012N > 0212012N
f 1012012N = 0212012N
g 1512012N < 0212012N
h 1512012N > 0212012N
i 1512012N = 0212012N
j 1012012N < 0512012N
k 1012012N > 0512012N
l 1012012N = 0512012N
m 1512012N < 0512012N
n 1512012N > 0512012N
o 1512012N = 0512012N
p 1512012N < 1012012N
q 1512012N > 1012012N
r 1512012N = 1012012N

TABLE 55.--Wilcoxon Signed Rank Test Comparing mA on 12" 120 kVp Without Filter[c]

	0512012N - 0212012N	1012012N - 0212012N	1512012N - 0212012N	1012012N - 0512012N	1512012N - 0512012N	1512012N - 1012012N
Z	-1.063(a)	-2.629(a)	-2.104(a)	-2.072(a)	-1.730(a)	-.216(b)
Asymp. Sig. (2-tailed)	.288	.009	.035	.038	.084	.829

a Based on negative ranks.
b Based on positive ranks.
c Based on Wilcoxon Signed Rank Test, p < 0.00833.

TABLE 56.--Friedman Test for 12" 120 kVp With Filter Images[a]

N	30
Chi-Square	25.400
Df	3
Asymp. Sig.	.000 †

[a] Based on Friedman Test, p < 0.05.

TABLE 57.--Ranks for 12" 120 kVp With Filter Images

		N	Mean Rank	Sum of Ranks
0512012Y - 0212012Y	Negative Ranks	14(a)	14.79	207.00
	Positive Ranks	16(b)	16.13	258.00
	Ties	0(c)		
	Total	30		
1012012Y - 0212012Y	Negative Ranks	6(d)	9.92	59.50
	Positive Ranks	24(e)	16.90	405.50
	Ties	0(f)		
	Total	30		
1512012Y - 0212012Y	Negative Ranks	8(g)	13.63	109.00
	Positive Ranks	22(h)	16.18	356.00
	Ties	0(i)		
	Total	30		
1012012Y - 0512012Y	Negative Ranks	3(j)	12.50	37.50
	Positive Ranks	27(k)	15.83	427.50
	Ties	0(l)		
	Total	30		
1512012Y - 0512012Y	Negative Ranks	10(m)	11.65	116.50
	Positive Ranks	20(n)	17.43	348.50
	Ties	0(o)		
	Total	30		
1512012Y - 1012012Y	Negative Ranks	20(p)	15.80	316.00
	Positive Ranks	10(q)	14.90	149.00
	Ties	0(r)		
	Total	30		

a 0512012Y < 0212012Y
b 0512012Y > 0212012Y
c 0512012Y = 0212012Y
d 1012012Y < 0212012Y
e 1012012Y > 0212012Y
f 1012012Y = 0212012Y
g 1512012Y < 0212012Y
h 1512012Y > 0212012Y
i 1512012Y = 0212012Y
j 1012012Y < 0512012Y
k 1012012Y > 0512012Y
l 1012012Y = 0512012Y
m 1512012Y < 0512012Y
n 1512012Y > 0512012Y
o 1512012Y = 0512012Y
p 1512012Y < 1012012Y
q 1512012Y > 1012012Y
r 1512012Y = 1012012Y

TABLE 58.--Wilcoxon Signed Rank Test Comparing mA on 12" 120 kVp With Filter

	0512012Y - 0212012Y	1012012Y - 0212012Y	1512012Y - 0212012Y	1012012Y - 0512012Y	1512012Y - 0512012Y	1512012Y - 1012012Y
Z	-.527(a)	-3.562(a)	-2.543(a)	-4.018(a)	-2.390(a)	-1.721(b)
Asymp. Sig. (2-tailed)	.598	**.000** †	.011	**.000** †	.017	.085

a Based on negative ranks.
b Based on positive ranks.
† $p < 0.00833$

APPENDIX 12

Intraexaminer and Interexaminer Reliability

In this document, we examine intra-rater reliability of 6 inch and 9 inch ranking data separately. The same agreement measures are used as we did for 12 inch measurements. We first use Kendall's tau-b to examine intra-rater agreement and then uses Kendall's coefficient of concordance.

1. Analysis using Kendall's tau-b

We first calculate Kendall's tau-b between time 1 and time 2 for each individual operator, then perform a meta analysis which combines (pools) the individual estimates of tau-b from the ten operators into a single combined estimate. The results of this analysis are given in Table 59 (6 inch ranking) and Table 60 (9 inch ranking).The results are shown graphically in Figure 49 and 50 for 6 inch and 9 inch ranking data respectively.

TABLE 59.--Kendall's tau-b of 6" Ranking by Each Operator at Time 1 and Time 2 with Pooled Coefficient.

Operator	Kendall's tau-b (asymptotic SE)	P-value
Operator 6	0.617 (0.110)	<.0001
Operator 7	0.667 (0.131)	<.0001
Operator 9	0.517 (0.097)	<.0001
Operator 12	0.800 (0.085)	<.0001
Operator 14	0.517 (0.141)	0.0003
Operator 22	0.650 (0.120)	<.0001
Operator 27	0.667 (0.133)	<.0001
Operator 32	0.517 (0.168)	0.0021
Operator 33	0.567 (0.140)	<.0001
Operator 34	0.583 (0.143)	<.0001
Pooled	0.631 (0.038)	<.0001

The Chi square statistic of heterogeneity test is 6.97, df = 9 and p-value = 0.640.

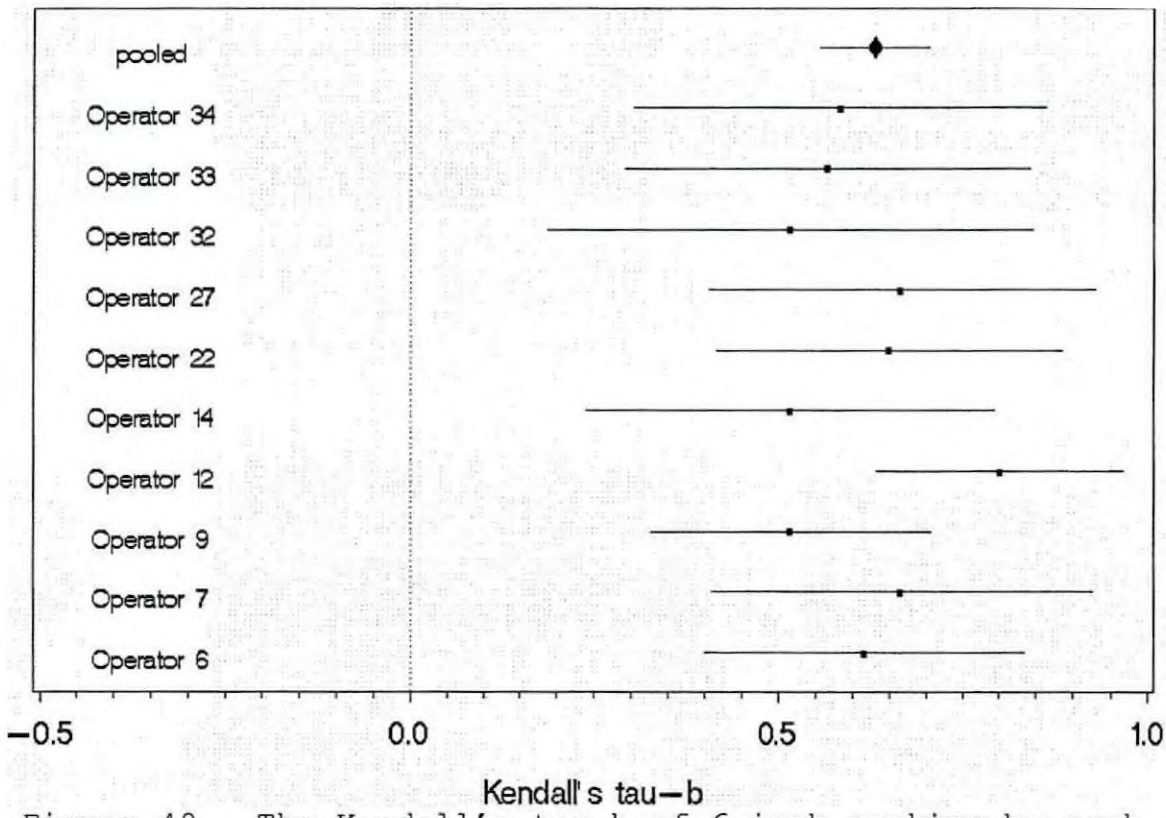


Figure 49. The Kendall's tau-b of 6 inch ranking by each operator at time 1 and time 2 and the pooled tau-b of all operators

Table 59 and Figure 49 show that tau-b from operator to operator do not differ significantly (p value = 0.640). The overall pooled estimate of tau-b across the ten readers was 0.631 ($p < 0.0001$), indicating a high intra-rater agreement.

TABLE 60.--Kendall's tau-b of 9" Ranking by Each Operator at Time 1 and Time 2 with Pooled Coefficient.

Operator	Kendall's tau-b (asymptotic SE)	P-value
Operator 1	0.350 (0.193)	0.0694
Operator 6	0.283 (0.139)	0.0418
Operator 13	0.217 (0.225)	0.3349
Operator 19	0.117 (0.224)	0.6016
Operator 21	-0.017 (0.173)	0.9233
Operator 24	-0.200 (0.156)	0.2008
Operator 25	-0.100 (0.164)	0.5424
Operator 26	0.317 (0.203)	0.1180
Operator 28	0.050 (0.161)	0.7567
Operator 31	-0.100 (0.215)	0.6424
Pooled	0.083 (0.064)	0.1950

The Chi square statistic of heterogeneity test is 11.31, df = 9 and p-value = 0.255.

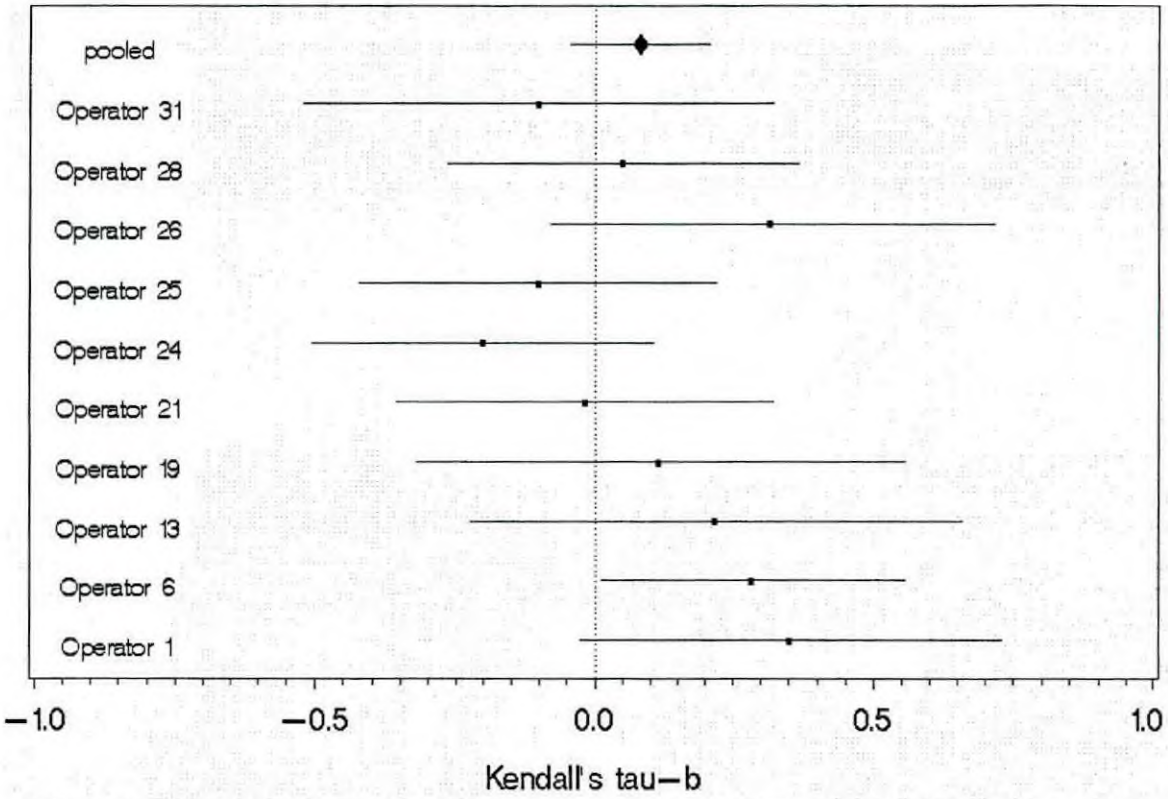


Figure 50. The Kendall's tau-b of **9 inch** ranking by each operator at time 1 and time 2 and the pooled tau-b of all operators along with 95% confidence interval (Table 1.b).

Table 60 and Figure 50 show that tau-b do not differ significantly among operators (p value = 0.255). The overall pooled estimate of tau-b across the ten readers was 0.083 (p = 0.1950), indicating a low non-significant intra-rater agreement.

2. Analysis of Kendall's Coefficient of Concordance W

We also calculate Kendall's coefficient of concordance for each of the ten individual operators and the average coefficient of concordance across the ten operators. Results are shown in Table 2.a (6 inch) and Table 2.b (9 inch).

TABLE 61.--Kendall's Coefficient of Concordance of 6" Ranking by Each Individual at Two Time Points with P-values.

Operator	Kendall's W	P-value
Operator 6	0.903	0.028
Operator 7	0.907	0.027
Operator 9	0.856	0.042
Operator 12	0.966	0.016
Operator 14	0.860	0.040
Operator 22	0.904	0.028
Operator 27	0.918	0.025
Operator 32	0.841	0.047
Operator 33	0.859	0.041
Operator 34	0.869	0.037
Average W =0.888 with 95% CI=(0.865, 0.912)		

Average W from 10 operators indicate a high level agreement of 6 inch rankings by each operator at two time points.

TABLE 62.--Kendall's Coefficient of Concordance of 9" Ranking by Each Individual at Two Time Points with P-values.

Operator	Kendall's W	P-value
Operator 1	0.751	0.094
Operator 6	0.706	0.131
Operator 13	0.646	0.698
Operator 19	0.584	0.289
Operator 21	0.487	0.480
Operator 24	0.371	0.744
Operator 25	0.440	0.588
Operator 26	0.726	0.113
Operator 28	0.516	0.417
Operator 31	0.444	0.577
Average W =0.567 with 95% CI=(0.484, 0.651)		

Average W from 10 operators indicates a low to medium level agreement of 9 inch rankings by each operator at two time points.

In this document, we examine intra-rater reliability in two ways. The first uses Kendall's tau-b, which is a nonparametric measure of correlation ranging from -1 (perfect negative concordance) to 1 (perfect positive concordance), where a value of 0 indicates no correlation. The second uses Kendall's coefficient of concordance, W, which ranges from 0 (no concordance) to 1.

Analysis using Kendall's tau-b

In this document we first calculate Kendall's tau-b between time 1 and time 2 for each individual operator, then perform a meta analysis which combines (pools) the individual estimates of tau from the ten operators into a single combined estimate, which is presented along with a confidence interval. The results of this analysis are given in Table 1, which presents the individual estimates of tau, and the pooled estimate. The results are shown graphically in Figure 60.

TABLE 63.--Kendall's tau-b of 12" Ranking by Each Operator and Pooled Coefficient with 95% CI

Operator	Kendall's tau-b (asymptotic SE)	P-value
Operator 1	0.350 (0.185)	0.0586
Operator 2	0.467 (0.135)	0.0117
Operator 3	0.533 (0.155)	0.0040
Operator 5	-0.267 (0.193)	0.1497
Operator 6	-0.050 (0.187)	0.7871
Operator 7	0.267 (0.184)	0.1497
Operator 10	0.067 (0.236)	0.7187
Operator 12	0.067 (0.176)	0.7187
Operator 13	0.600 (0.082)	0.0012
Operator 14	0.233 (0.212)	0.2074
Pooled	0.258 (0.082)	0.0017

The Chi square statistic of heterogeneity test is 30.827, df = 9 and p-value = 0.0003.

Table 1 and Figure 1 show that there was substantial heterogeneity from operator to operator in the levels of intra-rater agreement, as measured by tau. The footnote to Table 1 indicates that a test for heterogeneity was highly significant (p = 0.0003), indicating that the taus differed significantly among operators. The individual estimates ranged from -0.267 for operator 5 to 0.600 for operator 13. Three of the ten operators had estimates of tau significantly greater than 0 ($p < 0.05$). The overall pooled estimate of tau across the ten readers was 0.26 (p = 0.0017), indicating a low-moderate but significant level of intra-rater agreement.

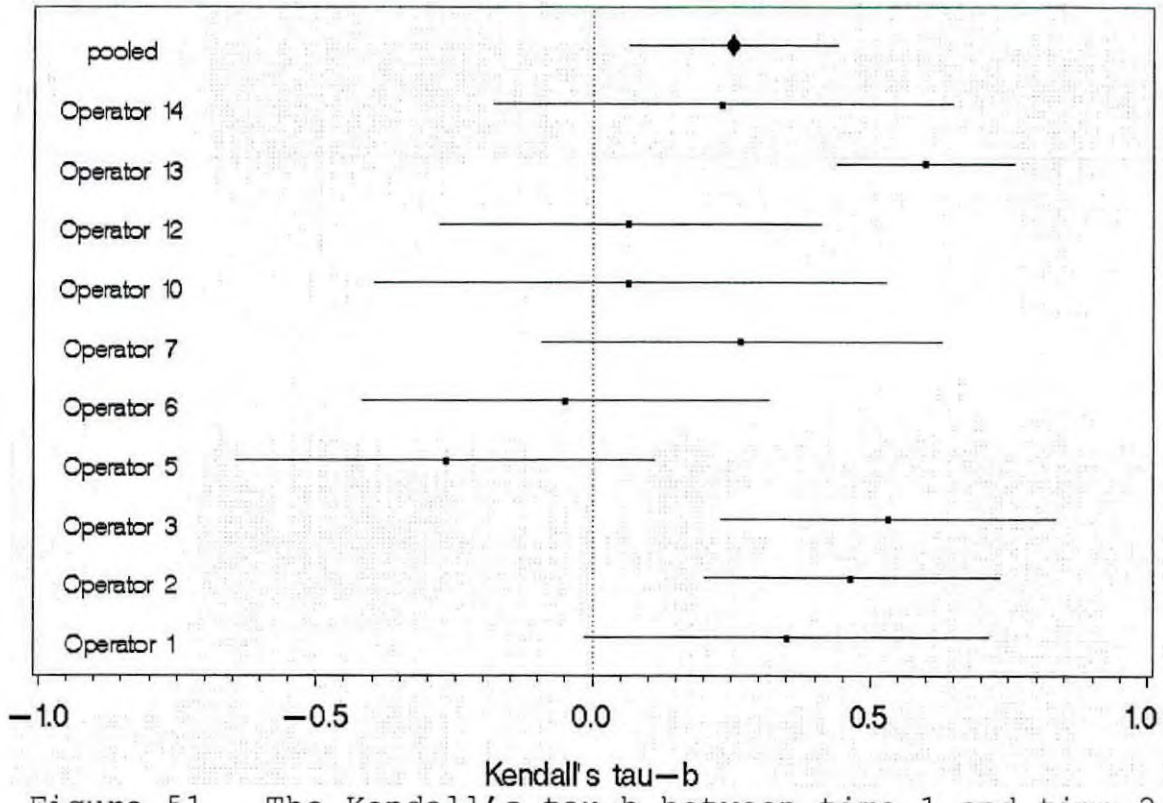


Figure 51. The Kendall's tau-b between time 1 and time 2 for each operator and the pooled tau-b of all operators along with 95% confidence interval (Table 1).

Analysis of Kendall's Coefficient of Concordance W

We also calculated Kendall's coefficient of concordance for of the each 10 individual operators and the average coefficient of concordance across the ten operators. Results are shown in Table 2. The individual estimates of W for the ten operators ranged from 0.322 to 0.897, and the average W across operators was 0.653 (95% CI: 0.527 to 0.780). This pooled estimate of W can be compared to value of W obtained when examining inter-rater agreement.

TABLE 64.--Kendall's Coefficient of Concordance for Each Individual at Two Time Points with P-values.

Operator	Kendall's W	P-value
Operator 1	0.718	0.121
Operator 2	0.822	0.055
Operator 3	0.846	0.045
Operator 5	0.322	0.840
Operator 6	0.504	0.442
Operator 7	0.675	0.163
Operator 10	0.541	0.367
Operator 12	0.565	0.322
Operator 13	0.897	0.029
Operator 14	0.643	0.201
Average W =0.653 with 95% CI=(0.527, 0.780)		

REFERENCES

Badr I, Thomas SM, Cotterrill AD, Pettetta Aduko JM, Fitzgerald M, Adam EJ. X-ray pelvimetry--which is the best technique? Clin Radiol 1997;52(2):136-41.

Bianchi SD, Rampado O, Luberto L, Genovesio AF, Bianchi CC, Ropolo R. Image quality analysis and low dose dental CT. In. *Proceedings of the 19th International Congress and Exhibition in Berlin, Germany, June 22 - 25, 2005,* by International Congress Series 1281, 1177-1181.

Bodner L, Bar-Ziv J, Becker A. Image accuracy of plain film radiography and computerized tomography in assessing morphological abnormality of impacted teeth. Am J Orthod Dentofacial Orthop 2001;120:623-8.

Bottollier-Depois JF, Chau Q, Bouisset P, Kerlau G, Plawinski L, Lebaron-Jacobs L. Assessing exposure to cosmic radiation on board aircraft. Adv Space Res 2003;32(1):59-66.

Bottollier-Depois JF, Trompier F, Clairand I, Spurny F, Bartlett D, Beck P, Lewis B, Lindborg L, O'Sullivan D, Roos H, Tommasino L. Exposure of aircraft crew to cosmic radiation: on-board intercomparison of various dosemeters. Radiat Prot Dosimetry 2004;110(1-4):411-5.

Cohnen M, Fischer H, Hamacher J, Lins E, Kötter R, Mödder U. CT of the head by use of reduced current and kilovoltage: relationship between image quality and dose reduction. Am J Neuroradiol 2000;21(9):1654-1660.

Curry TS, Dowdey JE, and Murry RC. 1990. *Christensen's Physics of Diagnostic Radiology.* 4th ed. Philadelphia: Lippincott, Williams and Wilkins

Danforth RA, Clark DE. Effective dose from radiation absorbed during a panoramic examination with a new generation machine. Oral Surg Oral Med Oral Pathol Oral Radiol Endod 2000;89(2):236-43.

Danforth R, Dus I, Mah J. 3-D volume imaging for dentistry: a new dimension. J Calif Dent Assoc 2003;31(11):817-23.

Elefteriadis JN, Athanasiou AE. Evaluation of impacted canines by means of computerized tomography. Int J Adult Ortho Orthognath Surg 1996;11:257-64.

Endo M, Tsunoo T, Nakamori N, Yoshida T. Effect of scattered radiation on image noise in cone beam CT. Med Phys 2001;28(4):469-474.

European Commission. European guidelines on quality criteria for diagnostic radiographic images, EUR 16260 EN. Brussels: CEC, 1996a.

European Commission. European guidelines on quality criteria for diagnostic radiographic images, EUR 16261 EN. Brussels: CEC, 1996b.

Farman AG, Farman TT. 1997 Digital imaging in dentistry: concept and applications. In *Towards an Electronic Patient Record' 97*, ed. Waegemann CP, 178-87. Broadview, IL: Kelvyn Press.

Farman AG. Fundamentals of image acquisition and processing in the digital era. Orthod Craniofacial Res 2003;6(suppl. 1):17-22.

Forsyth DB, Shaw WC, Richmond S, Roberts CT. Digital imaging of cephalometric radiography, Part 1: Advantages and limitations of digital imaging. Angle Orthod 1996a;66(1):1-42.

Forsyth DB, Shaw WC, Richmond S, Roberts CT. Digital imaging of cephalometric radiographs, Part 2: Image quality. Angle Orthod 1996b;66(1):43-50.

Franklin, JB. The effect of aluminum filter disks in roentgenographic cephalometry. Angle Orthod 1962;32(4): 252-269.

Frederiksen NL. X-Rays: What is the risk? Texas Dent J. 1995;112(2):68-72.

Gould RB. 1991. *Specification, Acceptance Testing and Quality Control of Diagnostic X-Ray Imaging Equipment.* Medical Physics Monograph, ed. Seibert JA, Barnes GT, Gould RG, no. 20. Woodbury: American Institute of Physics.

Gündogdu S, Mahmutyazicioglu K, Ozdemir H, Savranlar A, Asil K. Assessment of image quality of a standard and three dose-reducing protocols in adult cranial CT. Eur Radiol 2005;15(9):1959-1968.

Gray JE, Karsell PR, Becker GP, Gehring DG. Total digital radiology: is it feasible or desirable? Am J Roentgenology 1984;143:1345-1349.

Haaga JR, Miraldi F, MacIntyre W, LiPuma JP, Bryan PJ, and Wiesen E. The Effect of mAs variation upon computed tomography image quality as evaluated by *in vivo* and *in vitro* studies. Radiology 1981; 138(2): 449-454.

Hamada Y, Kondoh T, Noguchi K, Iino M, Isono H, Ishii H, Mishima A, Kobayashi K, Seto K. Application of limited cone beam computed tomography to clinical assessment of alveolar bone grafting: a preliminary report. Cleft Palate Craniofac J 2005;42(2):128-37.

Hatcher D, Dial C, Mayorga C. Cone beam CT for pre-surgical assessment of implant sites. J Calif Dent Assoc 2003;31(11)825-833.

Kiefer H, Lambrecht JT, Roth J. Digital exposition from intra- and extraoral dental radiography. In *Proceedings of the 18th International Congress and Exhibition, Chicago, USA, June 23 - 26, 2004a,* by International Congress Series 1268, 1147-1151.

Kiefer H, Lambrecht JT, Roth J. Dose exposure from analog and digital full mouth radiography and panoramic radiography. Schweiz Monatsschr Zahnmed 2004b;114(7):687-93. German.

Loubele M, Jacobs R, Maes F, Schutyser F, Debaveye D, Bogaerts R, Coudyzer W, Vandermeulen D, Van Cleynenbreugel, Marchal G, Suetens P. Radiation dose vs. image quality for low-dose CT protocols of the head for maxillofacial surgery and oral implant planning. Radiat Prot Dosimetry. 2005;117(1-3):211-6. Epub 2006 Feb 3.

Mah J, Enciso R, Jorgensen M. Management of impacted cuspids using 3-D volumetric imaging. J Calif Dent Assoc 2003;31(11):835-841.

Martin CJ, Sutton DG, Sharp PF. Balancing patient dose and image quality. Appl Radiat Isot 1999;50(1):1-19.

Mayo JR, Hartman TE, Lee KS, Primack SL, Vedal S, Muller NL. CT of the chest: minimal tube current required for good image quality with the least radiation dose. Am J Roentgenol 1995;164:603-607.

Motz JW, Danos M. Image information content and patient exposure. Med Phys 1978;(5)8-22.

Ortiz P, Maccia C, Padovani R, Vano E, Carlsson, GA, Schibilla H. Results of the IAEA-CEC coordinated research programme on radiation doses in diagnostic radiology and methods for reduction. Radiat Prot Dosimetry 1995;57:95-99.

Rustemeyer P, Streubühr U, Suttmoeller J. Low-dose dental computed tomography: significant dose reduction without loss of image quality. Acta Radiol 2004;45:847-853.

Schulze D, Heiland M, Thurmann H, Adam G. Radiation exposure during midfacial imaging using 4 and 16 slice computed tomography, cone beam computed tomography systems and conventional radiography. Dentomaxillofac Radiol 2004a;33(2):83-6.

Schulze D, Heiland M, Schmelzle, R, Rother, UJ. Diagnostic possibilities of cone-beam computed tomography in the facial skeleton. In *Proceedings of the 18th International Congress and Exhibition, Chicago, USA, June 23 - 26, 2004b*, by International Congress Series 1268, 1179-1183.

Seibert JA. Tradeoffs between image quality and dose. Pediatr Radiol 2004;34(suppl 3): S183-195.

Sohaib SA, Peppercorn PD, Horrocks JA, Keene MH, Kenyon GS, Reznek RH. The effect of decreasing mAs on image quality and patient dose in sinus CT. Br J Radiol 2001;74(878):157-161.

Warren-Forward HM, Haddaway MJ, McCall IW, Temperton DH. Influence of dose reduction recommendations on changes in chest radiography techniques. Br J Radiol 1996;69(824): 755-761.

Wenzel A. Effect of varying gray-scale resolution for detectability of bone lesions in intraoral radiographs digitized for teletransmission. Scan J Dent Res 1987;95(6):483-92.

83 35 CW TH 5417
01/07 00-104-07 Ohio
IFGroup

Department of Orthodontics